Molecular Fluorescence Endoscopy

Clinical development and validation
within the lower gastrointestinal tract

Jolien Tjalma

Colophon

The research presented in this thesis was financially supported by a grant from the Dutch Cancer Society (grant RUG 2012-5416); Center for Translational Molecular Medicine (project MAMMOTH 03O-201); European Union (ERC-OA-2012-PoC-324627), an unrestricted research grant from SurgVision BV; and an unrestricted research grant from Boston Scientific. It is registered in the ClinicalTrials.gov registry as NCT02113202 and NCT01972373.

Printing of this thesis was financially supported by Graduate School of Medical Sciences (GSMS) of the University Medical Center Groningen (UMCG), the Faculty of Medical Sciences of the University of Groningen, Stichting Werkgroep Interne Oncologie, SBOH, Surgvision, LI-COR and are all gratefully acknowledged.

Author	Jolien Tjalma
Cover design and layout	© evelienjagtman.com
Printing	Ridderprint	www.ridderprint.nl

ISBN printed version 978-94-6416-382-7

rijksuniversiteit
groningen

Molecular Fluorescence Endoscopy

Clinical development and validation within the lower gastrointestinal tract

Proefschrift

ter verkrijging van de graad van doctor aan de
Rijksuniversiteit Groningen
op gezag van de
rector magnificus prof. dr. C. Wijmenga
en volgens besluit van het College voor Promoties.

De openbare verdediging zal plaatsvinden op

maandag 22 maart 2021 om 16.15 uur

door

Jolien Jozefien Janneke Tjalma

geboren op 26 augustus 1987
te Noordoostpolder

Promotores
Prof. dr. W.B. Nagengast
Prof. dr. G.A.P. Hospers
Prof. dr. J.H. Kleibeuker

Beoordelingscommissie
Prof. dr. R.K. Weersma
Prof. dr. E.C.J. Consten
Prof. dr. J.F. de Boer

Paranimfen

Margreet Smit

Hanna Tjalma

CONTENT

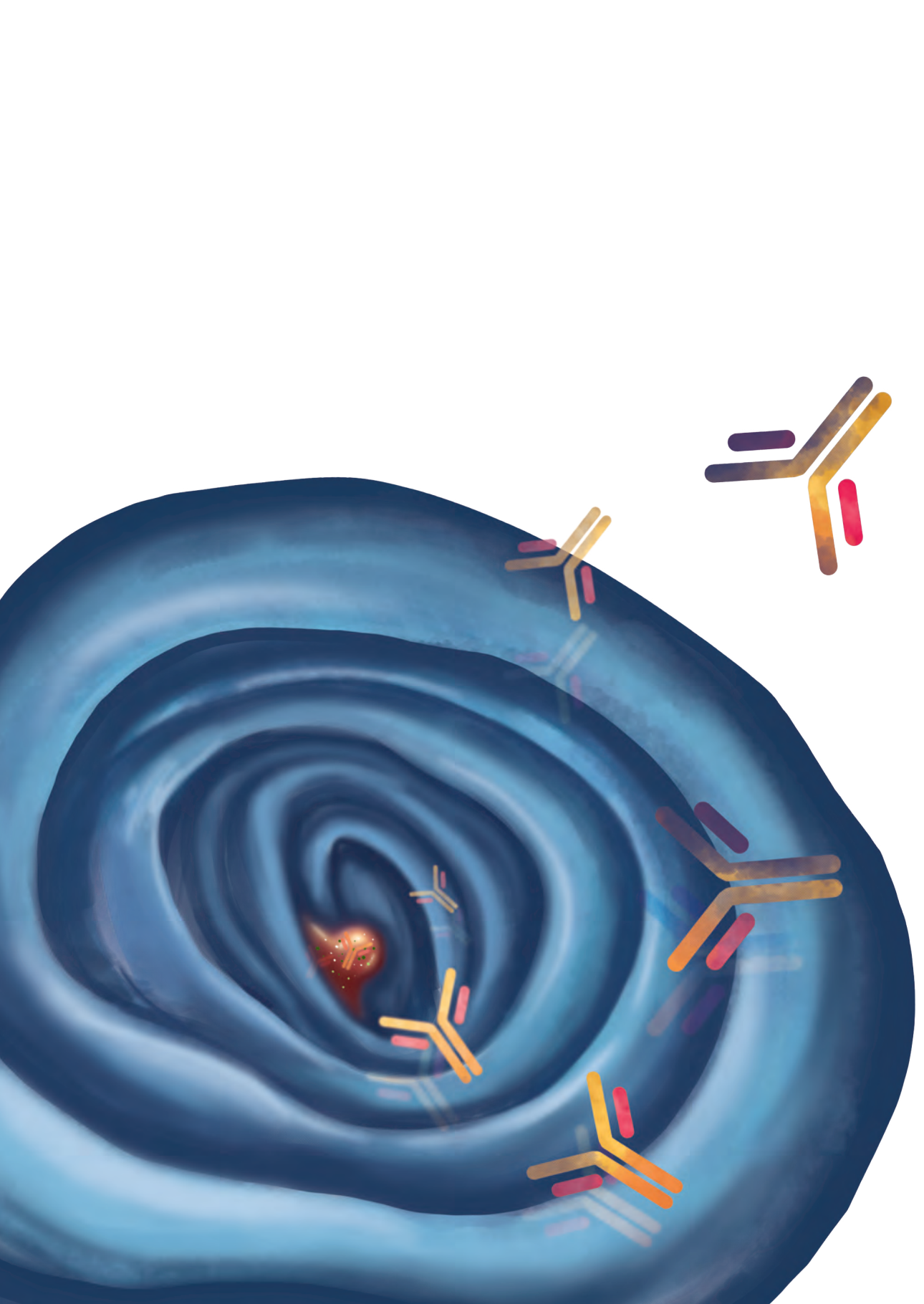

Chapter 1

General introduction and outline of the thesis

GENERAL INTRODUCTION

Colorectal cancer is the second most common cancer worldwide, accounting for 8% of all cancer related deaths.[1,2] Of all colorectal cancers, approximately 60% develops via the well-known adenoma-carcinoma sequence, one-third via the alternative serrated pathway and a small portion are hereditary, for example due to germline mutations in mismatch repair in Lynch syndrome (LS).[3] White-light endoscopy is considered the gold standard for colorectal cancer screening and diagnosis, and has a critical role in staging and response evaluation. During endoscopy, in current clinical practice, gastroenterologists rely on white-light images to evaluate aberrant tissue. Although they have different endoscopy techniques to enhance contrast, like narrow-band imaging, they still make an assessment based on morphological aspects and architectural changes only. Assessment on white-light images only is, however, suboptimal. For example, up to 20-26% of lesions are missed during white light endoscopy, and missed lesions are a main risk factor for the occurrence of interval cancers, particularly in high-risk patients such as patients with Lynch syndrome.[4-7]

Aside from its role in diagnosis and screening, endoscopy techniques may also be useful to evaluate treatment response. This is especially of relevance after neoadjuvant chemoradiotherapy in locally advanced rectal cancer (LARC), and during follow-up. The current standard consists of radiologic assessment by magnetic resonance imaging (MRI) and computed tomography (CT) and does not incorporate endoscopic imaging. The presence of tissue fibrosis, edema and ulcers after neoadjuvant chemoradiotherapy is however notoriously difficult to discriminate from residual tumor.

A novel imaging technique is optical molecular imaging, which can fluorescently tag (pre) malignant tissue and thereby function as a red-flag technique. It makes use of fluorescently-labeled antibodies or peptides that specifically bind their target molecule. As such, the molecular signature of cells is visualized in vivo, and when combined with white light imaging enables anatomic and molecular imaging in real time. The first proof-of-principle study in patients showing the potential of this technique was during surgery with a folate-fluorescein isothiocyanate (FITC) tracer in patients with ovarian cancer.[8]

In this thesis we describe the development and clinical validation of an optical imaging platform that can be used during gastrointestinal endoscopy, using a small fiber-bundle that can be inserted in the working channel of any clinical video-endoscope, and can detect and quantify near infra-red fluorescent light.[9-11]

The aim of this thesis is to address the clinical potential of molecular fluorescence endoscopy in the colon and rectum.

OUTLINE OF THE THESIS

Part I - Validation of molecular fluorescence endoscopy for screening purposes

The first step in the development of molecular fluorescence endoscopy is to find a molecular target that is specifically overexpressed in malignant and premalignant colorectal lesions. Therefore, in **chapter 2**, we determine the protein expression of vascular endothelial growth factor A (VEGFA) and epidermal growth factor receptor (EGFR) by immunohistochemistry in a large subset of 303 archival human colorectal samples: hyperplastic polyps, sporadic adenomas, sessile serrated adenomas/polyps (SSA/P), and adenomatous and carcinomatous tissue of patients with Lynch syndrome. Thereafter, we validate our molecular fluorescence endoscopy (MFE) approach with the near-infrared (NIR) fluorescent antibodies bevacizumab-800CW (anti-VEGFA) and cetuximab-800CW (anti-EGFR) in an artificial model. Intraperitoneal VEGFA- and EGFR-positive xenograft tumors were grown in mice, thereafter the mice were injected with one of the tracers or IgG control. Three days later, the tumors were stitched in a freshly resected human colon specimen to test the practical feasibility of molecular fluorescence endoscopy in visualizing small colorectal lesions in real time.

Given the relatively high detection miss rates of white light endoscopy, molecular fluorescence endoscopy may increase screening accuracy. In **chapter 3** we describe the first clinical proof-of-principal study towards the feasibility of VEGFA-targeted molecular fluorescence endoscopy for colorectal adenoma detection. This dose-escalation study is performed in 17 patients with familial adenomatous polyposis. These patients have a high probability of colorectal adenomas, which enables adequate evaluation of the optimal tracer dose. Patients received an intravenous injection with 4.5, 10 or 25 mg of bevacizumab-800CW and 2-3 days later they undergo molecular fluorescence endoscopy to detect colorectal adenomas. Next, to validate our in vivo wide-field molecular fluorescence endoscopy findings, the fluorescence in the freshly excised colorectal tissue is also quantified using spectroscopy to estimate local tracer concentration.

Part II - Imaging in locally advanced rectal cancer

Clinical decision-making in LARC is challenging. At baseline staging, patients receive a pelvic MRI scan for locoregional staging and a CT scan of chest and abdomen for detection of distant metastases. When LARC is diagnosed, patients receive neoadjuvant chemoradiotherapy to achieve regression of the primary tumor, thereby increasing chances of a successful surgical (R0) resection. However, in the time interval between diagnosis and surgery (at least eleven weeks) formerly non-detectable distant metastases may appear. Therefore, preoperative restaging is generally performed with MRI and CT scan of chest and abdomen, but this is not incorporated in national and international guidelines. **Chapter 4** describes a retrospective study in patients with LARC, determining the value of restaging CT scan. The aim of this

retrospective study was to determine the frequency of a change in treatment strategy after the restaging CT scan, in patients with LARC without distant metastases at initial staging. In total 153 LARC patients were included, of which the surgical treatment as planned before CRT was compared with the treatment ultimately received.

At restaging of LARC a second challenge comes along. Current clinical imaging modalities, MRI and conventional white-light endoscopy, suffer from a poor specificity and sensitivity partly because neoadjuvant chemoradiotherapy changes the local tissue architecture.[12] Especially identification of complete pathologic response (pCR, *i.e.* no residual cancer, ypT0N0) is difficult. White-light endoscopy (WLE) provides only morphological information of the superficial rectal mucosa, while MRI encounters difficulties distinguishing viable tumor from fibrosis. Studies have shown that 9%-16% of patients with suspected residual tumor following MRI and white-light endoscopy, in fact have a pCR in the resection specimen.[13-15] There is special interest in the approximately 15-27% of LARC patients who have a pCR after neoadjuvant chemoradiotherapy, as they could benefit from organ-preserving strategies instead of total mesorectal excision.[16] Since rectal surgery is accompanied by a relatively high morbidity rate, non-operative management for clinical complete responders could be an attractive option, and current studies show this is associated with high survival rates, reduced long-term morbidity and improved functional outcomes.[17-21] New systemic treatments and improved irradiation techniques may even increase the pCR rate in the nearby future, making it even more relevant to accurately determine response to assess whether refrainment from surgery is safe.

In **chapter 5** we investigate whether VEGFA-targeted molecular fluorescence endoscopy could identify the presence of residual tumor and aid in clinical response assessment in patients with LARC after neoadjuvant chemoradiotherapy. In 25 LARC patients VEGFA-targeted molecular fluorescence endoscopy is performed at the day of surgery. Fluorescence signals are measured in vivo, *i.e.* quantitative fluorescence endoscopy to ensure that the visualized fluorescence reflects the true accumulation of the tracer and thus the actual biology. Quantitative fluorescence endoscopy and conventional clinical restaging (MRI and white-light endoscopy) results are compared to the gold standard: pathological staging of the surgical specimen. In this way, we determine the potential additional value of quantitative fluorescence endoscopy to evaluate the response to neoadjuvant chemoradiotherapy; and its potential to predict pCR and aid organ-preserving strategies.

Unfortunately, a substantial part of surgical specimens of LARC patients turns out to have tumor in the circumferential resection margin (R1 resection) at histopathological evaluation (up to 18.6%).[22-24] The surgical success rate might improve if surgeons could assess whether the circumferential resection margin is tumor-positive peroperatively, as in this way resections

could be extended immediately or intraoperative radiation therapy (IORT) may be applied. On the other hand, when a margin is shown to be tumor-negative, extended resections could be avoided, thereby preventing substantial postoperative complications and the need for reinterventions.[25] **Chapter 6** describes a side-study of the VEGFA-targeted molecular fluorescence endoscopy study described in chapter 5. In this proof-of-concept study, we evaluate whether fluorescence imaging of the VEGFA-targeted surgical specimens could help the surgeon evaluating the circumferential resection margin at the surgical theatre. Fluorescence-guided imaging (FGI) is performed in a total of 8 specimens and the prediction of positive/negative resection margins by fluorescence imaging was compared to final pathology. Additionally, in 17 specimens the sensitivity and specificity of bevacizumab-800CW for tumor detection was determined and local tracer accumulation was three-dimensionally analyzed by light-sheet fluorescence microscopy.

The findings of this thesis are summarized in **chapter 7**, together with the current developments and future perspectives of this novel technique.

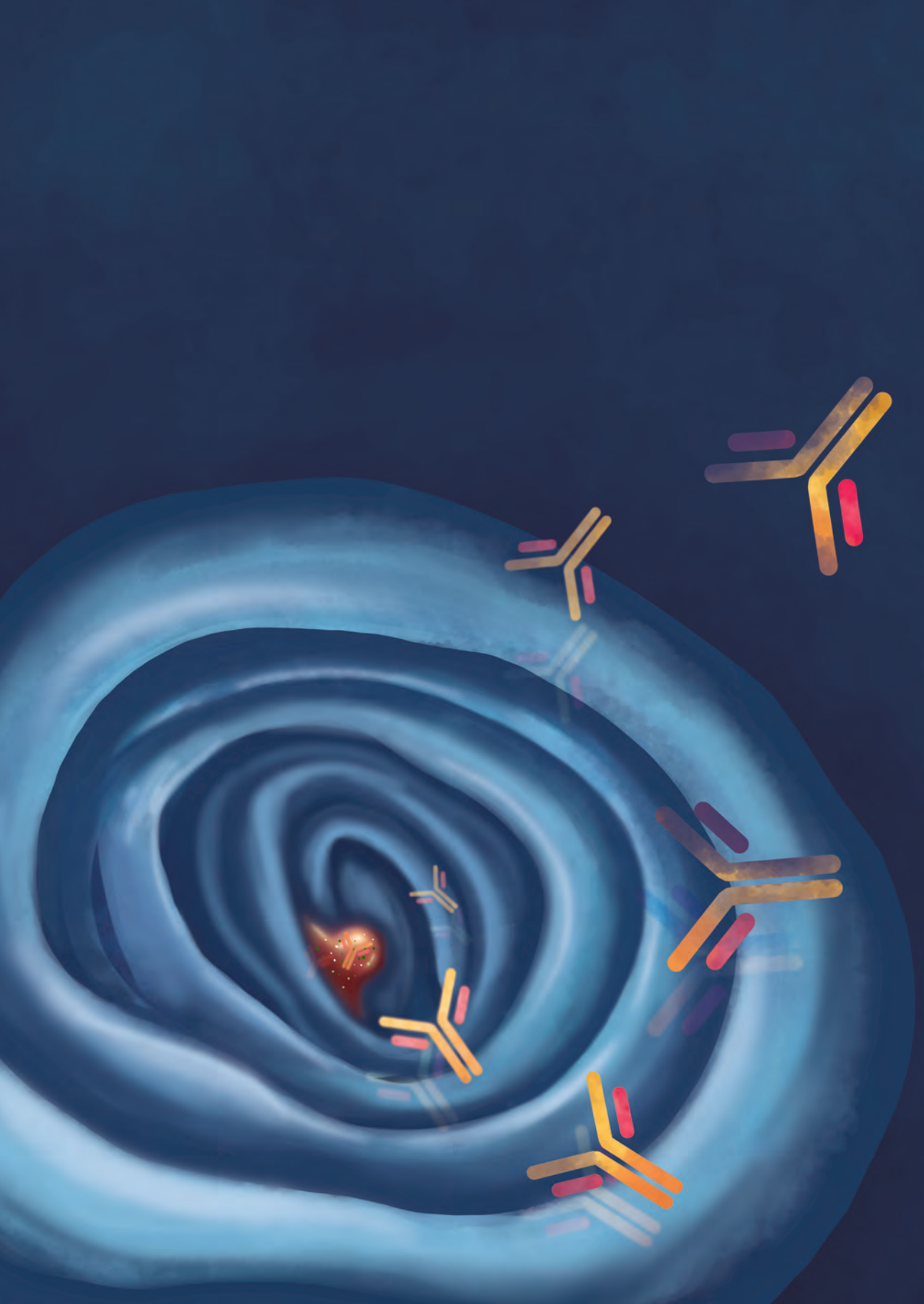



Part I

Validation of molecular fluorescence endoscopy for screening purposes

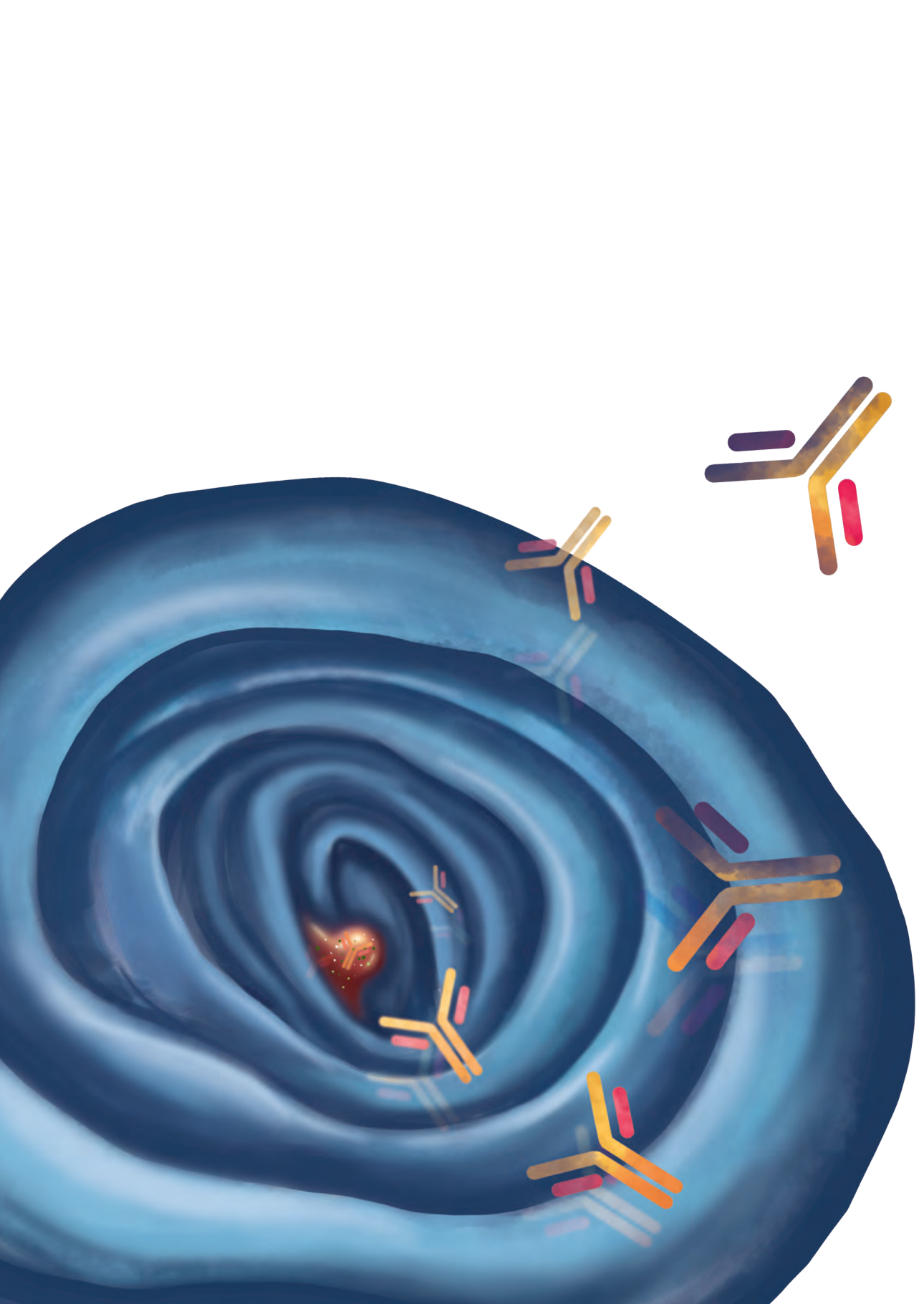

Chapter 2

Molecular-guided endoscopy targeting vascular endothelial growth factor A for improved colorectal polyp detection

Journal of Nuclear Medicine, 2016; 57(3): 480-485

Jolien JJ Tjalma[1*], P Beatriz Garcia-Allende[2*], Elmire Hartmans[1], Anton G Terwisscha van Scheltinga[3], Wytske Boersma-van Ek[1], Jürgen Glatz[2], Maximilian Koch[2], Yasmijn J van Herwaarden[4], Tanya M Bisseling[4], Iris D Nagtegaal[5], Hetty Timmer-Bosscha[6], Jan Jacob Koornstra[1], Arend Karrenbeld[7], Jan H Kleibeuker[1], Gooitzen M van Dam[8], Vasilis Ntziachristos[2], Wouter B Nagengast[1]

[*]Both contributed equally

[1]Department of Gastroenterology and Hepatology, [3]Department of Clinical Pharmacy and Pharmacology, [6]Department of Medical Oncology, [7]Department of Pathology, [8]Department of Surgery - University of Groningen, University Medical Center Groningen, Groningen, The Netherlands. [2]Chair for Biological Imaging & Institute for Biological and Medical Imaging - Technical University of Munich and Helmholtz Center Munich, Munich, Germany. [4]Department of Gastroenterology and Hepatology, [5]Department of Pathology - Radboud University Medical Center, Nijmegen, The Netherlands.

ABSTRACT

Introduction: Small and flat adenomas are known to carry a high miss-rate during standard white-light endoscopy. Increased detection rate may be achieved by molecular fluorescence endoscopy with targeted near-infrared (NIR) fluorescent tracers. The aim of this study was to validate vascular endothelial growth factor A (VEGFA) and epidermal growth factor receptor (EGFR)-targeted fluorescent tracers during ex vivo colonoscopy with an NIR endoscopy platform.

Methods: VEGFA and EGFR expression was determined by immunohistochemistry on a large subset of human colorectal tissue samples—48 sessile serrated adenomas/polyps, 70 sporadic high-grade dysplastic adenomas, 19 hyperplastic polyps— and tissue derived from patients with Lynch syndrome (LS)—78 low-grade dysplastic adenomas, 57 high-grade dysplastic adenomas and 31 colon cancer samples. To perform an ex vivo colonoscopy procedure, 14 mice with small intraperitoneal EGFR-positive HCT116^{luc} tumors received intravenous bevacizumab-800CW (anti-VEGFA), cetuximab-800CW (anti-EGFR), control tracer IgG-800CW, or sodium chloride. Three days later, 8 resected HCT116^{luc} tumors (2-5 mm) were stitched into 1 freshly resected human colon specimen and followed by an ex vivo molecular fluorescence colonoscopy procedure.

Results: Immunohistochemistry showed high VEGFA expression in 79-96% and high EGFR expression in 51-69% of the colorectal lesions. Both targets were significantly overexpressed in the colorectal lesions, compared with the adjacent normal colon crypts. During ex vivo molecular fluorescence endoscopy, all tumors could clearly be delineated for both bevacizumab-800CW and cetuximab-800CW tracers. Specific tumor uptake was confirmed with fluorescent microscopy showing, respectively, stromal and cell membrane fluorescence.

Conclusion: VEGFA is a promising target for molecular fluorescence endoscopy because it showed a high protein expression, especially in sessile serrated adenomas/polyps and LS. We demonstrated the feasibility to visualize small tumors in real time during colonoscopy using a NIR fluorescence endoscopy platform, providing the endoscopist a wide-field red-flag technique for adenoma detection. Clinical studies are currently being performed in order to provide in-human evaluation of our approach.

INTRODUCTION

White-light endoscopy is the gold standard for detection of premalignant and malignant colorectal lesions.[1] Despite the efficacy of current colonoscopy, small and especially right-sided flat or serrated adenomas are notoriously difficult to detect, resulting in substantial polyp detection miss-rates of 20-26%.[2,3] Missed lesions are a main risk factor for the occurrence of interval cancers, particularly in high-risk patients such as patients with Lynch syndrome (LS).[4-6] Advanced endoscopic imaging modalities, such as narrow-band imaging, autofluorescence imaging and chromoendoscopy, have been extensively investigated but did not show significant improvement in adenoma detection rates.[24-26] Ideally, white-light endoscopy is combined with a sensitive, wide-field-of-view, red-flag technique to assist the endoscopist in the immediate identification of aberrant lesions. Molecular optical imaging, that is, visualizing the molecular signature of cells in vivo, would be highly suitable for this aim. It enables real-time anatomic and functional imaging, and it is safe, fast and relatively inexpensive.[27] With selective optical agents functioning in the near-infrared (NIR) light spectrum, contrast between normal mucosa and dysplastic tissue could potentially be greatly enhanced, thereby reducing miss-rates.[28] These agents should target biomarkers known to be overexpressed in colorectal cancer such as epidermal growth factor receptor (EGFR) or shown to be overexpressed early in the adenoma-carcinoma sequence, as described for vascular endothelial growth factor A (VEGFA), due to the angiogenic switch.[7,9]

The aim of the current study was to validate VEGFA- and EGFR-targeting fluorescent antibodies in visualizing small colorectal lesions in real time with our novel NIR endoscopy platform. Therefore, we first determined the expression of potential targets VEGFA and EGFR in archival human colorectal samples, including sessile serrated adenomas/polyps (SSA/P) and adenomatous and carcinomatous tissue of patients with LS. Second, we performed a simulated endoscopy procedure to validate our VEGFA- and EGFR-targeting NIR fluorescent tracers.

MATERIALS AND METHODS

Immunohistochemistry of human colorectal lesions

The archival formalin-fixed and paraffin-embedded human colorectal tissue set consisted of SSA/P (*n* = 48; 42 different individuals), Lynch low-grade dysplasia (LGD) adenomas (*n* = 78; 62 individuals), Lynch high-grade dysplasia (HGD) adenomas (*n* = 57; 40 individuals), Lynch colon cancer tissue (*n* = 32; 31 individuals), sporadic adenomas with HGD (*n* = 70; 70 individuals), and hyperplastic polyps (HP) (*n* = 19; 18 individuals). The tissue was handled according to Dutch Code of Conduct for proper use of Human Tissue (www.federa.org), and the study was conducted according to the guidelines of the medical ethical committee of our hospital (www.ccmo.nl). To evaluate the clinical relevance of an anti-VEGFA and anti-EGFR fluorescent tracer for colorectal surveillance, the protein expression of VEGFA and EGFR was determined by immunohistochemistry. Slides were rehydrated via graded alcohols. Antigen was retrieved with 0.100M Tris/HCl (pH 9.0, 15 minutes) for VEGFA and 0.1% Proteinase K (30 min) for EGFR. Endogenous peroxidase blocking was performed during 30 min with 0.42% hydrogen peroxide, followed by avidin-biotin blocking. For VEGFA, sections were incubated for one hour with polyclonal rabbit anti-human VEGFA (Santacruz) (1:50) and consecutive for 30 minutes with swine anti-rabbit biotin (1:300 in phosphate-buffered saline (PBS) with 1% bovine serum albumin (BSA)) and Streptavidin (1:300 in PBS/1% BSA). For EGFR, sections were incubated for one hour with monoclonal mouse anti-EGFR (clone 31G7, Invitrogen) (1:50 in PBS/1% BSA) and consecutive for 30 minutes with rabbit anti-mouse peroxidase (1:100) and goat anti-rabbit peroxidase (1:100). Color development was achieved by applying a 3-3'-diaminobenzine-tetrahydorchloride (DAB) reagent (Sigma) for 10 minutes. PBS was used throughout for washing and all steps occurred at room temperature. Finally, sections were counterstained with Mayer hematoxylin, dehydrated in alcohol, and coverslipped. Staining intensities were independently evaluated by 2 individuals; consensus was achieved in discrepant cases by consulting an experienced pathologist. Dysplasia, cancer, and adjacent normal epithelium, if present, were separately scored and compared. Staining intensities were graded using a 0-3 scale (0, completely negative; 1, weak; 2, moderate; 3, strong staining).

Cell culture

The HCT116^{luc} human colon cancer cell line, stably transfected with the firefly gene *luciferase*, was obtained from Caliper Life Sciences. The cells were grown in a monolayer culture using McCoy 5A Medium (Gibco, Life Technologies) supplemented with 10% fetal bovine serum, in a humidified atmosphere containing 5% CO_2 at 37°C. EGFR cell surface expression was confirmed for HCT116^{luc} (data not shown) with the use of fluorescence-activated cell sorting (FACS Calibur, BD Biosciences).

Fluorescent labeling of monoclonal antibodies

As described previously, the monoclonal antibodies bevacizumab (Roche), cetuximab (Merck) and human IgG (Nanogram; Sanquin) were labeled with IRDye800CW-NHS (LI-COR Biosciences).[29,30] This NIR fluorescent dye underwent extensive toxicity testing and is a good-manufacturing-practice-compliant compound, registered at the U.S. Food and Drug Administration.[31,32]

HCT116^{luc} human xenograft tumors

All experiments were approved by the animal welfare committee of the University of Groningen and performed in accordance with the Dutch Animal Welfare Act of 1997. To obtain multiple small tumor lesions, fourteen male athymic nude mice (Harlan) received an intraperitoneal injection with 200µL of 2 x 10^6 HCT116^{luc} cells suspended in PBS. Tumor growth was monitored with intraperitoneal injections with D-luciferin reconstituted in PBS (1.5 mg in 100 µL; PerkinElmer), followed by bioluminescence imaging with an in vivo imaging system (IVIS Spectrum; Caliper Life Sciences). At day 14, all mice reached bioluminescent signals, indicating sufficient tumor growth, after which 100 µg of bevacizumab-800CW (n = 5), 100 µg of cetuximab-800CW (n = 5), 100 µg of human IgG-800CW (n = 2) or sodium chloride (n = 2) were injected in a total volume of 200 µL. Intravenous injection was performed via the penile vein under general anesthesia. The mice receiving IgG-800CW or sodium chloride served as negative controls. At day 3 after injection mice were euthanized by cervical dislocation and eight small intraperitoneal tumors (2-5 mm) were harvested for ex vivo colonoscopy purposes (2 per tracer). The remaining intraperitoneal tumors (varying in size between 2 and 5 mm) and mouse organs (liver, colon and muscle) were harvested for ex vivo analyses.

NIR fluorescence endoscopy platform

The NIR fluorescence endoscopy platform consists of a custom-made Micrendo fiber bundle containing 30,000 coherently arranged individual fibers (Schölly Fiberoptic GmbH). The imaging bundle conducts the images to the sensor module of a previously developed clinical prototype NIR camera system.[8,33] This camera system comprises of a color camera and a monochrome one, which operate in parallel for white-light and NIR fluorescence acquisition respectively. A beam splitter (T760lpxr, Chroma Technology) separates the color and NIR image components. Appropriate filtering is provided by a white light shortpass filter with a cut-off wavelength of 750 nm and a fluorescence emission bandpass filter with a central wavelength of 819 nm (bandwidth 44 nm) (THORLABS). Connection of the fiber bundle to the camera system is made feasible via a mechanical and focusing adapter, while a multi-branched fiber optic bundle (SEDI-ATI Fibres Optiques) realizes simultaneous white-light illumination and fluorescence excitation (laser at 750 nm) coupling. The performance of the clinical endoscopy platform, namely the characterization of the optical resolution and the sensitivity, was determined in the same manner as for the preclinical platform.[34]

Simulation of NIR molecular fluorescence endoscopy procedure

To simulate a clinical colonoscopy procedure, an 11 cm long human colon specimen was derived from a right hemicolectomy of a patient with colon cancer (requirement to obtain informed consent was waived by the Medical Ethical Committee Groningen, METC nr. 2013.446). Immediately after the surgical resection, the healthy part of the colon specimen was transported to the endoscopy suite. Two freshly resected HCT116^{luc} intraperitoneal tumors (2-5 mm in diameter) per tracer (bevacizumab-800CW, cetuximab-800CW, IgG-800CW or sodium chloride) were stitched onto the luminal side of the colon wall (Figure 1). Molecular fluorescence endoscopy was performed using a clinical video endoscope (Olympus Exera II GIF-180 series, Olympus), with the fiber bundle of the NIR fluorescence endoscopy platform inserted through the working channel. The images were displayed on two separate screens, one for the video endoscope derived images and the other for the composite images of the fiber bundle, combining color and fluorescence. A qualitative assessment of tumor visualization was made during endoscopy and video footage and photo material was collected.

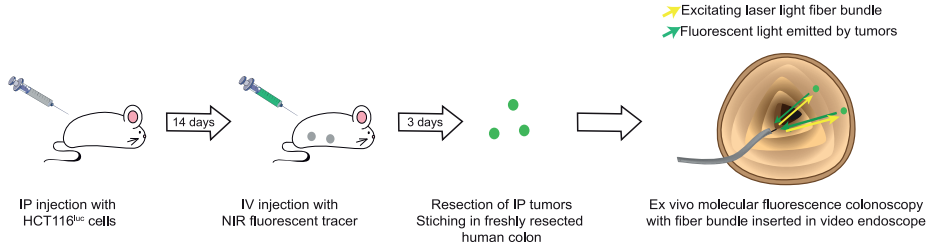

Figure 1. HCT116^{luc} tumor cells were intraperitoneal inoculated in athymic nude mice. After tumor establishment, targeted NIR fluorescent tracer (bevacizumab-800CW or cetuximab-800CW), non-targeted NIR fluorescent tracer (IgG-800CW), or sodium chloride was administered intravenously. Three days after administration, intraperitoneal tumor lesions (diameter, 2-5 mm) were harvested and stitched in a freshly resected human colon. Ex vivo molecular fluorescence colonoscopy was performed using a standard video endoscope, with the fiber bundle of NIR fluorescence endoscopy platform passed through the working channel.

Ex vivo analyses

To further validate the findings of the simulated endoscopy procedure, the remaining harvested HCT116^{luc} human xenograft tumors, mouse organs and a part of the human colon tissue were formalin-fixed and paraffin-embedded for microscopic analysis. To detect if 800 nm fluorescence signals were present, 4 µm slides were obtained, deparaffinized (10 minutes xylene), scanned on an Odyssey Infrared Imaging System (intensity 5; LI-COR Biosciences) and subsequently stained with hematoxylin and eosin. Hoechst staining (33258; Invitrogen) was used to visualize nuclei. Fluorescence microscopy was performed using a Leica DM6000B inverted wide-field microscope (63x

magnification, immersion oil), with a mercury short-arc reflector lamp (HXP-R120W/45C VIS), DFC365FX camera (Leica) and a filter set (49037ET; Chroma Technology). Images were processed with LAS-AF2 software (Leica Microsystems).

Statistical analysis

Statistical analysis was performed using IBM SPSS Statistics 20. Per tissue type, the difference in staining intensity between aberrant tissue and adjacent normal tissue was determined via non-parametric Mann-Whitney U testing. The correlation between histological stage of Lynch tissue (LGD adenomas, HGD adenomas and cancer tissue) and staining intensity (0-3) was tested using a Kruskal Wallis test, corrected for multiple testing. Data are presented using Prism (version 5; GraphPad Software) and Adobe Illustrator CS6.

RESULTS

High VEGFA expression in human colorectal lesions

Immunohistochemistry for VEGFA showed a homogeneous staining pattern within dysplastic and carcinomatous areas (Figure 2 and Supplemental Figure 1A). From normal colon crypts towards dysplastic and cancerous areas, a gradually increasing staining intensity was observed (Supplemental Figure 1B). Moderate to strong VEGFA expression was observed in 96% of Lynch LGD adenomas, 79% of Lynch HGD adenomas, 94% of Lynch colon cancer tissue and 94% of SSA/P. No significant differences in staining intensities could be observed between the different histological stages (LGD, HGD, carcinoma) of the LS samples. In addition, VEGFA demonstrated to be a relevant target for other polyps as well, showing a 94% VEGFA expression in HGD sporadic adenomas and 95% in HP lesions (Figure 3). For all adenomas, the VEGFA expression was significantly higher compared to the adjacent normal colonic crypts ($P < 0.001$), signifying the potential of this target for adenoma detection.

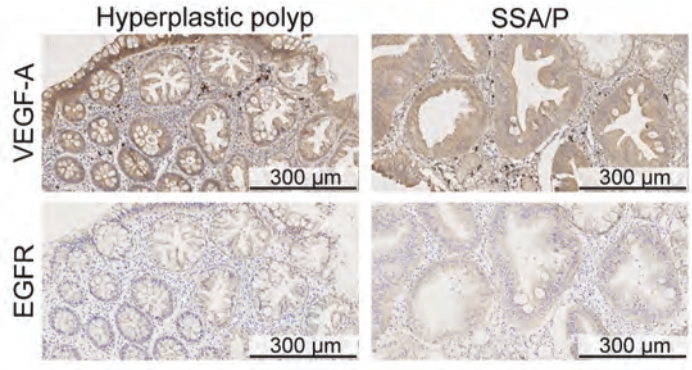

Figure 2. Representative immunohistochemistry staining of VEGFA and EGFR in 1 HP and 1 SSA/P. Both lesions were scored 3 (strong) for VEGFA and 2 (moderate) for EGFR.

The percentage of EGFR positive samples was lower for all tissue types: 52% of Lynch LGD adenomas, 51% of Lynch HGD adenomas, 68% of Lynch cancer samples, 52% of SSA/P lesions, 51% of sporadic HGD adenomas and 58% of HP lesions showed a positive receptor staining (Figure 3). In contrast to VEGFA, EGFR immunohistochemistry results showed a heterogeneous expression pattern throughout the neoplastic lesions, resulting in both EGFR-negative and EGFR-positive crypts within 1 adenoma (Figure 2 and Supplemental Figure 1A). The EGFR expression was significantly higher in neoplastic lesions than in the adjacent normal colon crypts ($P < 0.001$). A gradient of increased EGFR expression from normal towards dysplastic crypts was not observed.

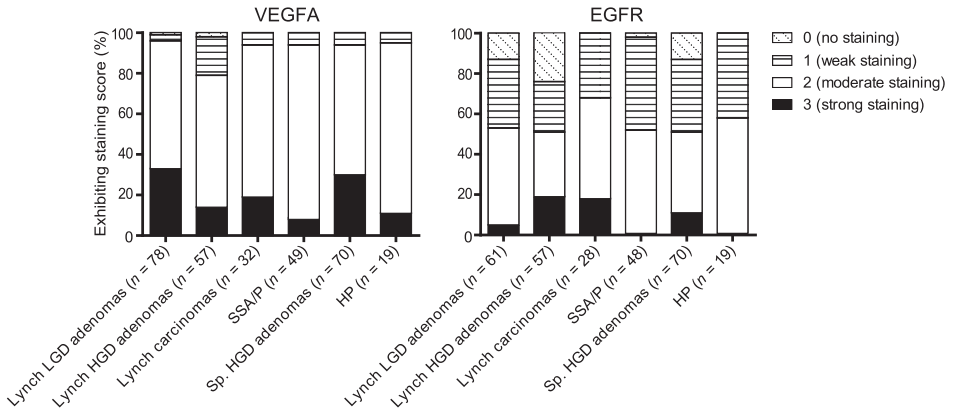

Figure 3. VEGFA and EGFR expression for colorectal adenomas with LGD of patients with LS, adenomas with HGD of patients with LS, carcinomas of patients with LS, SSA/P, sporadic (Sp.) adenomas with HGD, and HPs.

Performance of the NIR fluorescence endoscopy platform

The resolution of the fluorescence endoscopy platform was characterized by imaging the USAF 1951 resolution test chart with the system's color channel (Figure 4A). Here we can distinctly identify the vertical and horizontal lines in Element 3 of Group 1, which translates to a spatial resolution of 198.42 µm at a distance of 2 cm. The signal-to-noise ratios were determined for a dilution series of IRDye800CW with concentrations ranging between 26.05 µM and 1.55 pM (Figure 4B). Each subsequent dilution was obtained of a halved concentration of IRDye800CW dissolved in PBS. The detection limit was defined as the concentration where the signal is three times higher than the noise, which corresponds to a signal-to-noise ratio of 9.5 dB. The detection limit, calculated from the regression line, lies at a concentration of 19.80 nM.

Ex vivo colonoscopy procedure: real-time visualization of NIR fluorescent lesions

During the ex vivo colonoscopy procedure, the NIR fluorescence endoscopy platform exhibited sufficient sensitivity and resolution for the visualization of all small HCT116^{luc} tumors that were labeled with bevacizumab-800CW and cetuximab-800CW (Figure 5 and Supplemental Figure 2 and Supplemental Video 1). The endoscopist was able to instantly detect the specifically targeted tumors (2-5 mm) and differentiate these from the control tumors. White-light, fluorescence and composite images were displayed real-time and with a wide field of view. Fluorescence was also clearly visible when the fiber was retracted to a larger distance (~5 cm) of the fluorescent tumors. Control tumors from mice that were given IgG-800CW or sodium chloride showed negligible fluorescence signals and there was no interference of autofluorescence of the human colon tissue.

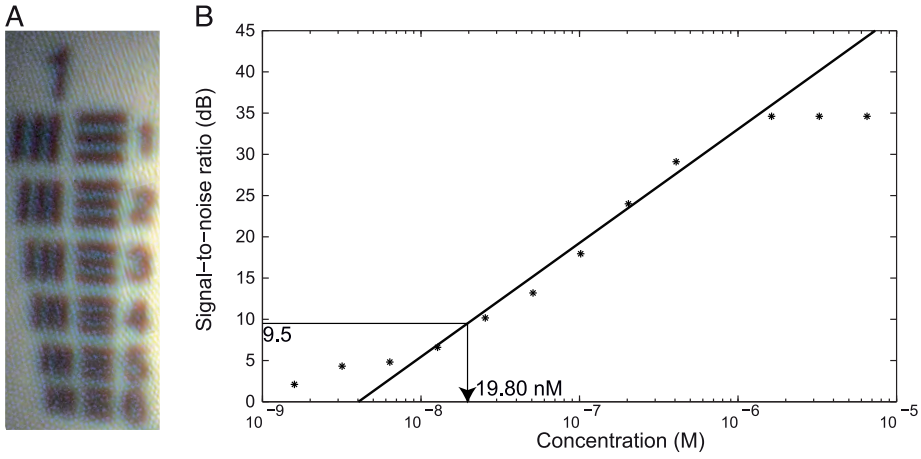

Figure 4. (**A**) Detail of USAF 1951 resolution target image, in which vertical and horizontal lines in element 3 of group 1 can be distinctly identified, which translates to a spatial resolution of 198.42 µm at a distance of 2 cm. (**B**) Signal-to-noise ratio over IRDye800CW concentration measured from the dilution series. Detection limit of 9.5 dB lies at concentration of 19.80 nM.

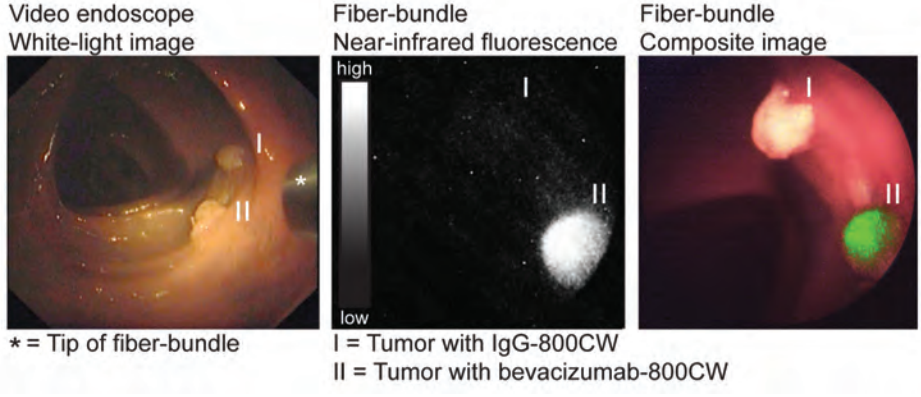

Figure 5. Images acquired during ex vivo molecular fluorescence colonoscopy of IgG-800CW (I) and bevacizumab-800CW (II) targeted tumors (3 x 3 mm in size). Endoscopy images were obtained with video endoscope and fiber bundle. White-light, fluorescence and composite images of fiber bundle were real-time-projected.

IRDye800CW-labeled tracers: ex vivo established target specificity

Odyssey imaging system and fluorescence microscopy

Ex vivo macroscopic NIR fluorescence imaging of the deparaffinized tissue slides revealed highly fluorescent tumors with clear tumor delineation (Figure 6B and Supplemental Figure 3B) for both bevacizumab-800CW and cetuximab-800CW. IgG-800CW and negative tumors showed low autofluorescence signals (Supplemental Figure 3E). NIR fluorescence was

low in the HE-confirmed necrotic areas of the tumors and healthy adjacent mouse tissue (Figure 6A and Supplemental Figures 3A and 3D, orange arrows). Fluorescence microscopy confirmed the localization of bevacizumab-800CW and cetuximab-800CW in the vital parts of the HCT116^{luc} tumors (Figure 6C and Supplemental Figure 3C). For bevacizumab-800CW, the fluorescent signal was mainly located in the tumor stroma and surrounding the tumor blood vessels, corresponding with our previous observations for ^{89}Zr- and ^{111}In-labeled bevacizumab.[29,35] A more homogeneous distribution was seen for cetuximab-800CW in the tumor lesions, with membranous and cytoplasmic localization of the NIR fluorescence signals.[36]

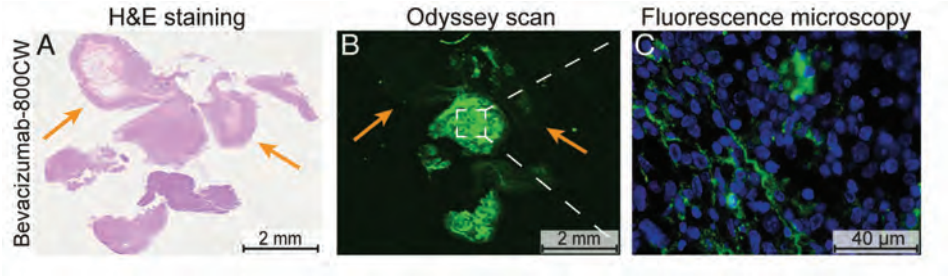

Figure 6. Hematoxylin and eosin (HE) staining (**A**), corresponding fluorescence image obtained with Odyssey Scanner (**B**), and corresponding fluorescence microscopy image (**C**) of HCT116^{luc} tumor targeted with bevacizumab-800CW. Odyssey scan shows clear fluorescence in all tumor tissue at 800nm, whereas uptake was negligible in histologic normal tissue (colon and muscle of mice, see orange arrows). Fluorescence microscopy showed bevacizumab-800CW to be mainly localized in stroma of tumors.

DISCUSSION

This study demonstrated, in a simulation model, that it is feasible to visualize colorectal lesion in real-time, using a novel fluorescence endoscopy platform combined with VEGFA- and EGFR-targeting NIR fluorescent tracers. Given the observed overall VEGFA overexpression in colorectal lesions, this target appears to be the most relevant for molecular colorectal screening purposes. Especially in colorectal lesions that are easily missed during endoscopy, such as SSA/P lesions and Lynch adenomas, VEGFA was highly overexpressed. The ability to visualize colon lesions in the simulation model used in this study, in combination with the good manufacturing practice production of 800CW-labelled antibodies, allows rapid translation of this technique towards the clinic.

To the best of our knowledge, no prior data are available on VEGFA expression in SSA/P or neoplastic lesions from high-risk patients, such as those with LS. We found a moderate to strong VEGFA expression in most SSA/P and Lynch adenomas. The high VEGFA expression in sporadic adenomas was in concordance with literature.[7,9] VEGFA expression was significantly higher in adenoma crypts than in adjacent normal colon crypts, which is a key requirement for successful visualization of target lesions by molecular imaging. Moreover, we observed a gradually increased staining intensity from normal colon crypts towards dysplastic and cancerous areas in many of the samples, which can be explained by the fact that VEGFA expression is regulated by several growth factors present in the microenvironment of premalignant and malignant lesions.[37]

In contrast, EGFR is overexpressed in only approximately 50% of all adenoma lesions, including those of LS patients, and was expressed more heterogeneously throughout the lesions. The observed EGFR expression is in line with previous findings in sporadic adenomas.[38] Therefore, VEGFA seems the most suitable target for screening purposes. In contrast, cetuximab-800CW may still be valuable in evaluating the EGFR expression status of an already identified lesion. In this setting, our approach could play an assisting role in molecular treatment decision-making processes, whereas EGFR-targeting therapeutics are currently being applied in colorectal carcinomas.

The use of a fiber bundle-based approach is relatively inexpensive and can easily be incorporated in standard clinical endoscopy procedures, because the fiber bundle fits through the working channel of a routine clinical video endoscope. Although the fiber images have a significant lower resolution compared to high-definition video endoscope images, the molecular-guided approach is sensitive and provides strong contrast between the NIR fluorescent-targeted lesions and the surrounding normal tissue. Because the images are in real time and with a wide field of view, this approach can assist in the screening of large surfaces, with the high-definition white-light endoscope providing morphological orientation while the fiber can support as a red-flag method.

The technique described in this study has several advantages when compared to other molecular-guided endoscopy approaches. First, confocal laser endomicroscopy, has shown promising results both preclinically and clinically, but has a limited field of view.[39-41] Therefore, confocal laser endomicroscopy is not suitable for screening purposes, as our technique is, but rather a tool for lesion characterization. Second, other research groups have described topical spraying of tracer products to improve detection of dysplastic regions, but this is most attractive for relatively small areas and therefore not practical in the colon.[42-44] An approach using intravenously injected tracers can circumvent these issues. Finally, the use of a fluorescent tracer emitting in the NIR light spectrum likely improves specificity and tumor-to-background signals when compared to fluorescent dyes of the visible spectrum, because autofluorescence is negligible in the NIR range (Supplemental Figures 4 and 5).[45]

Previously, in an HCT116^{luc} xenograft model, a tumor-to-background ratio of 3.2 ± 0.9 was seen for bevacizumab-800CW and 5.7 ± 3.0 for cetuximab-800CW 3 days after injection (Supplemental Figure 4). However, the commonly used tumor-to-background ratio cannot be reliable evaluated in mice, because the tracers are targeted toward human VEGFA and EGFR. As a consequence, the used artificial model, targeted intraperitoneal xenograft tumors stitched in a human colon specimen, demonstrates the practical feasibility of the proposed technique, but no statements can be made regarding specific tumor or adenoma accumulation in comparison to uptake in healthy human colon tissue. However, clinical studies evaluating the use of ^{89}Zr-labeled bevacizumab in breast and kidney cancer patients did not show aspecific accumulation of the tracer in the colon.[46] Also, the significant higher VEGFA expression in colorectal adenomas compared to adjacent normal tissue implies that bevacizumab-800CW could be a promising tracer from a diagnostic point of view. The initiated clinical studies (NCT01972373 and NCT02113202) should give insight into the in vivo sensitivity and specificity of bevacizumab-800CW towards VEGFA in different colorectal lesions, as well as the safety and optimal tracer dose to perform the molecular-guided endoscopy procedure.

CONCLUSION

Molecular-guided NIR fluorescence endoscopy is a promising technique that allows real-time, wide-field visualization of both tissue morphology and molecular characteristics. In this study we demonstrated that our good manufacturing practice-produced NIR tracers, targeting VEGFA and EGFR, could be clearly visualized during a simulated molecular-guided NIR fluorescence endoscopy procedure. On the basis of the expression profiles observed in a large set of different colorectal samples, including those in high-risk patients with SSA/P and LS, VEGFA seems a suitable target for molecular-guided endoscopic screening purposes. Clinical studies have been initiated and are currently recruiting patients to validate the potential of this technology during colonoscopy (clinicaltrials.gov: NCT01972373 and NCT02113202).

Disclosures: The research leading to these results was partially supported by the European Union under the grant agreement ERC-OA-2012-PoC-324627 and partially supported by the Dutch Cancer Society, RUG 2012-5416.

SUPPLEMENTAL FIGURES

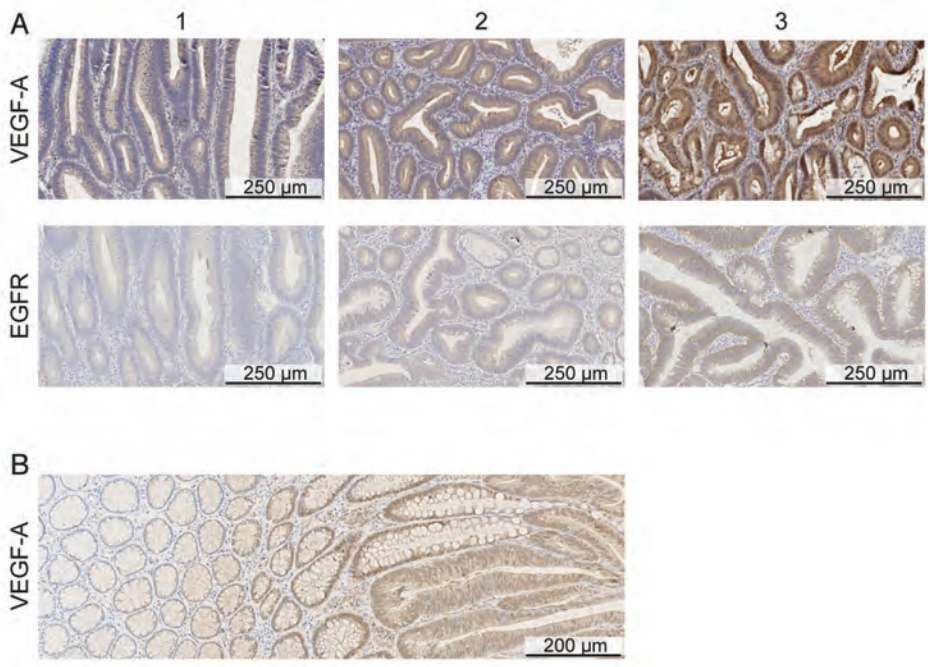

Supplemental Figure 1. (**A**) Representative immunohistochemical staining (intensity 1-3) of VEGFA and EGFR in sporadic colorectal adenomas. (**B**) Notice a clear gradient in staining intensity of VEGFA from normal colon crypts towards dysplastic area.

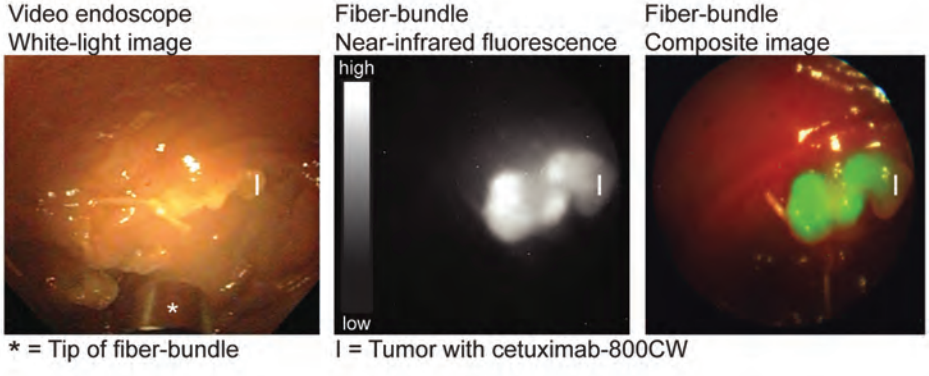

Supplemental Figure 2. Images acquired during ex vivo molecular fluorescence colonoscopy of a cetuximab-800CW targeted tumor (2 x 4 mm). Endoscopy images were obtained with video endoscope and fiber bundle. The fluorescence and composite fiber bundle images were in real time projected.

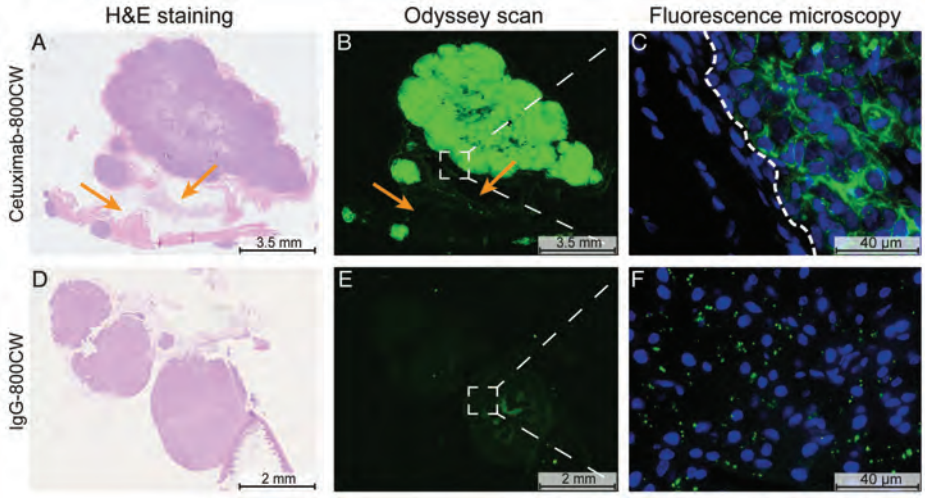

Supplemental Figure 3. Hematoxylin and eosin (HE) staining (**A, D**) and corresponding fluorescence images obtained with Odyssey scanner (**B, E**) and fluorescence microscopy (**C, F**) of an HCT116^{luc} tumor-positive mouse lymph node targeted with cetuximab-800CW (**A-C**) and an intraperitoneal HCT116^{luc} tumor targeted with IgG-800CW (**D-F**). Cetuximab-800CW showed clear fluorescence in all tumor tissue at 800nm with Odyssey scanner, while uptake of IgG-800CW was negligible. Cetuximab-800CW was almost absent in necrotic tumor areas and in histologic normal tissue (orange arrows, colon and muscle of mice). Fluorescence microscopy demonstrated tumor cell membrane binding and uptake in tumor cytoplasm for cetuximab-800CW. White dashed line = tumor border.

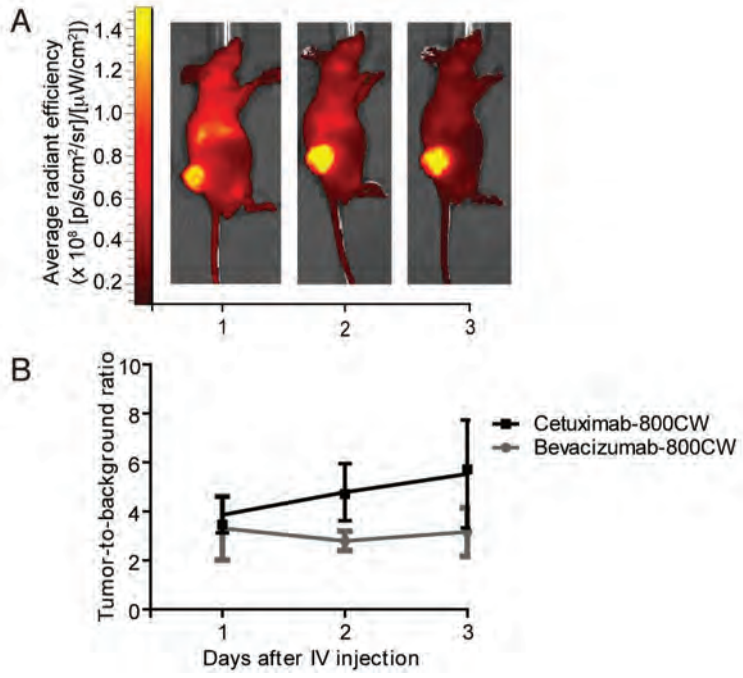

Supplemental Figure 4. (**A**) Representative near-infrared (NIR) fluorescence images of an athymic nude mouse with a subcutaneous HCT-116^{luc} tumor. Imaging performed with IVIS spectrum (Caliper Life Sciences) (ex745/em800, binning small, f/2, exposure time 20 seconds); 1, 2 and 3 days after intravenous injection with cetuximab-800CW. (**B**) The tumor-to-background ratios of in total 6 athymic nude mice with a subcutaneous HCT116^{luc} tumor, measured with the IVIS spectrum 1, 2 and 3 days after intravenous injection of 100 µg bevacizumab-800CW (*n* = 3) or cetuximab-800CW (*n* = 3). The Living Image software (V4.3.1; Caliper Life Sciences) was used for data acquisition and analysis. Two regions of interests (ROI) of equivalent areas were drawn; the first corresponding to the tumor and the second corresponding to an area of normal tissue in the abdominal region. The tumor-to-background ratios were calculated by dividing the mean fluorescence intensity of the tumor ROI by the mean fluorescence intensity from the background ROI. The tumor-to-background ratio 3 days after injection is for bevacizumab-800CW 3.2 ± 0.9 and for cetuximab-800CW 5.7 ± 3.0. In contrast to bevacizumab-800CW, the uptake of cetuximab-800CW increased in time in the HCT116^{luc} subcutaneous model.

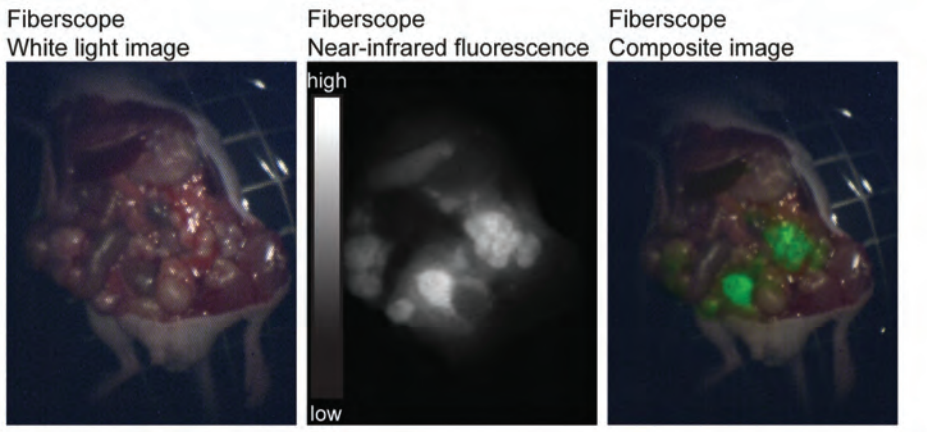

Supplemental Figure 5. White-light, fluorescence and composite image of the opened abdomen of an athymic nude mouse with intraperitoneal HCT-116^{luc} tumors, three days after intravenous injection with cetuximab-800CW. The NIR fluorescence matches all the intra-abdominal tumor masses present. Background fluorescence is negligible. Images were acquired with the preclinical platform, consisting of a fiberscope (GIF-XQ20, Olympus, Center Valley, US-PA), as described previously.[34] Detailed distribution of bevacizumab and cetuximab labeled with IRDye800CW and Zr^{89} has been previously described.[29,35]

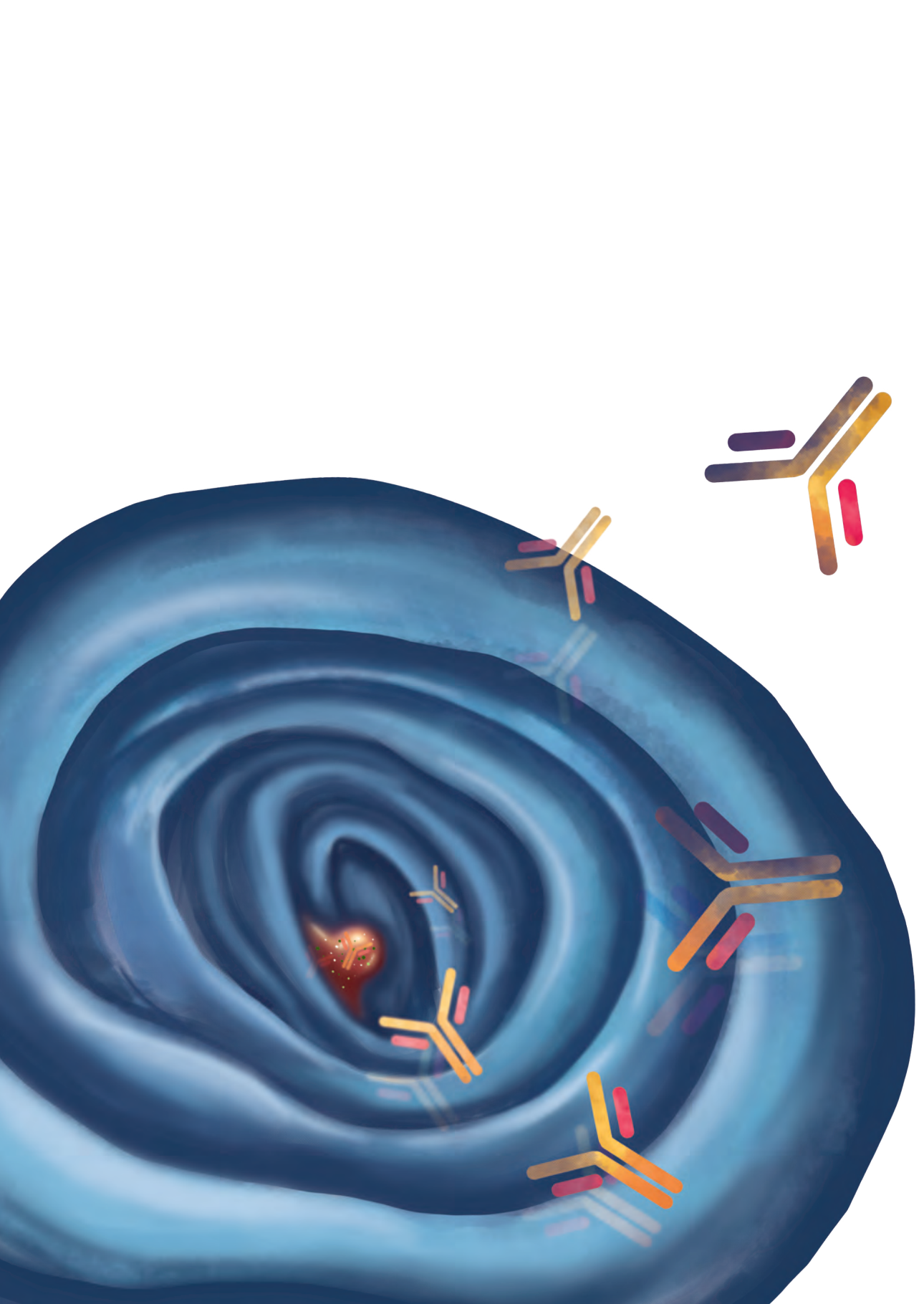

Chapter 3

Potential red-flag identification of colorectal adenomas with wide-field molecular fluorescence endoscopy

Theranostics, 2018; 8(6): 1458-1467

Jolien JJ Tjalma[1*], Elmire Hartmans[1*], Matthijs D Linssen[1,2], P Beatriz Garcia Allende[3], Marjory Koller[4], Annelies Jorritsma-Smit[2], Mariana e Silva de Oliveira Nery[1], Sjoerd G Elias[5], Arend Karrenbeld[6], Elisabeth GE de Vries[7], Jan H Kleibeuker[1], Gooitzen M van Dam[4,8], Dominic J Robinson[9], Vasilis Ntziachristos[3], Wouter B Nagengast[1]

[*]Both contributed equally

[1]Department of Gastroenterology and Hepatology, [2]Department of Clinical Pharmacy and Pharmacology, [4]Department of Surgery, [6]Department of Pathology, [7]Department of Medical Oncology, [8]Department of Nuclear Medicine and Molecular Imaging and Intensive Care - University of Groningen, University Medical Center Groningen, Groningen, The Netherlands. [3]Institute for Biological and Medical Imaging - Technical University of Munich and Helmholtz Center Munich, Munich, Germany. [5]Julius Center for Health Sciences and Primary Care - University Medical Center Utrecht, Utrecht, The Netherlands. [9]Otolaryngology and Head & Neck Surgery - Erasmus MC, University Medical Center Rotterdam, Rotterdam, The Netherlands.

ABSTRACT

Introduction: Adenoma miss rates in colonoscopy are unacceptably high, especially for sessile serrated adenomas / polyps (SSA/P) and in high-risk populations, such as patients with Lynch syndrome. Detection rates may be improved by molecular fluorescence endoscopy (MFE), which allows morphological visualization of lesions with high-definition white-light imaging as well as fluorescence-guided identification of lesions with a specific molecular marker. In a clinical proof-of-principal study, we investigated MFE for colorectal adenoma detection, using a fluorescently labelled antibody (bevacizumab-800CW) against vascular endothelial growth factor A (VEGFA), which is highly upregulated in colorectal adenomas.

Methods: Patients with familial adenomatous polyposis (n = 17), received an intravenous injection with 4.5, 10 or 25 mg of bevacizumab-800CW. 3 days later, they received NIR-MFE.

Results: VEGFA-targeted NIR-MFE detected colorectal adenomas at all doses. Best results were achieved in the highest (25 mg) cohort, which even detected small adenomas (<3 mm). Spectroscopy analyses of freshly excised specimen demonstrated the highest adenoma-to-normal ratio of 1.84 for the 25 mg cohort, with a calculated median tracer concentration in adenomas of 0.64 mmol/mL. Ex vivo signal analyses demonstrated NIR fluorescence within the dysplastic areas of the adenomas.

Conclusion: These results suggest that NIR-MFE is clinically feasible as a real-time, red-flag technique for detection of colorectal adenomas.

INTRODUCTION

Colorectal cancer (CRC) is the second most common cancer worldwide, accounting for 8% of all cancer related deaths.[10] Of all CRCs, approximately 60% develops via the well-known adenoma-carcinoma sequence, one-third via the alternative serrated pathway and a small portion from Lynch syndrome (LS).[11] White-light endoscopy is considered the gold standard for detection and removal of colorectal lesions, to prevent CRC development. However, detection of small adenomas (<5 mm) and sessile serrated adenomas / polyps (SSA/P) is difficult since conventional endoscopy relies upon aspecific morphological tissue signatures and thus on the experience of the endoscopist. As a result, the reported adenoma detection miss rate for the general population is relatively high (27%).[12] For patients with LS, adenoma miss rates are even up to 55%. In this high-risk population small adenomas are more common, and these often already contain high-grade dysplasia (HGD) since the adenoma-carcinoma sequence is known to be accelerated.[3,5] Therefore, missed lesions can rapidly progress to cancer which results in an unacceptable cumulative cancer risk of up to 35% at the age of 60, despite intensive screening programs. This underscores the necessity of improving endoscopic detection strategies.[4]

One way to improve endoscopic lesion identification is the incorporation of wide-field molecular fluorescence endoscopy (MFE). MFE visualizes lesions based on their biological properties rather than their morphology; it uses exogenous fluorescent tracers that bind to specific proteins, thereby fluorescently highlighting the tissue of interest as a red-flag for the endoscopist. A recently published study showed a higher adenoma detection rate with MFE following an intravenous injected anti-cMET tracer using an old white-light fiber endoscope for both fluorescence and white-light imaging, which hampers clinical translation.[45] Moreover, MFE in the visible spectrum limits the sensitivity and contrast available to the fluorescence method. Separation of weak fluorescence signals in the presence of strong white-light illumination requires several orders of magnitude spectral separation through filters, which also reduces significantly the transmission of fluorescence signals. Moreover, the visible light exhibits strong autofluorescence, reducing contrast.

Therefore, we labelled the monoclonal antibody bevacizumab with a near-infrared (NIR) fluorescent dye, IRDye 800CW, and used a NIR-MFE platform that enables concurrent fluorescence and high-definition white-light imaging. Bevacizumab-800CW binds vascular endothelial growth factor A (VEGFA), which is present in all stages of colorectal neoplasms, including low grade dysplastic (LGD) adenomas and in up to 90% of difficult to detect but clinically important sessile serrated adenomas/polyps (SSAPs).[7,47] We evaluated VEGFA-targeted NIR-MFE for adenoma detection in a dose-escalation study, performed in patients with familial adenomatous polyposis (FAP) who have a high probability of occurrence of

colorectal adenomas. We choose FAP patients due to the abundance of colorectal adenomas in this condition, to enable adequate evaluation of the different dose steps. To validate our in vivo NIR-MFE findings, we quantified the fluorescence of excised colorectal tissue by correcting for the influence of tissue optical properties using Multi-Diameter Single Fiber Reflectance and Single Fiber Fluorescence (MDSFR/SFF) spectroscopy (Figure 1).

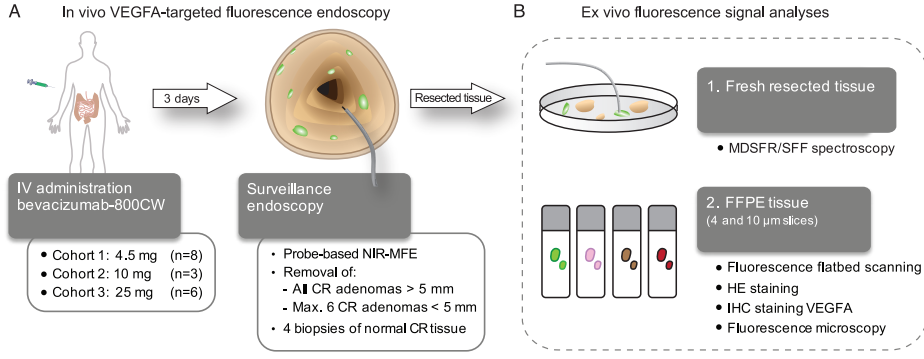

Figure 1. Study design. (**A**) Intravenous administration of the fluorescent tracer bevacizumab-800CW, three days later followed by VEGFA-targeted fluorescence endoscopy. (**B**) Ex vivo fluorescent signal analyses: 1) quantification of the fluorescence signals with MDSFR/SFF spectroscopy, performed on fresh resected tissue, and 2) qualitative evaluation of tracer distribution performed on FFPE tissue.

MATERIALS AND METHODS

Study population and design

Patients with FAP that were 18 years of age or older, and scheduled for surveillance endoscopy at the University Medical Center Groningen (UMCG), were invited to participate in the study. Trial enrolment required FAP to be genetically proven or clinically diagnosed by >100 colorectal adenomatous polyps at earlier endoscopy. Patients with a *MutY* human homolog gene (*MUTHY*) mutation or who had a proctocolectomy were excluded. The study protocol was approved by the Medical Ethics Committee of the UMCG. All patients gave their written informed consent for participation in the study before inclusion. The study was registered with ClinicalTrials.gov (NCT02113202).

This non-randomized, non-blinded, single center proof-of-principle study consisted of three tracer-dose cohorts: 4.5, 10 and 25 mg of bevacizumab-800CW (Figure 1A).[48] These tracer dosages are low compared to the therapeutic dose of bevacizumab (5-10 mg/kg).[49] Three days after intravenous tracer injection, patients underwent surveillance endoscopy with a clinical video endoscope followed by NIR-MFE to visualize fluorescent signals. Afterwards, we validated the observed fluorescence by ex vivo signal quantification on fresh resected tissue with MDSFR/SFF spectroscopy. Additionally, to specify tracer distribution and enable correlation to histopathology, we performed NIR-fluorescence flatbed scanning, fluorescence microscopy and VEGFA immunohistochemistry (IHC) on formalin-fixed, paraffin-embedded (FFPE) tissue (Figure 1B).

In the 4.5 mg cohort, 6 FAP patients with adenomas were included. The interim analysis incorporated in our study protocol allowed for a tracer dose escalation if the 4.5 mg tracer dose appeared suboptimal. As a result, 3 patients were included in the subsequent dose cohorts (10 and 25 mg); the best-performing tracer-dose cohort (25 mg) was expanded to 6 FAP patients in total. All observed adverse events were noted until 72 h after intravenous tracer injection. This period was chosen as bevacizumab-800CW had shown a good safety profile in previous studies in patients with primary breast cancer and peritoneal carcinomatosis of colorectal origin.[50]

NIR-MFE procedure

Endoscopy was performed after standard bowel preparation, optionally under conscious sedation with midazolam and fentanyl. All procedures were performed with a routine clinical high-definition video endoscope, which is standard of care during surveillance endoscopies (CF-H180AL/I or GIF-H180J; EVIS EXERA II; Olympus Corporation, Tokyo, Japan). White light was provided by a standard xenon light source (CLV-180 Evis Exera II; Olympus Corporation), in which a short pass filter was installed (<750 nm, E700SP-2P; Chroma, Bellows Falls, VT, USA).

When the caecum or ileorectal anastomosis was reached, the NIR-MFE probe was introduced in the working channel of the video endoscope (Supplemental Figure 1A).[34] During withdrawal, adenomas were concurrently visualized with both the video endoscope and the NIR-MFE probe. The NIR-MFE images (color, fluorescence and overlay) were displayed on a separate monitor (Figure 2). Subsequently, all large adenomas (≥5 mm; standard clinical care) and a maximum of six small adenomas (<3 mm) were excised. Additionally, four biopsies of normal appearing colorectal mucosa were taken for research purposes only. See supplementary materials for detailed information on tracer production and the technical background of the NIR-MFE system.

MDSFR/SFF spectroscopy

The freshly resected adenomas and normal mucosa biopsies were placed on ice with the mucosal side upwards. Directly after the endoscopy the MDSFR/SFF spectroscopy probe was placed on top of the fresh tissue for quantitative measurements of NIR fluorescence. This device gains two reflectance spectra via two different optical fibers and subsequently one raw fluorescence spectrum (Supplemental Figures 1B and 2). From the reflectance spectra, the scattering and absorption coefficients were determined, which were used to determine the intrinsic fluorescence. The intrinsic fluorescence was afterwards used to calculate the actual bevacizumab-800CW concentration present in the fresh resected tissue. Subsequently, the majority of resected adenomas and normal tissue biopsies were formalin-fixed and paraffin-embedded (FFPE), while some were snap-frozen in liquid nitrogen and stored at -80 °C. In one patient (25 mg cohort) no quantitative measurements could be collected due to a technical malfunction of the MDSFR/SFF spectroscopy device. See supplementary materials for more detailed information on the MDSFR/SFF spectroscopy device, spectral fitting and determination of the local bevacizumab-800CW concentration.

Histological fluorescence mapping

Per FFPE tissue block, one 10 mm section and three 4 mm sections were sliced, mounted on silane-coated slides and dried overnight at 37 °C. The 10 mm FFPE tissue sections were deparaffinized (10 min xylene) and imaged with the NIR fluorescence flatbed. Afterwards, the 10 mm tissue sections and the subsequent 4 mm tissue sections were stained with hematoxylin and eosin (HE). The HE slides were digitalized by the Nanozoomer 2.0-HT slide scanner (Hamamatsu) and viewed with use of NanoZoomer Digital Pathology viewer software (Hamamatsu). Blinded for the fluorescence signals and under supervision of an experienced gastrointestinal pathologist (A.K.), different tissue areas were selected: low-grade dysplasia (LGD) areas within the adenoma, normal adjacent tissue within the adenoma section and normal colon crypts within the normal tissue biopsies. Afterwards, these areas were superimposed on the NIR fluorescence Odyssey images. Ex vivo analyses of the snap frozen tissue was shown to be unreliable, as bevacizumab-800CW signals diminished during thawing of the samples.

Fluorescence microscopy

For fluorescence microscopy, 4 mm FFPE tissue sections were deparaffinized, rehydrated and stained with Hoechst to visualize nuclei (33258; Invitrogen, Thermo Fisher Scientific). Fluorescence microscopy was performed using an inverted wide-field microscope (63-100x magnification, immersion oil; DMI6000B, Leica Biosystems GmbH, Nussloch, Germany), with a LED light source that is able to excite up to 900 nm (X-Cite 200DC; Excelitas Technologies, Waltham, MA, USA), a monochrome camera also sensitive in the NIR range (1.4M Pixel CCD, DFC365FX; Leica Biosystems GmbH) and an adapted filter set (two band-pass filters 850-90m-2p and a long-pass emission filter HQ800795LP; Chroma Technology). All tissue slides were assessed using the same settings to enable visual comparison. Following acquisition, the images were processed with LAS-AF2 software (Leica Microsystems).

Immunohistochemical analysis of VEGFA expression

We previously demonstrated the relevance of VEGFA as a target for colorectal neoplasia.[47] To determine if the prior VEGFA results hold true for our current patient population, we immunostained all FFPE colorectal tissue collected during this study (polyclonal rabbit anti-human VEGFA, RB9031 1:300; Thermo Fisher Scientific, Waltham, Ma, USA). To ascertain specific binding of the anti-VEGFA antibody, a positive tissue control and a negative IgG control were included. Dysplastic crypts, normal crypts within the adenoma section and normal mucosa derived from the biopsies were scored separately for their staining intensity (0-3 scale) and the percentage of cells stained. This visual scoring was performed by two separate observers (E.H. and J.J.J.T.). Subsequently, H-scores were generated (continuous scale: 0-300) by combining the evaluated intensity and the corresponding percentage of cells stained.[51] See Supplemental Material and Methods for detailed description of the IHC methods and H-score formula.

Statistics

For statistical analysis of the MDSFR/SFF spectroscopy and flatbed scanning results IBM SPSS 22.0 (IBM Corporation, Armonk, NY, USA) and GraphPad Prism 5.0 (GraphPad Software Inc, La Jolla, CA, USA) were used. A two-tailed *t* test, Mann-Whitney U test or Kruskal-Wallis test was used, according to sample-size and distribution. *P*-values <0.05 were considered statistically significant.

RESULTS

Near-infrared molecular fluorescence endoscopy (NIR-MFE)

In total, 17 patients participated in the study (Table 1). Eight patients received 4.5 mg, three patients 10 mg and another six patients 25 mg bevacizumab-800CW intravenously. No tracer-related adverse events were observed (0/17). Two patients in the 4.5 mg cohort did not have any lesions at endoscopy and were excluded from further analyses.

Table 1. Patient and adenoma characteristics

Number of patients, *n* (%)	17	
Complete colon *in situ*	5	(29.4%)
Ileorectal anastomosis	12	(70.6%)
Sex, *n* (%)		
Male	5	(29.4%)
Female	12	(70.6%)
Age, in years		
Median (range)	42	(20-65)
Total number of observed adenomas per patient, *n* (%)		
0	2[A]	(11.8%)
1-5	4	(23.5%)
6-20	10	(58.8%)
>20	1	(5.9%)
Histology of resected lesions, *n* (%)	51	(100%)
LGD adenomatous polyp	50	(98%)
HGD adenomatous polyp	1	(2%)

[A] The two patients without any adenomas at endoscopy were left out of the ex vivo fluorescent signal analyses.

For all 3 tracer-dose cohorts, VEGFA-targeted NIR-MFE fluorescently visualized all adenomas identified with white-light high-definition inspection concurrently (sensitivity 100%) (Figure 2).

All larger adenomas (≥5 mm) showed sufficient fluorescent contrast for direct in vivo detection at video rate (10 frames per second). Small adenomas (<3 mm) were clearly fluorescent in the 25 mg bevacizumab-800CW dose cohort enabling real-time visualization of all adenomas at video rate (Figure 3 and Supplemental Video 1 and 2), though the fluorescence signal varied in the 4.5 mg bevacizumab-800CW dose cohort hampering real-time detection in this lowest dosing cohort. Moreover, we were even able to detect small adenomas (<3 mm) present in the background of bright fluorescent adenomas (Figure 3 – *second row*). Normal colorectal mucosa showed only minimal fluorescence, resulting in a clear delineation of

the fluorescent adenomas. We did not observe false positives in this feasibility study since normal-appearing colorectal tissue during high-definition inspection showed no significant NIR fluorescence with NIR-MFE. In a few cases, where bowel preparation was insufficient, we did observe a detectable amount of NIR fluorescence in remaining feces. This NIR fluorescence is probably due to the native fluorescence present in fecal remnants, most likely originating from unrefined chlorophyll-containing ingredients like spinach.[52]

MDSFR/SFF spectroscopy: fluorescent signal quantification

In total, the intrinsic fluorescence intensities were determined of 39 adenomas and 27 normal colon biopsies. This revealed a median adenoma-to-normal ratio for the 25 mg dose cohort of 1.84. There was a 40% increase of intrinsic fluorescence of adenomas for the 25 mg cohort compared to the 10 mg cohort (Figure 4). In contrast, the intrinsic fluorescence intensities of normal tissue remained constant for all dose cohorts. The correction factor to correct the raw fluorescence for tissue optical properties ranged between 1.65 and 3.57. Tissue absorption, mainly by hemoglobin, was the main actor in this, while differences in scattering made a smaller but still significant contribution. The resulting intrinsic fluorescence spectra resembled the emission spectrum of bevacizumab-800CW in PBS, which confirms that the measured fluorescent signals are tracer derived (Supplemental Figure 2).

Based on the intrinsic fluorescence determined with MDSFR/SFF spectroscopy, an estimation could be made of the tracer concentration present in the tissue. This showed a median bevacizumab-800CW concentration 0.48 mmol/mL in the 10 mg adenomas, compared to 0.69 mmol/mL in the 25 mg adenomas. The median tracer concentration in normal tissue was 0.38 mmol/mL (10 mg cohort) vs 0.37 mmol/mL (25 mg cohort). These quantified measurements confirm our in vivo NIR-MFE results, in which we observed improved fluorescence visualization of adenomas in the 25 mg dose cohort.

Figure 2. Wide-field VEGFA-targeted fluorescence endoscopy. Three adenomas per tracer-dose cohort. The clinical white-light images gained with a high-definition video endoscope (*first column*), combined with representative overlay images (*second column*) and NIR fluorescence images (*third column*) gained with the NIR fiber bundle. The overlay images are automatically generated by the software, showing the highest fluorescence intensities in bright green and the very low fluorescence intensities as absent. The fluorescence images were taken with different exposure times. ►

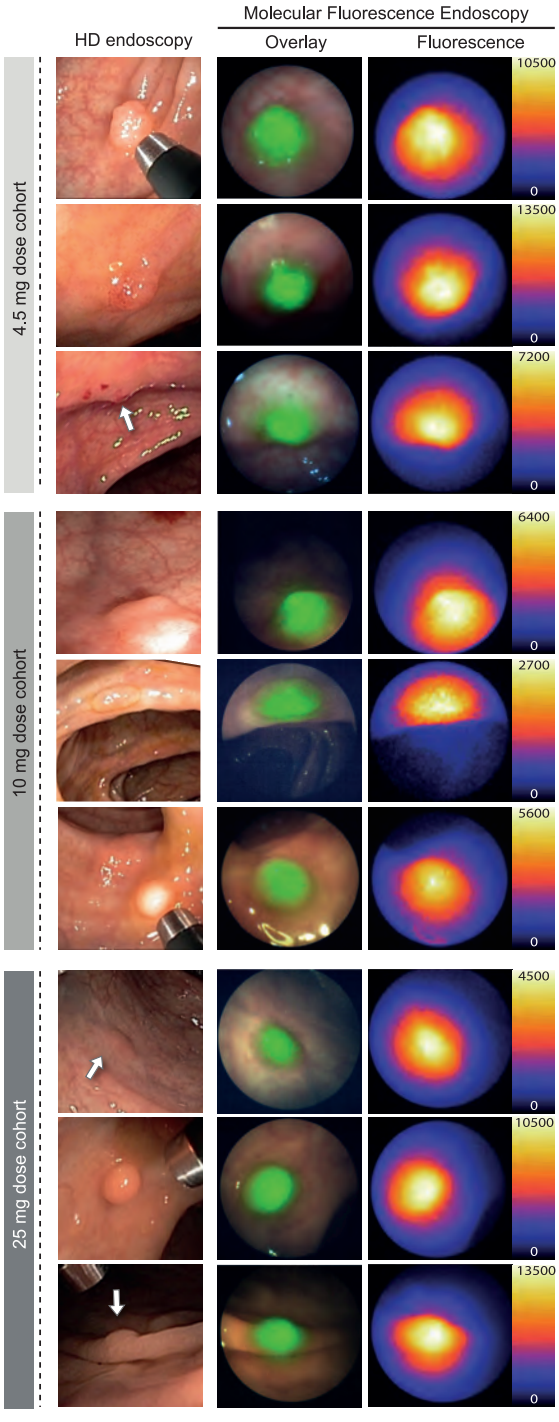
Molecular Fluorescence Endoscopy
HD endoscopy
Overlay
Fluorescence
4.5 mg dose cohort
10 mg dose cohort
25 mg dose cohort
10500
0
13500
0
7200
0
6400
0
2700
0
5600
0
4500
0
10500
0
13500
0

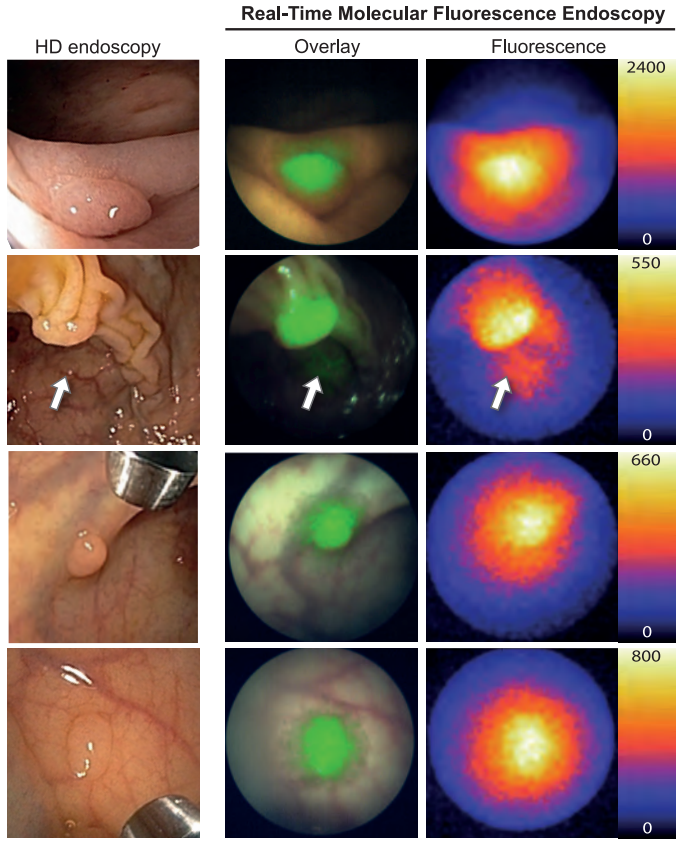

Figure 3. Real-time in vivo NIR-MFE images. Adenomas from the 25 mg dose cohort demonstrating the ability of the NIR-MFE system to visualize small and flat adenomas at video frame rate (10 frames per second). The white arrow indicates a second small adenoma. The overlay images are automatically generated by the software, showing the highest fluorescence intensities in bright green and the very low fluorescence intensities as absent.

Ex vivo tissue analyses: fluorescent signal qualification.

In total, 49 FFPE adenomas (4.5 mg *n* = 21; 10 mg *n* = 11; 25 mg *n* = 17) and 24 normal tissue biopsies (4.5 mg *n* = 8; 10 mg *n* = 4; 25 mg *n* = 12) were analyzed. Of the 49 FFPE adenomas, 48 contained LGD and one showed HGD. Within the adenomas, the tracer was mainly localized in the dysplastic areas compared to the normal tissue within the adenoma section (Figure 5A). NIR fluorescence was localized between the adenomatous crypts, within the stromal tissue (Figure 5B). Normal colorectal tissue within the sections of adenomas and in the normal mucosa biopsies both showed negligible NIR fluorescence (Figure 5C).

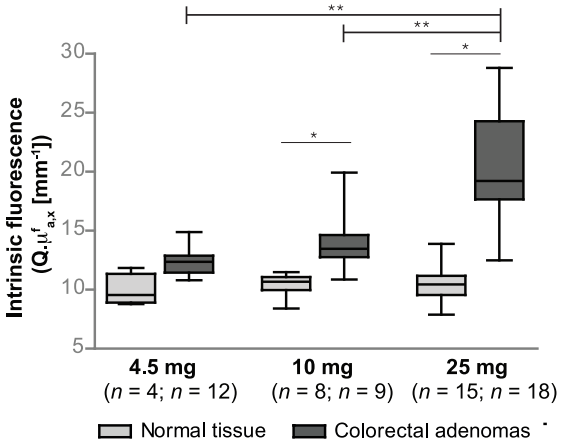

Figure 4. Fluorescence quantification by MDSFR/SFF spectroscopy. Box plot (median, 10-90 percentile) showing the intrinsic fluorescence ($Q.\mu^{f}_{a,x}$) per bevacizumab-800CW tracer-dose cohort for both LGD containing adenomas and the normal colorectal tissue (biopsies). For all dose cohorts, a significant difference in fluorescence intensity can be observed between the benign and premalignant tissue, which increases with increasing tracer dosages. Note that the fluorescence in the normal tissue stays constant in the 10 and 25 mg cohorts, regardless of the tracer dose used. The median adenoma-to-normal ratio of intrinsic fluorescence was 1.84 for the 25 mg cohort. * = $P < 0.05$; ** = $P < 0.001$.

Target-validation: VEGFA immunohistochemistry

We observed a clear difference in VEGFA expression levels between the dysplastic crypts and the normal colon crypts (Figure 6). All adenoma samples expressed VEGFA, of which 96% showed a high staining intensity and 4% an intermediate staining (mean H-score: 286). In contrast, the normal colon tissue showed a lower mean intermediate H-score, namely 123 for normal crypts within the adenoma sections, versus 174 for biopsies of normal mucosa.

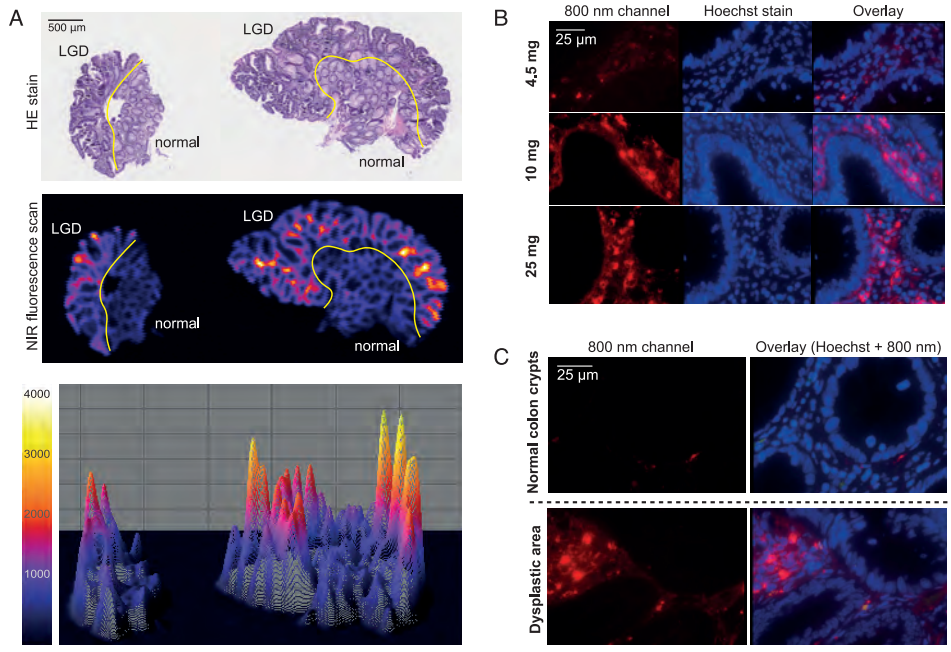

Figure 5. Ex vivo fluorescent signal analyses. (**A**) Representative NIR fluorescence flatbed scan of a fluorescent adenoma (10 mg dose cohort), containing both dysplasia and normal colon crypts in the same section (HE staining). The fluorescence scan and interactive surface plot demonstrate that the fluorescence intensities are the highest at the sites of dysplasia, a phenomenon that was observed in all three tracer-dose cohorts. (**B**) 3 representative fluorescence microscopy images, demonstrating an observable difference in fluorescence intensities between the three dose cohorts: the 4.5 mg cohort shows a lower signal in the 800 nm channel, compared to the 2 higher dose cohorts. Fluorescence microscopy did not show a clear difference between the 2 highest dose cohorts (10 mg vs 25 mg). The left column represents the fluorescence of the tracer (800 nm channel), the middle column shows Hoechst staining of the nuclei and third column displays an overlay of the previous two channels. (**C**) Representative microscopy images of 1 adenoma of the 25 mg dose cohort, showing a clear difference in NIR fluorescent signal between areas containing dysplasia and areas containing normal colon crypts; the areas can be distinguished based on the appearance of the crypts, since stacking of the nuclei is typical for dysplasia.

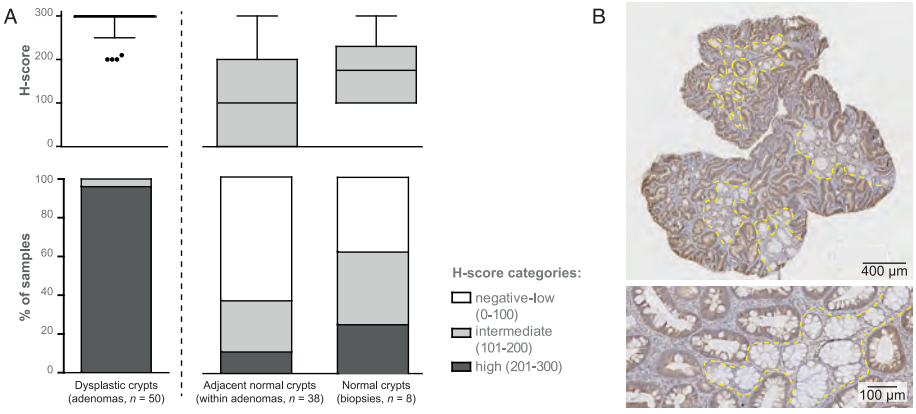

Figure 6. VEGFA immunohistochemistry results. (**A**) Box plot (median, 10-90 percentile) and bar graph, both presenting VEGFA IHC results (H-score) of adenomatous colorectal polyps (LGD and normal crypts) and normal colorectal biopsies; a clear difference in H-score can be observed between the adenomatous crypts and the normal surrounding tissue and normal biopsies. (**B**) Representative images illustrating the clear difference in VEGFA staining intensities (brown) between dysplastic and normal crypts (areas within dashed yellow lines display normal crypts).

DISCUSSION

In this study, we demonstrated that colorectal adenomas can be identified with VEGFA-targeted NIR-MFE with concurrent high-definition white-light endoscopy. Based on the real-time observations in FAP patients, we identified 25 mg bevacizumab-800CW as the best-performing tracer dose. With this dose, we were able to identify all small (<5 mm) adenomas at video-rate, even if those were situated in the background of the image, behind a larger fluorescent adenoma. Detailed ex vivo fluorescent signal analyses with MDSFR/SFF spectroscopy and microscopy confirmed the specificity of the obtained results. As such, we believe that VEGFA-targeted NIR-MFE has the potential to improve real-time, wide-field colorectal adenoma identification. With this first feasibility and dose-finding study, the way is cleared to start a study in high risk patients, to objectify its red-flag ability in identifying and improving detection of flat and depressed adenomas.

Previously described targeted MFE approaches have been mainly restricted to preclinical application; they described the potential of a wide range of molecular targets, fluorescent labels and administration routes, as well as the use of both wide-field macroscopic and microscopic imaging systems.[40,53] Clinically, different approaches have been tried to obtain wide-field MFE for colorectal adenoma detection. Mayinger showed in a feasibility study improved detection of small adenomas after topical application of hexaminolevulinate (HAL). Since HAL absorption time is around 60 min, tracer administration is challenging. In this study the tracer was administered via an enema which might hamper detection of right-sided lesions.[54] A fluorescent tracer targeting cMET showed promising positive results, though fluorescence imaging was compared with outdated fiber white-light detection which does therefore not reflect current clinical practice.[45] Joshi *et al*. nicely demonstrated specific binding, using ex vivo quantification and correction, of a small fluorescent peptide after topical administration on SSA/Ps in the proximal colon identified with high-definition white-light endoscopy.[55] Future studies applying the tracer before identification of the lesions should elucidate the real-time identification potential of promising tracers as red-flag technique.

Our MFE approach is distinctive from former approaches since we used a tracer in the NIR range to optimally provide *instant* red-flag identification of colorectal lesions. The fluorescence and white-light images could concurrently be captured, as bevacizumab-800CW emits fluorescent light outside of the visible light spectrum; in the NIR light spectrum. Hence, the fluorescent signals could instantly be superimposed on the white-light images shown to the endoscopist. The clear discrimination between colorectal adenomas and normal tissue is a result of the accumulation of the intravenous injected bevacizumab-800CW specifically in colorectal adenomas, and the negligible attribution

of human autofluorescence in the NIR light spectrum. Future software improvements could automatically alert the endoscopist and thereby even reduce the human factor which might improve adenoma detection rates.

Most likely the optimal tracer dose used during NIR-MFE will have to be determined per tracer, organ of interest and indication. The aim of this study was to identify the best dose of intravenous bevacizumab-800CW for colorectal adenoma identification purposes. In cancer lesions it is thought that, due to the enhanced permeability and retention (EPR) effect, antibodies will accumulate easily, even when only a microdose of tracer is used.[56] However, in case of precancerous lesions, such as adenomatous polyps in which vascular hyperpermeability is not yet present, a higher tracer dose may be required to ensure sufficient fluorescent signal strength.

To identify the optimal dose, adequate fluorescent signal quantification is essential since it validates the observed in vivo fluorescent signals. The background tissue optical properties, i.e., absorption and scattering, make quantitative measurements on in vivo NIR-MFE images complicated. MDSFR/SFF spectroscopy can correct raw fluorescent signals for the influence of the local tissue optical properties and was previously validated in silico and in optical phantoms, and has been used in in vivo pre-clinical models.[13,57-59] The spectroscopy results showed that an adenoma-to-normal tracer concentration ratio of 1.84 was sufficient to gain real-time visualization of adenomas (25 mg dose cohort). As this ratio is based on actual quantification using spectroscopy, it is not comparable to the usual adenoma-to-normal ratios given in other studies, only obtained by comparing contrast in reflectance images, as is signified by the clear contrast in our in vivo images. The applied bevacizumab dose of 25 mg is still far below the conventional therapeutic dose of 5-10 mg/kg and did not show any side-effects.[49] In addition, we subsequently calculated the actual bevacizumab-800CW concentration in the tissue with the assumption that the in silico measured fluorescence quantum yield and extinction coefficient of bevacizumab-800CW are representative for the in vivo conditions.

Although our results are promising, our proof-of-principle study has some limitations. First, as the lesions were concurrently detected by white-light endoscopy and NIR-MFE, this study cannot address the effect of NIR-MFE on improving the adenoma detection rate. Secondly, FAP patients are not an ideal patient population for evaluating adenoma detection miss rates, since they are known to have multiple areas with aberrant crypt foci, and most patients have an ileorectal anastomosis. Nevertheless, we deliberately performed this proof-of-principle study in FAP patients to ensure sufficient adenoma numbers to identify the optimal tracer dose, despite the limited number of available patients. Twenty-five mg bevaciumab-800CW may well be universally used to detect the important SSA/P and high-risk Lynch lesions,

since we previously showed 94% overexpression of VEGFA in sporadic adenomas (with similar etiology as adenomas of FAP patients), and a comparable 95% in SSA/P and 79-96% overexpression in LS patients.[47]

In conclusion, this study demonstrates that VEGFA-targeted NIR-MFE is a promising optical molecular red-flag imaging approach for colorectal adenoma detection: our novel probe-based NIR-MFE approach meets the current clinical standards since it provides real-time molecular guidance, and thus functional information, without interfering with the regular morphological information of high-definition white-light endoscopy. Following intravenous administration of 25 mg of bevacizumab-800CW, NIR-MFE highlighted very small dysplastic adenomas with high in vivo fluorescent contrast at video-rate, which was confirmed by MDSFR/SFF spectroscopy. Future studies are required to determine the effect of NIR-MFE using 25 mg of bevacizumab-800CW on improving the adenoma detection rate of flat and depressed adenomas compared to white-light endoscopy, and thereby the clinical benefit for patients at high risk of developing colorectal cancer, for example patients with Lynch syndrome.

Acknowledgments: This work was in part supported by the Dutch Cancer Society (personal grant W.B.N., RUG 2012-5416), Center for Translational Molecular Medicine (project MAMMOTH 03O-201), Royal Netherlands Academy of Arts and Sciences (KNAW, professorship to E.G.E.d.V.), ERC advanced grant OnQview and unrestricted research grants from SurgVision B.V. and Boston Scientific.

Competing interest: G.M.v.D. and W.B.N. received an unrestricted research grant made available to the institution for the development of optical molecular imaging from SurgVision BV (Groningen, The Netherlands). G.M.v.D. and V.N. are members of the scientific advisory board of SurgVision BV. Other authors declare no competing financial interests.

SUPPLEMENTAL MATERIALS AND METHODS

NIR fluorescent tracer: bevacizumab-800CW

Tracer production and administration

Clinical grade bevacizumab-800CW was produced at the University Medical Centre Groningen (UMCG, Groningen, The Netherlands), according to good manufacturing practice (GMP) guidelines.[48] The labelling of the monoclonal antibody bevacizumab (Avastin, Roche, Hertfordshire, United Kingdom) with the near infrared (NIR) fluorophore IRDye 800CW (IRDye800CW-NHS ester; LI-COR Biosciences, Lincoln, NE, USA) was performed in a 4:1 or 2:1 dye-to-protein [D:P] molar ratio in a phosphate-buffered saline (PBS, pH 8.5) solution (Supplemental Table 1). The D:P molar ratio was lowered from 4:1 to 2:1 to guarantee stability of tracer compound. The lower ratio was administered in the 10 mg and 25 mg groups.[30,48,60]

Supplemental Table 1. Tracer production characteristics.

Dose group	D:P[A]	Labelling efficiency (%)	Theoretical D:P
4.5 mg	4:1	80 %	3.20:1
10 and 25 mg	2:1	83.4 %	1.67:1

[A]Dye-to-protein molar labelling ratio

After conjugation, the product was purified by buffer exchange, formulated, passed over a sterile 0.2 µm filter and filled into injection vials (1 mg/mL). During and after production, quality control was performed to assess identity, chemical quality, chemical purity and biological activity of the tracer. Endotoxin levels and bioburden were assessed in accordance with the European Pharmacopoeia 8.0. Labelling efficiency, theoretical D:P molar ratio, quality and purity were determined by a validated size-exclusion high-performance liquid chromatography (SE-HPLC) method (Supplemental Table 1). Bevacizumab-800CW was infused intravenously (infusion rate 75 mL/h) three days before the surveillance endoscopy. This time interval was chosen based on experience with ^{89}Zr-bevacizumab PET-scans in renal cell cancer patients.[46] Patients were observed during 1 h, with close monitoring of blood pressure, pulse and temperature. Based on the toxicity study of cetuximab-800CW in cynomolgus macaques, which showed increased QTc time, and in-human results regarding elevated levels of aspartate aminotransferase (AST), patients included in the 10 and 25 mg dose groups also received an ECG and baseline routine blood levels (full blood count, serum creatinine, liver enzymes, magnesium, calcium and ß-HCG in women of childbearing potential), prior to infusion of the tracer.[32,61]

Near-infrared molecular fluorescence endoscopy (NIR-MFE)

Probe-based NIR-MFE system

The NIR-MFE system (SurgVision, Groningen, The Netherlands) is developed in such a way that it can be easily incorporated in clinical endoscopy procedures. It is a probe-based system, making use of a custom-made Micrendo fiber bundle, containing 30,000 coherently-arranged individual fibers (Schölly Fiberoptic GmbH, Denzlingen, Germany). The fiber bundle has a field of view of 85° and a diameter of 2.4 mm, making it suitable for insertion through the working channel of a commercially available video endoscope. White-light illumination of the fiber was provided by a LED light source (KL 2500 LED, Schott AG, Mainz, Germany) with a shortpass dichroic filter (E700SP-2P; Chroma, Bellows Falls, VT, USA). Fluorescence excitation was achieved by two class IIIb lasers (750nm, max. power 300 mW; BWF1, B&WTEK, Newark, DE, USA). Both light sources are coupled to the fiber bundle via a multi-branched fibre-optic bundle (SEDI-ATI Fibres Optiques, Courcouronnes, France). The fibre bundle itself is connected to a mechanical and focusing adapter (Schölly Fiberoptic, Denzlingen, Germany). This connection conducts the fiber images via a dichroic mirror and bandpass filter (819 nm, ±44 nm, Semrock inc, Rochester, NY, USA) to a charge-coupled digital (EM-CCD) camera, sensitive for NIR light, and a separate camera for color detection (Supplemental Figure 1A). The cameras are installed at a movable arm with two swivel joints. The software generates an overlay image of both cameras and projects this real-time during the procedure on a second screen. In this way, fluorescence molecular guidance is realized with little impact to current workflow of clinical endoscopy procedures. The performance of the NIR-MFE system was characterized as described before, with a spatial resolution of 198.42 µm at a distance of 2 cm, and a detection limit at a concentration of 19.80 nM.[47]

MDSFR/SFF spectroscopy

Instrument description

The MDSFR/SFF spectroscopy device uses an optical fiber probe, consisting of two adjacent optical fibers with different diameters (0.4 and 0.8 mm). White-light from a tungsten halogen lamp (HL-2000-FHSA; Ocean Optics, Duiven, The Netherlands), was directed trough these fibers, for the sequential acquisition of a reflection measurements using two spectrometers (SD-2000; Ocean Optics). Subsequently, 775 nm laser light was directed through the 0.8 mm fiber to obtain a fluorescence spectrum using a separate sensitive spectrometer (QE-65000; Ocean Optics). A long pass filter (785 nm) was used to block scattered excitation light (Supplemental Figure 1B). The tip of the probe has an angle of 15° to minimize internal specular reflections. Spectrometers and light sources were controlled by a custom made LabView program (LabView 7.1; National Instruments Corporation, Austin, TX, USA) as described previously.[13,62] Before every procedure, a calibration was performed to correct for fiber alignment and transmission efficiency, using a 1.3% intralipid phantom.[63] An ex vivo MDSFR/SFF spectroscopy measurement took approximately 3 sec per location.

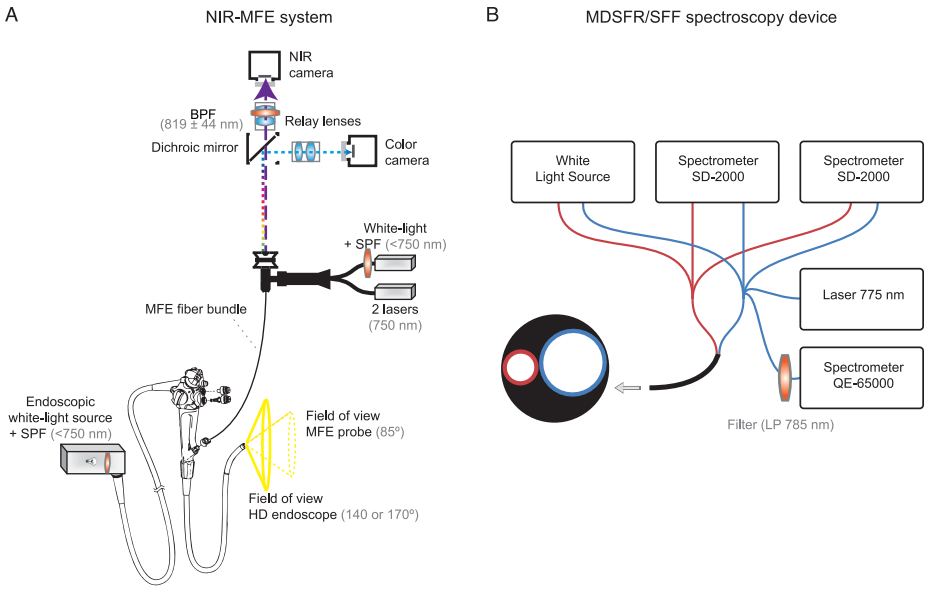

Supplemental Figure 1. Schematic representation of the NIR-MFE system and the MDSFR/SFF spectroscopy device. (**A**) Fluorescence excitation is provided by two laser sources (750 nm); fluorescence and white-light detection is simultaneously derived by a charge-coupled digital (EM-CCD) NIR camera and a color camera. The optical fiber bundle is inserted through the working channel of a clinical high-definition video-endoscope, creating wide-field MFE. (**B**) Reflection spectra are measured by the two bundled optical fibers (Ø 0.4 and 0.8 mm), followed by one fluorescence spectrum measurement via the largest fiber (Ø 0.8 mm, 775 nm fluorescence excitation light).

Spectral fitting and the determination of intrinsic fluorescence

The MDSFR/SFF spectroscopy device was used to quantify the NIR fluorescent signals of the freshly resected colorectal tissue. The approach is based on the measurement of multiple, in the case of the current study, two single fiber reflectance spectra. From these spectra the wavelength dependence of the reduced scattering coefficient m'_s and the parameter γ (l), which is related to the angular distribution of light scattering in tissue, is determined. It is then possible to determine the absorption coefficient m_a (l) of the tissue based on a set of specific chromophores: bilirubin, oxygenated hemoglobin and deoxygenated hemoglobin. By combining the measurements of the tissue optical properties (m'_s and m_a) at both the fluorescence excitation wavelength (775 nm) and the fluorescence emission wavelength range of the tracer (780 – 850 nm) with a measurement of the raw fluorescence from the tissue, it is possible to recover the intrinsic fluorescence $Q.\mu^f_{a,x}$. The intrinsic fluorescence $Q.\mu^f_{a,x}$ is defined as the product of the quantum efficiency across the emission spectrum,

Q[-], where Q is the fluorescence quantum yield of IRDye 800CW and m_{af} [mm^{-1}] is the tracer absorption coefficient at the excitation wavelength. The methodology of the determination of the correction factor has been previously described in detail.[13] Quantitative fluorescence spectra were fitted as a linear combination of background autofluorescence basis spectra, determined from adenomatous polyps of a FAP patient that had not received the fluorescent tracer and average basis spectra formed from 2 patients that received the highest dose of tracer (25 mg). To overcome the problem of noise in the fluorescence signal between 780 and 790 nm (where our detection filter blocks both scattered excitation and fluorescence light) and to satisfy our intention to include the whole of the emission spectrum in the calculation of $Q.\mu^{f}_{a,x}$, we utilized a spectrum of bevacizumab-800CW in PBS to fit spectral data below 790 nm.

Supplemental Figure 2A and 2B show the measured reflection spectra of two LGD adenomas, both derived from the 25 mg dose cohort. In adenoma A the estimated optical properties are m'_s (at 775 nm) = 2.53 mm^{-1} and m_a (at 775 nm) = 0.0004 mm^{-1} and of adenoma B m'_s (at 775 nm) = 0.61 mm^{-1} and m_a (at 775 nm) = 0.0087 mm^{-1}. The characteristic wavelength dips around 400 nm and between 500-600 nm are caused by the strong absorbance properties of hemoglobin. When comparing the reflectance spectra of both adenomas, note the significantly higher reflectance over the whole wavelength range in adenoma A (0.8 mm diameter fiber; blue). This is because this polyp contained significantly less hemoglobin compared to adenoma B, which clearly shows the characteristic double absorption dip centered on 575 nm due to oxygenated hemoglobin. The measured raw fluorescence was subsequently corrected for the estimated optical properties to yield the intrinsic fluorescence $Q.\mu^{f}_{a,x}$. Adenoma B needed a higher correction factor to yield the intrinsic fluorescence because of the higher light absorption by oxygenated hemoglobin. That the tissue optical properties differed over all tissue samples, is reflected in the correction factor that ranged from 1.65 to 3.57. Supplemental Figure 2C shows a representative example of an intrinsic fluorescence spectrum (and its fit in blue). The in vivo fluorescence spectrum closely resembles the fluorescence spectrum of bevacizumab-800CW in PBS (data not shown).

Determination of bevacizumab-800CW concentration

In the calculations of in-tissue bevacizumab-800CW concentration, we assumed that all IRDye800CW fluorescence originated of intact bevacizumab-800CW. With knowledge of the intrinsic fluorescence, $Q.\mu^{f}_{a,x}$, it is interesting to determine an estimation of the actual concentration of bevacizumab-800CW present in the tissue. To estimate its extinction at 775 nm, we first acquired an absorption spectrum of bevacizumab-800CW (D:P molar ratio of 2:1, in 50 mM phosphate NaCl) (Supplemental Figure 2D). From this, we calculated the extinction coefficient of bevacizumab-800CW at 775 nm of approximately 311,204 M^{-1} mm^{-1}. The best available data in the literature suggests that fluorescence quantum yield

of IRDye800CW is 0.09.[64] When we assume that the extinction coefficient as well as the fluorescence quantum yield are representative for the in vivo conditions, we can calculate the tissue tracer concentration by dividing the intrinsic fluorescence $Q.\mu^{f}_{a,x}$ by the extinction coefficient and the fluorescence quantum yield. Under these assumptions, the median measured bevacizumab-800CW concentration in LGD adenomas after the intravenous administration of 25 mg was 0.69 mmol mL^{-1}.

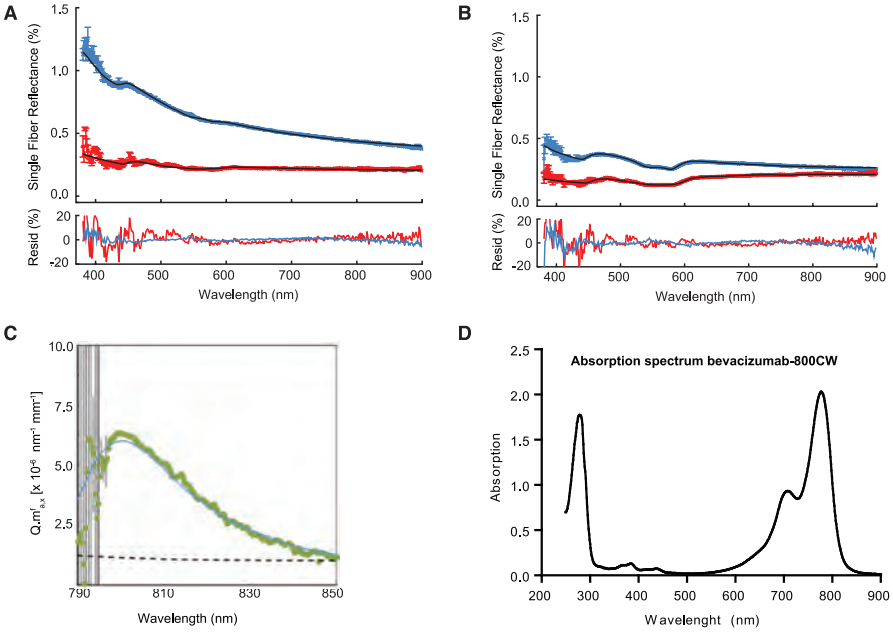

Supplemental Figure 2. MDSFR/SFF spectroscopy. (**A-B**) Two examples of MDSFR spectra measured for two resected colorectal adenomas with LGD. The percentage of reflected light is plotted against wavelength, blue for the large fiber (Ø 0.8 mm) and red for the small fiber (Ø 0.4 mm) plus standard deviations. The larger fiber measurement always shows a higher reflectance compared to the smaller fiber due to the larger collection area. Underneath, the corresponding residual lines are plotted to show the difference between the mathematical fit and the actual data. Both fibers show a higher percentage of noise in the lower and higher wavelengths. (**C**) A representative corrected SFF spectrum of an adenoma from the 25 mg cohort depicted in green. The measured fluorescence is here corrected for the optical properties (tissue absorbance and scattering) calculated from the measured MDSFR spectra. The large error bars around 790 nm are due to the filters applied to block the excitation light. This green spectrum resembles the fluorescence spectrum of bevacizumab-800CW in PBS, which confirms that the measured fluorescent signals are tracer derived. The blue line is the mathematical fit to the data. (**D**) The absorption spectrum of bevacizumab-800CW dissolved in a 50 mM fosfate NaCl solution. A protein peak is detected 280 nm and the bevacizumab-800CW absorption peak at 775 nm. This spectrum was used to calculate the absorption coefficient at 775 nm.

Ex vivo signal analyses

NIR fluorescence flatbed scanner

The Odyssey CLx imaging system (LI-COR Biotechnology, Lincoln, NE, USA) is a NIR fluorescence flatbed scanner. It contains a solid-state laser diode to excite at 785 nm and silicon avalanche photodiodes to detect at 800 nm, creating high quality and resolution NIR fluorescence images (laser intensity set at 6; spatial resolution of 21 µm, focus 0 mm, scanning speed 5 cm/s).

Immunohistochemical analysis of VEGFA expression

At start, 4 µm FFPE tissue sections were deparaffinized and rehydrated. Heat-induced antigen retrieval was performed with citrate buffer (10mM, pH 6.0; 15 min microwave), followed by endogenous peroxidase blocking with 1.5 mL 30% hydrogen peroxide in 48.5 mL PBS (30 min). After PBS washing steps, the sections were incubated overnight at 4°C with polyclonal rabbit anti-human VEGFA (RB9031; Thermo Fisher Scientific, Waltham, MA, USA; 0.2 µg/mL, dissolved 1:300 in PBS with 1% bovine serum albumin (BSA)). Tissue was stained using goat-anti-rabbit-HRP IgG (DAKO, Glostrup, Denmark; 1:50 in PBS, 1% BSA, 1 % antibody serum) for 30 min at room temperature, followed by rabbit-anti-goat-HRP (DAKO; 1:50 in PBS, 1% BSA, 1% antibody serum). Visualization took place with diaminobenzidine (DAB) for 10 min. Finally, the sections were counterstained with Mayer hematoxylin, dehydrated and mounted with a glass cover slip. Dysplastic crypts, normal crypts in the adenoma sections and biopsy derived normal mucosa were scored separately for their staining intensity (0-3 scale) and the percentage of cells stained. This visual scoring was performed by two observers (J.J.J.T. and E.H.). Subsequently, H-scores were generated (continuous scale: 0-300) by combining the evaluated intensity and the corresponding percentage of cells stained (formula used: *1x (percentage of cells weakly stained [1+] + 2x (percentage of cells moderately stained [2+]) + 3x (percentage of cells strongly stained [3+])*, creating expression categories representative for overall protein expression per tissue type (0-100, negative/low; 101-200, intermediate; 201-300, high).[51]

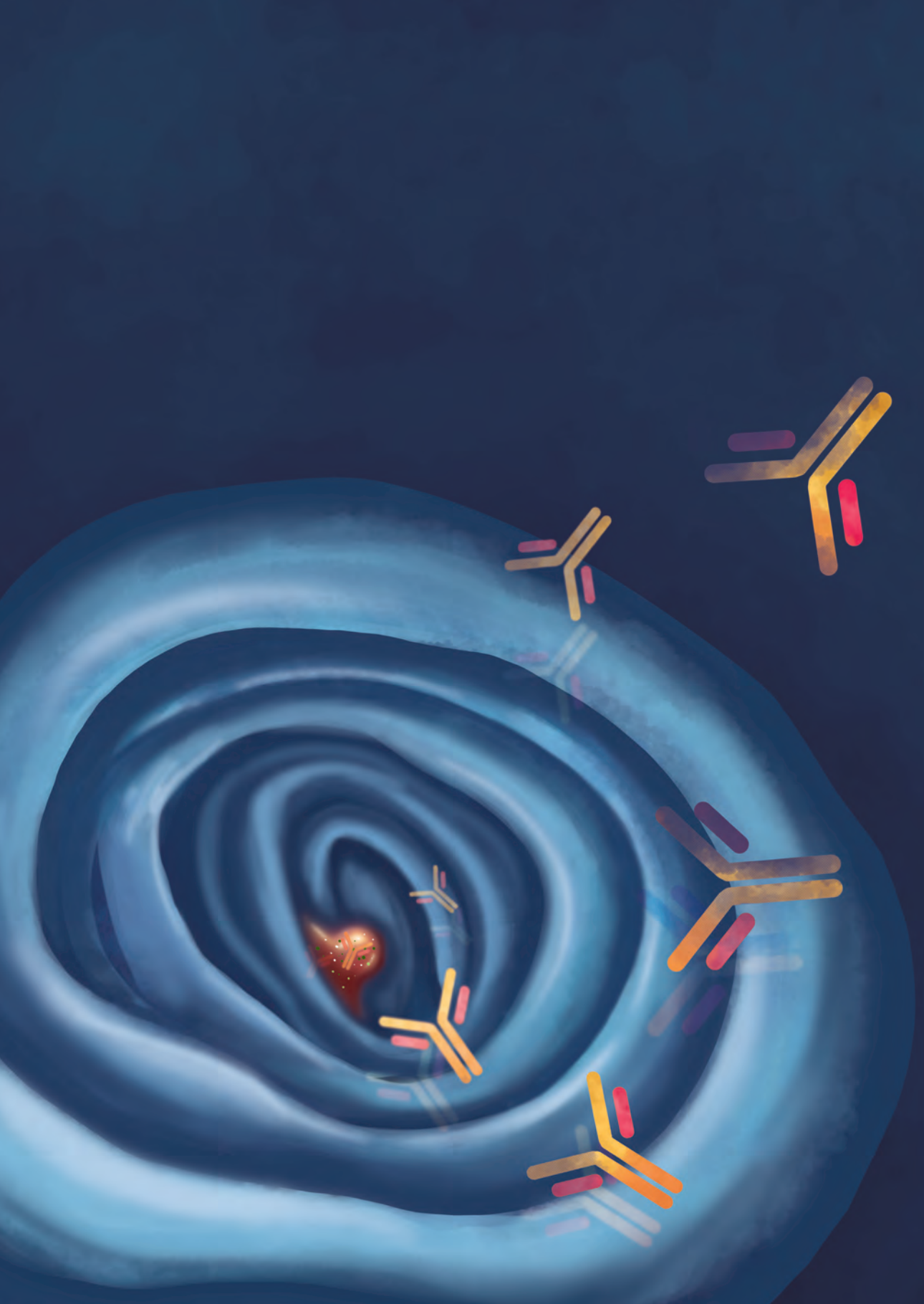



Part II

Imaging in patients with locally advanced rectal cancer

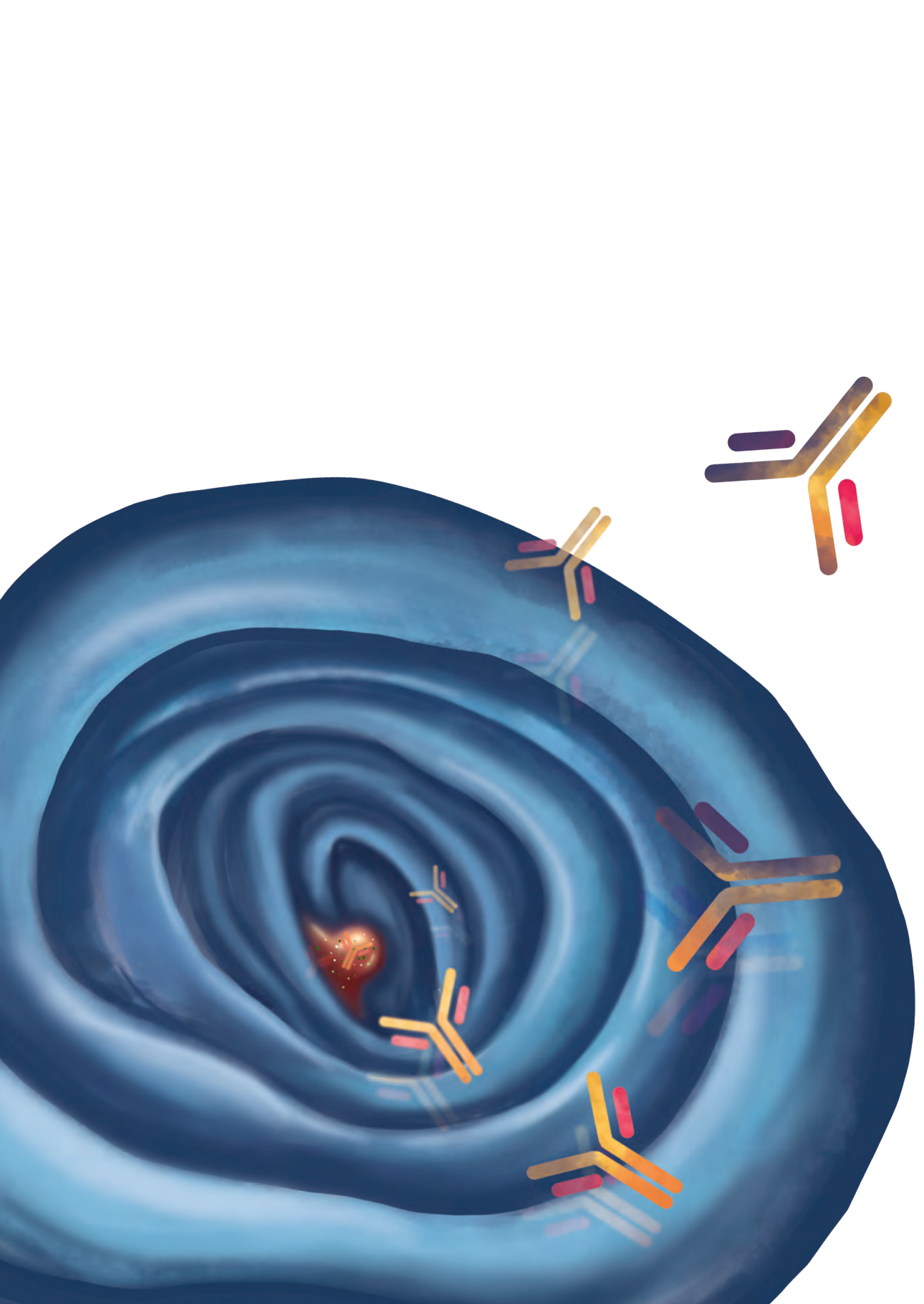

Chapter 4

Consequence of restaging after neoadjuvant treatment for locally advanced rectal cancer

Annals of Surgical Oncology, 2015; 22(2): 552-556

Kees Bisschop[1], Jolien JJ Tjalma[2], Geke AP Hospers[1], Dick van Geldere[3], Jan Willem B de Groot[4], Erwin M Wiegman[5], Miranda van 't Veer-ten Kate[6], Miek G Havenith[7], Juda Vecht[8], Jannet C Beukema[9], Gürsah Kats-Ugurlu[10], Shekar VK Mahesh[11], Boudewijn van Etten[12], Klaas Havenga[12], Hans GM Burgerhof[13], Derk Jan A de Groot[1], Wouter H de Vos tot Nederveen Cappel[8].

[1]Department of Medical Oncology, [2]Department of Gastroenterology and Hepatology, [9]Department of Radiation Oncology, [10]Department of Pathology, [11]Department of Radiology, [12]Department of Surgical Oncology, [13]Department of Epidemiology - University of Groningen, University Medical Center Groningen, Groningen, The Netherlands. [3]Department of Surgery, [4]Department of Medical Oncology, [5]Department of Radiation Oncology, [6]Department of Radiology, [7]Department of Pathology, [8]Department of Gastroenterology and Hepatology - Isala Hospital, Zwolle, The Netherlands.

ABSTRACT

Introduction: Locally advanced rectal cancer is customarily treated with neoadjuvant chemoradiotherapy (CRT) followed by a total mesorectal excision (TME). During the course of CRT, previously non-detectable distant metastases can appear. Therefore, a restaging CT scan of the chest and abdomen was performed prior to surgery. The aim of this study was to determine the frequency of a change in treatment strategy after this restaging CT scan.

Methods: Patients treated with neoadjuvant CRT for locally advanced rectal cancer between January 2003 and July 2013 were included retrospectively. To determine the value of the restaging CT scan, the surgical treatment as planned before CRT was compared with the treatment ultimately received.

Results: A total of 153 patients (91 male) were eligible, and median age was 62 (32–82) years. The restaging CT scan revealed the presence of distant metastases in 19 patients (12.4, 95% confidence interval [CI] 7.0–17.8). In 17 patients (11.1, 95% CI 6.1-16.1), a change in treatment strategy occurred due to the detection of metastases with a restaging CT scan.

Conclusion: A restaging CT scan after completion of neoadjuvant CRT may detect newly developed metastases and consequently alter the initial treatment strategy. This study demonstrates the added value of the restaging CT scan prior to surgery.

INTRODUCTION

Colorectal malignancies are diagnosed frequently, with an incidence of nearly 1.4 million worldwide.[65] In about one-quarter of cases, the tumor is located in the rectum. In about half of the patients with rectal cancer, the tumor is already in an advanced T and/or N stage at the time of diagnosis, referred to as locally advanced rectal cancer. Furthermore, rectal cancer carries a significant risk of distant metastases; 19% of patients with colorectal cancer present with synchronous hepatic metastases, and pulmonary metastases are found in 7.5% of patients.[66-68]

In the diagnostic work-up of rectal cancer, several imaging techniques are available for staging. Staging is built on two principals. The first is defining the local anatomy, allowing for surgical planning, and the second is to estimate the prognostic stage by revealing any distant metastases. The imaging techniques most appropriate for local staging are magnetic resonance imaging (MRI) and endorectal ultrasonography.[69,70] MRI is more accurate in determining the higher T stages, locoregional lymph node involvement, and circumferential resection margin involvement, and is therefore used generally for local staging. To rule out distant metastases, a computed tomography (CT) scan of the chest and abdomen is the most appropriate strategy.[69,71]

Although surgical resection, by means of total mesorectal excision (TME), remains the cornerstone of curative treatment, in recent decades progress has been made in the development of neoadjuvant treatment.[72-76] Standard treatment of locally advanced rectal cancer currently consists of neoadjuvant chemoradiotherapy (CRT) followed by TME, which has led to a local recurrence rate of less than 10%.[66] Generally, the chemotherapeutic agent of choice is capecitabine.[77] This agent acts as a radiosensitizer. CRT has the ability to achieve regression of the primary tumor and hence to transform an unresectable tumor into a resectable one.

Since neoadjuvant CRT became the standard treatment for locally advanced rectal cancer, an interval between diagnosis and surgery of at least 11 weeks was created in which formerly non-detectable distant metastases may appear. Therefore, it is justifiable to restage patients with a CT scan of the chest and abdomen preoperatively. If this scan reveals metastatic spread to the liver or lungs, the decision could be made to refrain from TME or change the surgical plan.

Although a restaging CT scan is generally performed in the work-up of patients with locally advanced rectal cancer, it is not incorporated in national and international guidelines. Both the European (Integraal Kankercentrum Nederland [IKNL], National Institute for Health and Care

Excellence [NICE], and European Society for Medical Oncology [ESMO]) and North American (American Society of Colon and Rectal Surgeons [ASCRS], and National Comprehensive Cancer Network [NCCN]) guidelines provide information about the most appropriate staging modalities, but do not mention the need for distant staging after neoadjuvant CRT.[78-82] The most important reason for this is that the value of this scan has not been demonstrated in prospective research. In 2013, Dutch researchers published a retrospective study that investigated the value of a restaging CT scan in 153 patients with locally advanced rectal cancer.[83] The authors reported a change in treatment strategy in 12% of the patients due to new findings on the restaging CT scan; 8% of the patients were spared rectal surgery due to progressive metastatic disease.

The aim of the present retrospective study was to determine the value of the restaging CT scan in a homogenous cohort of patients with locally advanced rectal cancer who were preoperatively treated with CRT.

MATERIALS AND METHODS

Study population

We used a retrospective cohort analysis design. Patients were included from a secondary and a tertiary medical center in The Netherlands (Isala Clinics Zwolle and University Medical Center Groningen [UMCG], respectively). Patients were included from a search in the Dutch National Pathology Registry (PALGA). For this search, the following search terms were used: 'colorectal' and 'carcinoma'. At the UMCG, a prospectively maintained database was available that included all rectal cancer patients who were discussed in the weekly multidisciplinary meetings. This database was used to add patients to our search who were not found by the local PALGA search. The inclusion period covered January 2003 to July 2013, since neoadjuvant CRT became the standard of therapy around 2003. All patients included were diagnosed with locally advanced rectal cancer and received neoadjuvant CRT. Locally advanced rectal cancer was defined as a T4 tumor, a T3 tumor with close relation to the circumferential resection margin (≤1 mm) or the presence of 4 or more tumor-positive lymph nodes. Patients with rectal tumors that did not fulfill these criteria on the standard radiology report were included as locally advanced tumors based on the reassessment of the scan by the radiologist of the multidisciplinary tumor board. Lymph nodes were considered tumor-positive when short-axis measured 5 mm or more by MRI.[78] Patients with a local recurrence or distant metastases at the time of diagnosis were excluded from the study because these factors could affect the initial treatment strategy. Additional eligibility criteria are described in Table 1.

Table 1. Eligibility criteria

Inclusion criteria
Carcinoma located in the rectum
Locally advanced rectal cancer
Neoadjuvant treatment with chemoradiotherapy
CT scan of chest and abdomen performed before and after chemoradiotherapy
Exclusion criteria
Local recurrence of rectal cancer
Distant metastases present at staging
Neoadjuvant therapy with an experimental scheme

CT computed tomography

Study procedures

All patients included in this study received a work-up for locally advanced rectal cancer that included an MRI scan of the rectum for local staging, and a CT scan of the chest and abdomen for distant staging. The CT scan was performed both before and after CRT. CT

images were acquired after administration of an intravenous, oral, and rectal contrast agent. Images of the chest were acquired in the arterial phase of contrast enhancement, whereas images of the abdomen were acquired in the venous phase. The liver was scanned in both phases.

All newly diagnosed patients were discussed during meetings of a multidisciplinary tumor board consisting of medical oncologists, surgical oncologists, radiation oncologists, gastroenterologists, radiologists, nuclear medicine specialists, pathologists, and case managers. If they concluded that a patient had locally advanced rectal cancer, treatment with neoadjuvant CRT was recommended. This treatment generally consisted of long-course radiotherapy with a total dose of 50.4 Gy delivered in 28 fractions of 1.8 Gy, and the concomitant administration of chemotherapy, consisting of a twice daily bolus of capecitabine. Neoadjuvant therapy was followed by TME of the tumor after an interval of at least 6 weeks. The resection could comprise an (extralevator) abdominoperineal resection (APR) or a low anterior resection (LAR), and was performed according to the principles of the TME. At the UMCG, a pelvic exenteration could also be performed. In addition, at this center, patients could be treated with intraoperative brachytherapy if resection margins were suspected to be tumor-positive intraoperatively.

Data collection

To investigate the value of the restaging CT scan, several variables were collected for each patient, including the CT scan outcomes before and after CRT, the surgical treatment as planned before CRT, and the ultimate treatment. The intention of treatment, which could be either curative or palliative, was also determined.

Statistical analysis

The collected data was principally analyzed by means of descriptive statistics. Descriptive variables were expressed as numbers and percentages. All statistical analyses were executed by SPSS statistical software (IBM Corporation, Armonk, NY, USA).

Ethical analysis

The study was approved by the Institutional Review Boards of both participating centers, and was conducted according to the Dutch guidelines for research involving human subjects.

RESULTS

With the local PALGA search, 3037 colorectal cancer patients were found, of which 1089 patients had rectal cancer. From this group, a total of 153 patients were eligible for the study. Most patients (618) were excluded because their cancer was not locally advanced and consequently were not treated with neoadjuvant CRT. An additional 125 patients were excluded because no CT scan of the chest and abdomen was performed before and after CRT. Baseline characteristics of the study population are described in Table 2. The majority of the patients were included in the final years of the study.

Table 2. Baseline characteristics of the study population

Characteristics	
Number of patients	153
Age – Years	
Median	62
Range	32–82
Sex – no. (%)	
Male	91 (59.5)
Female	62 (40.5)
Period of diagnosis – no. (%)	
2003–2008	21 (13.7)
2009–2013	132 (86.3)
Distance to anal verge – no. (%)[a]	
0–5 cm	91 (59.5)
6–10 cm	37 (24.2)
>10 cm	18 (11.8)
Not documented	7 (4.6)
cT-stage – no. (%)[b]	
T1	0 (0.0)
T2	13 (8.5)
T3	71 (46.4)
T4	65 (42.5)
Tx	4 (2.6)

a) Measured at colonoscopy

b) Based on pelvic MRI

The median intervals between the various diagnostic and treatment modalities are shown in Table 3. The median interval between the end of CRT and the possible TME of the tumor was 9 weeks.

Table 3. Time interval between diagnostic and treatment modalities

Period	Median interval (weeks)	Interquartile range (weeks)
Staging CT scan – start CRT	3.9	(3.0 – 5.8)
Start CRT – end CRT	5.4	(5.3 – 5.6)
End CRT – restaging CT scan	4.0	(3.1 – 4.9)
Restaging CT scan – surgery	5.0	(3.9 – 6.6)

CRT = chemoradiotherapy

Change in treatment strategy

The restaging CT scan showed new findings in a substantial number of patients. It revealed distant metastases in 19 of the 153 patients (12.4, 95% confidence interval [CI] 7.0–17.8), previously unknown with distant metastatic spread. The metastases were localized in the liver (9), lung (4), both liver and lung (4), adrenal gland (1), and bone (1). Due to these new findings on the restaging CT scan, the treatment strategy was changed for 17 patients in this group (89%). This constitutes 11.1% of the study population (95% CI 6.1–16.1). Due to the detection of new metastases, 15 patients (9.8%) were spared rectal surgery. These patients received either palliative treatment or supportive care. The remaining 2 patients received a partial liver resection for curative treatment of liver metastases in addition to TME of the primary tumor. The individual changes in treatment strategy are described in Table 4. The 2 patients with distant metastases who did not receive a different treatment, still underwent TME of the tumor for palliative reasons.

Table 4. Changes in treatment strategy based on new findings on the restaging CT scan

Treatment strategy based on staging CT scan	Treatment strategy post-restaging CT scan	Patients
LAR	Palliative chemotherapy	5
APR	Palliative chemotherapy	1
LAR	Supportive care	2
APR	Supportive care	5
Total exenteration	Liver resection + supportive care	1
APR	Palliative radiotherapy + supportive care	1
LAR	LAR + liver resection	1
APR	APR + liver resection	1

CT computed tomography, *LAR* low anterior resection, *APR* abdominoperineal resection

DISCUSSION

In the present study, we determined the value of the restaging CT scan after neoadjuvant treatment for locally advanced rectal cancer. The study showed a change in treatment strategy in 11% of patients due to the detection of new metastases on the restaging CT scan. Moreover, approximately 1 in 10 patients was spared rectal surgery due to this CT scan. These results underscore the relevance of the CT scan after CRT in patients with locally advanced rectal cancer.

The results of our study confirm those of a recent study reported by Ayez et al., also conducted in The Netherlands.[83] They noted a change in treatment strategy in 12% of their study population. However, our study differed from theirs in two major respects. We created a more homogenous cohort of patients with no detectable metastases at the time of diagnosis. When patients with distant metastases were excluded from the study of Ayez et al., a change in treatment strategy was seen in only 9% of patients. Second, we only included patients who received a CT scan before and after CRT. Patients who were staged with an X-ray instead of a CT scan of the thorax were excluded, since a chest X-ray does not have sufficient resolution to diagnose metastases. Moreover, the difference in imaging modality before and after CRT makes it difficult to compare their results with ours. Furthermore, the results of the MERRION study were recently published, which evaluate the value of MRI for local staging post-CRT and besides the value of CT for distant staging.[84] They noted a change in treatment strategy in 18 of 267 (6.7%) patients due to metastases on the restaging CT scan. This percentage is smaller than the percentage we have detected in our study and could be explained by the inclusion of patients with American Joint Committee on Cancer (AJCC) stage 2 rectal cancer (17%) who not fulfill the criteria for locally advanced rectal cancer and are less likely to develop distant metastases.

Although many practitioners question the value of the restaging CT scan, our study indicates that a substantial proportion of the patients could be spared a mutilating and probably unnecessary surgical intervention by this restaging scan. TME of rectal cancer is also relatively hazardous, with a morbidity rate of 31% and mortality rate of 1.6%.[85] Moreover, our study demonstrates that, on average, 10 restaging CT scans can spare 1 patient from rectal surgery.

A potential confounding factor is that the accuracy of CT for detection of distant metastases is questionable. Lung lesions are especially difficult to define, which is most likely due to the frequent detection of indeterminate lesions.[86] The presence of a parenchymal lung nodule (≥1 cm if single and ≥0.5 cm if multiple) with a soft-tissue component and without calcification on lung and mediastinal window settings, is considered positive for the presence of metastasis.

Two studies showed a sensitivity of 70–78% for detection of pulmonary metastases with helical CT, by confirming CT results with intraoperative inspection of the lungs.[87,88] However, in our study all patients with evidence of pulmonary metastases on the restaging CT scan had multiple lung lesions. Consequently, we believe that the diagnosis of pulmonary metastases in patients who underwent a change in treatment strategy was trustworthy.

The restaging CT scan also has several disadvantages, including radiation exposure and added cost. Moreover, the detection of distant metastases may not necessarily alter the surgical treatment plan, since surgical resection could serve as an adequate palliative treatment by alleviating local complaints such as pain, defecation problems and rectal bleeding. Another consideration is that detection of distant metastases may not necessarily imply incurable disease because some metastases can be treated with curative intent.

Due to the retrospective character of this study, selection bias may have occurred. The strict criteria for inclusion in this study resulted in a homogenous cohort of patients, but this cohort does not necessarily resemble the general population of locally advanced rectal cancer patients. Furthermore, the retrospective study design depends on the completeness of the documentation. This documentation was limited due to suboptimal description of the surgical approaches before and after neoadjuvant treatment.

As CT scanners will be replaced during a study period of 10 years, different CT scans might be used for distant staging of rectal cancer throughout the years. As newer CT scanners often have a higher resolution, smaller metastases could be detected.

CONCLUSION

In this study, we have demonstrated the value of the restaging CT scan for patients with locally advanced rectal cancer without distant metastases at initial staging. This CT scan not only reveals a significant number of formerly unknown metastases, but also leads to changes in treatment strategy in a substantial proportion of patients.

Acknowledgments: The authors would like to thank Stichting PALGA, The Netherlands, for providing a database of pathological specimens from patients who were eligible for inclusion in the study.

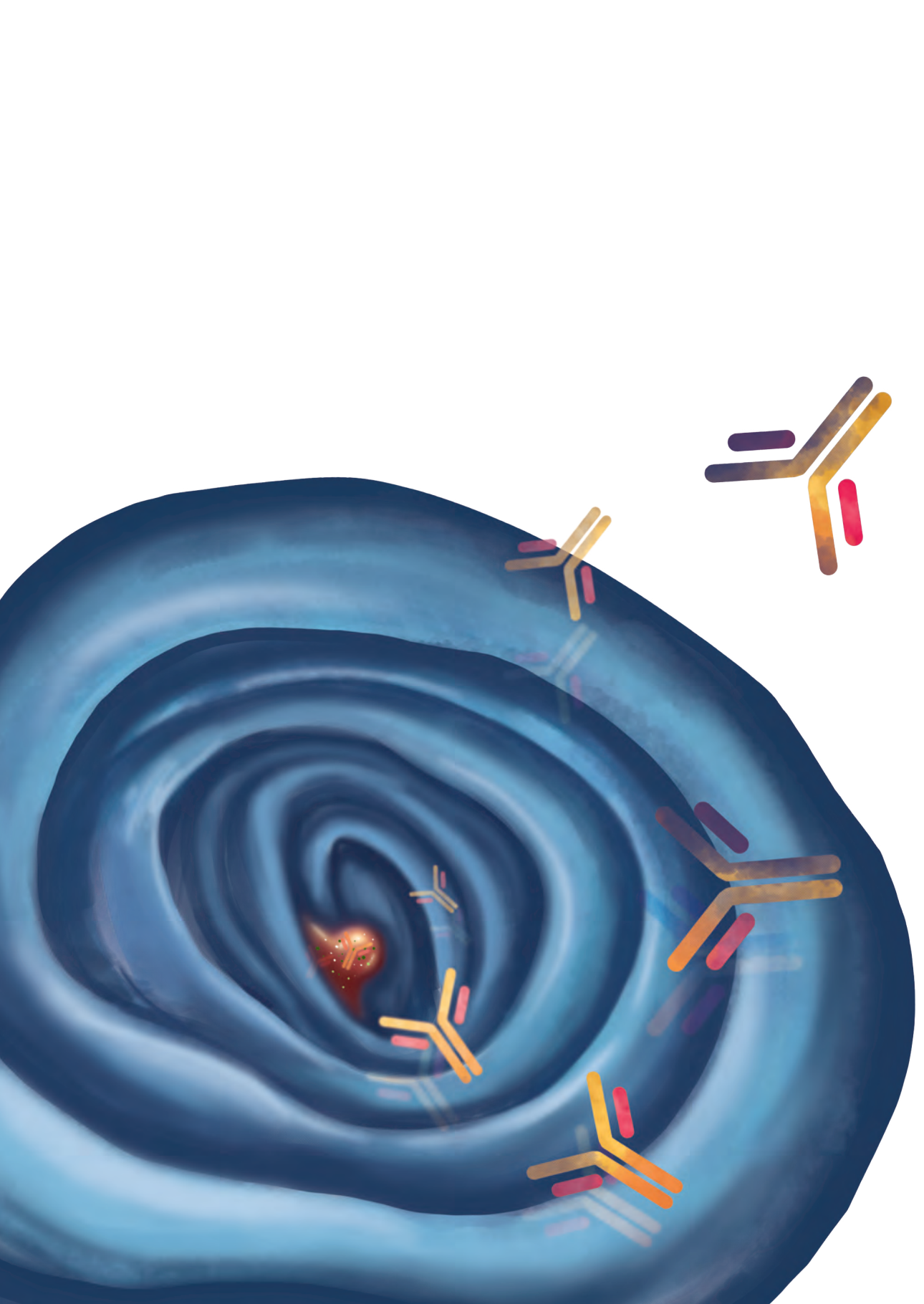

Chapter 5

Quantitative fluorescence endoscopy: an innovative endoscopy approach to evaluate neoadjuvant treatment response in locally advanced rectal cancer

This chapter is based on: Gut, 2020; 69(3): 406-410

Jolien JJ Tjalma[1*], Marjory Koller[2*], Matthijs D Linssen[1,3], Elmire Hartmans[1], Steven J de Jongh[1], Annelies Jorritsma-Smit[3], Arend Karrenbeld[4], Elisabeth GE de Vries[5], Jan H Kleibeuker[1], Jan Pieter Pennings[6], Klaas Havenga[2], Patrick HJ Hemmer[2], Geke A.P. Hospers[5], Boudewijn van Etten[2], Vasilis Ntziachristos[7], Gooitzen M van Dam[2,8], Dominic J Robinson[9], Wouter B Nagengast[1]

**contributed equally*

[1]Department of Gastroenterology and Hepatology, [2]Department of Surgery, [3]Department of Clinical Pharmacy and Pharmacology, [4]Department of Pathology, [5]Department of Medical Oncology, [6]Department of Radiology, [8]Department of Nuclear Medicine and Molecular Imaging and Intensive Care - University of Groningen, University Medical Center Groningen, Groningen, The Netherlands. [7]Institute for Biological and Medical Imaging - Technical University of Munich and Helmholtz Center Munich, Munich, Germany. [9]Otolaryngology and Head & Neck Surgery - Erasmus MC, University Medical Center Rotterdam, Rotterdam, The Netherlands.

ABSTRACT

Introduction: Patients with locally advanced rectal cancer (LARC) who obtain a pathological complete response (pCR) after neoadjuvant chemoradiotherapy may benefit from a watchful waiting strategy. Conventional restaging modalities lack sensitivity and specificity to optimally identify patients with a pCR. We aimed to study whether novel quantitative fluorescence endoscopy (QFE) could aid in clinical response assessment by identifying residual tumor in patients with LARC after neoadjuvant chemoradiotherapy.

Methods: In 25 patients with LARC, we investigated QFE with the fluorescent tracer bevacizumab-800CW, targeting vascular endothelial growth factor A (VEGFA), for tumor response evaluation. QFE measurements were correlated to gold standard: pathological staging of the surgical specimen.

Results: Tumor tissue showed higher fluorescence compared to normal rectal tissue and fibrosis, with an area under curve of 0.925. When correlating QFE and conventional clinical restaging modalities with pathological staging of the surgical specimen, we observed an initial positive predictive value of 95% for QFE vs 87.5% for MRI and 90% for white-light endoscopy; and accuracy of 92% for QFE vs 84% for MRI and 80% for white-light endoscopy.

Conclusion: QFE would have changed the restaging diagnosis correctly in four patients (16%), indicating QFE as promising tool to aid response assessment in combination with MRI and white-light endoscopy after neoadjuvant chemoradiotherapy in patients with LARC. To realize this strategy, QFE needs further evaluation in a larger prospective cohort. ClinicalTrials.gov (NCT01972373).

INTRODUCTION

The management of locally advanced rectal cancer (LARC) has evolved in recent decades. Currently, patients receive neoadjuvant chemoradiotherapy (nCRT) followed by total mesorectal excision (TME) to achieve local disease control. In 15-27% of the patients the neoadjuvant treatment alone results in a *pathological* complete response (pCR), which is defined as no residual cancer present on histological examination of the TME specimen (i.e. ypT0N0).[89-91] Since pCR is associated with superior disease-free and overall survival, regimens that could further increase the pCR rate in patients with LARC are gaining interest.[90-92] Moreover, the observed high pCR rate (approximately 15-27%) has led to a growing interest in organ-preserving strategies as an alternative to TME surgery.[93] Non-operative management for *clinical* complete responders (cCR) following nCRT is associated with high survival rates, reduced long-term morbidity and improved functional outcomes.[19-23] However, correct identification of cCR is difficult: white-light endoscopy provides only morphological information of the superficial rectal mucosa, while magnetic resonance imaging (MRI) cannot always distinguish viable tumor from fibrosis. For example, studies of patients with suspected residual tumor following MRI and white-light endoscopy have shown that 9%-16% did not have tumor in the resection specimen.[15-17] And studies of patients categorized as cCR (i.e. no signs of residual tumor on MRI and white-light endoscopy) have shown that 31% still develop an early or late local or pelvic recurrence.[94] Therefore, imaging techniques that improve clinical response assessment in LARC patients will help support accurate selection of patients who would benefit from organ-preserving strategies.[18]

Quantitative Fluorescence Endoscopy (QFE) is a novel endoscopy technique that visualizes and quantitatively measures the presence of targeted fluorescent tracers in tissue. In this study, we used the fluorescent tracer bevacizumab-800CW, targeting vascular endothelial growth factor A (VEGFA), to visualize locally advanced rectal tumors. VEGFA is involved in the upregulation of tumor-associated angiogenesis and is highly upregulated in the microenvironment of many solid tumors, including colorectal cancer.[95] In the present study, we investigate whether VEGFA-targeted QFE could identify the presence of residual tumor and aid in clinical response assessment in patients with LARC after nCRT.

METHODS

Summary of the study design

Patients with LARC were given a single dose of bevacizumab-800CW intravenously and QFE was performed after the completion of nCRT, at day of surgery. Optionally, patients underwent QFE also at baseline. Tracer uptake in LARC was compared to normal tissue at both timepoints. Tracer uptake was evaluated to detect residual tumor and aid clinical response assessment after completion of nCRT. Patients also underwent conventional clinical restaging (MRI and white-light endoscopy). All results were compared to the gold standard: pathological staging of the TME specimen.

Study population

A total of 25 patients with proven LARC were enrolled between October 2013 and December 2016, in this non-blinded, prospective, single center feasibility study. Patients were required to have histopathologically confirmed adenocarcinoma, with the lower margin within 16 cm from the anal verge. The pelvic MRI indicated at least one of the following criteria: cT4a, cT4b, N2, presence of tumor cells in the vasculature beyond the muscularis propria –extramural venous invasion–, presence of tumor or lymph node <1 mm from the mesorectal fascia or positive lateral lymph nodes. Patients were eligible only if the multidisciplinary team decided on long-course nCRT. The sample included patients who were also included in the RAPIDO trial (ClinicalTrials.gov: NCT01558921). Key exclusion criteria were concurrent uncontrolled medical conditions and pregnancy or breast-feeding. Eligible patients were identified during the multidisciplinary colorectal cancer meeting at the University Medical Center Groningen (UMCG, Groningen, The Netherlands). All patients gave written informed consent for participation in the study before inclusion. The study protocol was approved by the Medical Ethics Committee of the UMCG and registered with ClinicalTrials.gov (NCT01972373).

Patient and public involvement

The study was supported by the Dutch Cancer Society. There was no patient involvement in study design, interpretation of results or writing of the manuscript.

Clinical procedures

Neoadjuvant treatment

Patients underwent nCRT before surgery, consisting of 28 doses of 1.8 Gy and oral capecitabine (825 mg/m^2 twice daily during radiotherapy course or 1000 mg/m^2 twice daily during 2 cycles of 14 days during radiotherapy course) or according to the study arm of the RAPIDO trial (*n*=2): 5 doses of 5 Gy, followed by 6 courses every 3 weeks of oxaliplatin intravenously (130 mg/m^2) at day 1 and oral capecitabine (1000 mg/m^2) twice

daily for 14 days starting at day 1 of the course. Dose adjustments were made in the event of side effects. No post-operative chemotherapy was administered, in line with our national guideline.[96]

Clinical restaging

All patients underwent radiological restaging after nCRT, which consisted of a computer tomography (CT) scan of chest and abdomen and a diffusion-weighted MRI scan of the pelvis. Tumor (T), lymph node (N) and metastasis (M) stage were assessed, together with extramural venous invasion and mesorectal fascia involvement, according to the TNM classification off the American Joint Committee on Cancer (5th edition).

Surgical resection

After the restaging CT and MRI, the TME plan was formulated. Surgery consisted of abdominoperineal resection, low anterior resection or a more extended procedure like partial or full pelvic exenteration in order to reach a tumor-free circumferential resection margin. Although watchful waiting is not part of standard clinical care in our institution, two patients requested this even though MRI and white-light endoscopy were inconclusive. Both showed tumor regrowth. One patient who chose watchful waiting underwent surgical resection of the regrown tumor 9 months after the final radiotherapy dose, and QFE was performed on the day of surgery. The second patient received QFE at the first restaging and underwent surgical resection 5 months after the final radiotherapy dose.

Pathological examination

Standard pathologic tumor staging of the resected specimen was performed by dedicated gastrointestinal cancer pathologist blinded for QFE results. The pathologic stage (ypTN) was recorded according to the fifth edition of the TNM classification, the clinical standard for the Netherlands. Circumferential resection margin involvement and lymphovascular invasion status were documented. pCR was defined as absence of viable adenocarcinoma cells in the surgical specimen (ypT0N0).

Study procedures

QFE procedures were scheduled at two time points: the first at baseline (prior to the start of nCRT) and the second after nCRT. The baseline QFE was optionally, as many patients were referred to our tertiary center after receiving nCRT at a regional hospital. The second QFE procedure was planned after nCRT, preferably at the day of the surgery, enabling direct correlation with the current clinical standards: radiological restaging (cTNM), white-light video endoscopy and the pathological outcome of the surgical specimen (ypTNM).

Tracer production and administration

The monoclonal antibody bevacizumab (Roche, Hertfordshire, United Kingdom) was labeled under cGMP conditions with the near-infrared fluorophore IRDye800CW (IRDye800CW-NHS ester; LI-COR Biosciences, Lincoln, NE) at the Department of Clinical Pharmacy and Pharmacology of the UMCG.[48] This was originally performed in a 4:1 dye-to-protein molar ratio. After the first 6 patients, the dye-to-protein molar ratio was changed to 2:1 to improve long term stability. No changes were seen in immunoreactivity tests. Patients received 4.5 mg of bevacizumab-800CW in accordance with microdosing limits as defined by the FDA.[97] Tracer was administered via intravenous bolus injection, 2 to 3 days prior to the QFE procedure, the optimal time-to-imaging interval based on experience with ^{89}Zr-bevacizumab PET-scans.[46] No tracer-related serious adverse events were reported, in accordance with previous clinical studies.[14,50,98,99]

White-light endoscopy procedure

All study subjects first received white-light endoscopy with a routine clinical high-definition video endoscope, immediately followed by QFE. Tumor response was endoscopically assessed by a dedicated gastroenterologist (W.B.N.) according to watchful waiting criteria: CR was diagnosed if residual tumor was absent, and only a flat, white scar with or without telangiectasia was present. Potential CR was diagnosed when a small, flat ulcer with smooth edges without signs of residual polypoid tissue was present. Every other type of ulcer or mass was considered as definite residual tumor.[100]

QFE procedure

After high-definition white-light inspection of the rectum with a routine clinical high-definition video endoscope, the wide-field optical fiber was inserted through the working channel of the endoscope for wide-field QFE. The gastroenterologist observed the presence, distribution and intensity of fluorescence signals in normal rectal tissue and in all rectal lesions present at endoscopy. Fluorescence was visually categorized as low (no difference with surrounding normal rectal tissue), intermediate (elevated, but difficult to clearly differentiate from surrounding normal rectal tissue) or high (clear differentiation from surrounding normal rectal tissue based on fluorescent signals). Images of normal tissue and LARC cancer tissue were digitally recorded with an exposure time of 1 frame per second and at video rate (10 frames per second). Subsequently, the spectroscopy fiber was inserted through the working channel of the endoscope and held onto tissue of interest, to perform in vivo point measurements for quantification of the NIR fluorescence. Quantification of minimal 3 different tumor areas and normal rectal mucosa was performed, preferably 10 cm proximal of the rectal tumor. At the end of the QFE procedure, four small forceps biopsies were taken of normal rectal tissue and of every tumor location where quantification was performed. Ex vivo spectroscopy measurements

were performed on these fresh biopsies to enable direct correlation of NIR fluorescence with histopathology. Afterwards, the tissue biopsies were formalin-fixed and paraffin-embedded (FFPE) or snap-frozen in liquid nitrogen and stored at -80° Celsius.

QFE system

Wide-field fluorescence imaging was provided by an imaging platform (Surgvision BV, 't Harde, The Netherlands) consisting of an optical fiber-bundle coupled to a charge-coupled digital (EM-CCD) camera, sensitive for NIR light, and a separate camera for color detection, as described previously.[14,99] Fluorescence excitation was provided by two class IIIb lasers (750 nm); white-light was provided by a LED light source. The wide-field fiber images (color, fluorescence and composite) were displayed live on a separate monitor for the gastroenterologist.

Fluorescence quantification was performed with a Multi Diameter Single Fiber Reflectance and Single Fiber Fluorescence (MDSFR/SFF) spectroscopy device. The in vivo measurements were performed with a fiber-bundle consisting of two concentric rings, the ex vivo measurements were performed with a different fiber-bundle consisting of 2 adjacent fibers (0.4 and 0.8 mm) (Supplemental Figure 1). During a measurement, two consecutive reflection spectra were acquired from which the tissue light absorbance and light reflection were calculated.[59,62,101] This was immediately followed by a fluorescence spectrum measurement. The intrinsic fluorescence ($Q.\mu^f_{a,x}$) of bevacizumab-800CW was acquired by correcting the fluorescence spectrum for the calculated tissue optical properties.[13,58,59]

Calculating local tissue concentration of bevacizumab-800CW

We calculated the local tracer concentration based on the in vivo quantified fluorescence, the molar extinction of the tracer and the fluorescence quantum yield.[14] The intrinsic fluorescence $Q.\mu^f_{a,x}$ is defined as the product of the quantum efficiency across the emission spectrum, Q[-], where Q is the fluorescence quantum yield of IRDye 800CW and m_{af} [mm^{-1}] is the tracer absorption coefficient at the excitation wavelength.

To estimate the molar extinction of bevacizumab-800CW (e) at a certain wavelength (775 nm), we divided the measured absorption (A) by the tracer concentration (c). This resulted in a molar extinction of bevacizumab-800CW at 775 nm of approximately 311,204 M^{-1} mm^{-1}. The *in vivo* measured intrinsic fluorescence ($Q.\mu^f_{a,x}$) was then divided by the fluorescence quantum yield of IRDye800CW (Q, 0.09), resulting in the tracer absorption coefficient at the excitation wavelength (m_{af} [mm^{-1}]).[64] The local tissue concentration of bevacizumab-800CW was then calculated by dividing $\mu^f_{a,x}$ by the extinction coefficient (e). In these calculations, we assumed that *in vitro* determined e and Q are representative for the *in vivo* conditions, and that all IRDye800CW fluorescence originated of intact bevacizumab-800CW.

Correlation of QFE findings with radiological and pathological staging

To assess the value of QFE after nCRT, QFE findings were compared to the clinical restaging findings (MRI and high-definition white-light endoscopy) and correlated to the gold standard: pathological staging (ypTNM).

Ex vivo analyses

For fluorescence microscopy, 4 µm FFPE tissue sections of the tissue biopsies were deparaffinized and stained with Hoechst solution (33258; Invitrogen, Thermo Fisher Scientific) to counterstain the cell nuclei.[14] The hematoxylin and eosin (HE), CD31, D2-40 and erg staining were performed on 4 µm FFPE tissue sections as standard clinical staining by our Pathology Department.

Statistical methods

Descriptive statistics were generated to describe patient characteristics and the association between QFE and pathological outcome. The intrinsic fluorescence ($Q{\cdot}\mu^{f}_{a,x}$) measurements of different tissue types after nCRT was analyzed with a one-way ANOVA test with Tukey post-hoc analysis. A receiver-operating characteristic (ROC) curve was generated from the fluorescence measurements obtained from normal rectal tissue versus tumor tissue. Normal rectal tissue included normal rectal tissue measurements of all patients and fibrosis measurements of pathological complete responders. Tumor tissue included all lesion measurements of all patients with residual tumor at pathological examination. The median and maximum values of the intrinsic fluorescence measurements ($Q{\cdot}\mu^{f}_{a,x}$) were correlated, showing a good correlation ($R^2 = 0.84$; $P < 0.0001$, data not shown). P values lower than 0.05 were regarded as statistically significant. IBM SPSS Statistics, version 23.0 (SPSS inc.) was used for all statistical analyses. All authors had access to the study data and reviewed and approved the final manuscript.

RESULTS

Patient characteristics

25 patients diagnosed with LARC were enrolled in the study. Ten of these patients received a baseline QFE prior to nCRT, and all 25 patients received QFE after nCRT (Table 1).

Baseline QFE prior to neoadjuvant chemoradiotherapy

We used the baseline QFE data to verify that the tracer indeed accumulates specifically in rectal cancer tissue. In all 10 baseline QFE procedures, tumor tissue showed clearly enhanced fluorescence compared to normal rectal tissue (Figure 1A, Supplemental Figure 2). Quantification of the fluorescence of bevacizumab-800CW ($Q{\cdot}\mu^{f}_{a,x}$; e.g., the intrinsic fluorescence measured) showed a median fluorescence of $3.75{\cdot}10^{-2}$ ($\pm 0.90{\cdot}10^{-2}$) in tumor tissue compared to $1.20{\cdot}10^{-2}$ ($\pm 0.20{\cdot}10^{-2}$) in normal rectal tissue ($P < 0.001$), corresponding to a tumor-to-normal ratio of 3.1 (Figure 1B). This showed that bevacizumab-800CW can visualize tumor tissue in rectal cancer. In addition, it also showed that sufficient bowel preparation is required to prevent interference with the fluorescent signals from the tracer, as feces also emitted near-infrared (NIR) fluorescence signals.

Bevacizumab-800CW distribution per tissue type after neoadjuvant chemoradiotherapy

To differentiate between tumor tissue and normal rectal tissue and fibrosis, we determined the cut-off fluorescence value. To this end we grouped the fluorescence measurements per tissue type. The fluorescence of tumor tissue was significantly higher than normal rectal tissue and fibrosis ($P < 0.001$) (Figure 2A). The receiver operating characteristic (ROC) curve generated from all fluorescence measurements of tumor areas ($n = 155$) compared to normal rectal tissue and fibrosis areas ($n = 100$), showed an area under the curve of 0.925 with a cut-off value of $2.00{\cdot}10^{-2}$ (Figure 2B). Ex vivo fluorescence microscopy showed NIR fluorescence in tumor tissue, localized in the stroma (Supplemental Figure 3).

QFE after neoadjuvant chemoradiotherapy

In all 25 patients (100%), normal rectal mucosa (median fluorescence $1.26{\cdot}10^{-2}{\pm}0.20{\cdot}10^{-2}$) showed low fluorescence levels $<2.00{\cdot}10^{-2}$. An overview of representative images of all included patients for each procedure is presented in Supplemental Figure 4.

Table 1. Patient and tumor characteristics

Characteristic	No.	%
Median age, in years (range)	61 (31-76)	
Sex		
Male	15	60%
Female	10	40%
Endoscopic findings at time of diagnosis		
Non-passable stenosis	*7*	*28%*
Radiologic staging (MRI pelvis and CT chest+abdomen)		
*c*T3 N0	2	8%
*c*T3 N1	5	20%
*c*T3 N2	10	40%
*c*T4 N1	4	16%
*c*T4 N2	4	16%
Neoadjuvant chemoradiotherapy regimen		
Capecitabine 825 mg/m^2 bid day 1-28 + 28x1.8Gy radiotherapy	18	72%
Capecitabine 1000 mg/m^2 bid day 1-14 and 25-38 + 25x2Gy radiotherapy	5	20%
6 cyles of capecitabine/oxaliplatin + 5x5Gy radiotherapy	2	8%
Main endoscopic findings at restaging		
Residual tumor / polypoid tissue	19	76%
Ulcer >3 cm	2	8%
Ulcer <3 cm	3	12%
White-scar tissue	1	4%
QFE procedure		
With fluorescence quantification	19	76%
Without fluorescence quantification	6*	24%
Type of Surgery		
Low anterior resection	14	56%
Abdominoperineal resection	11	44%
Pathological staging		
*yp*T0 N0 (pCR)	3	12%
*yp*T2 N0	4	16%
*yp*T3 N0	6	24%
*yp*T3 N1	3	12%
*yp*T3 N2	6	24%
*yp*T3 N0 M1	1	4%
*yp*T4 N0	2	8%

* in 2 patients fluorescence quantification was not yet available, in 4 patients the device malfunctioned.

QFE showed a clear fluorescence signal of ≥ $2.00{\cdot}10^{-2}$ in 22 of 25 patients. In 17 of these 22 (77%) patients, white light endoscopy revealed endoluminal tumor remnants confirmed by histology (median of max fluorescence $3.52{\cdot}10^{-2}{\pm}0.65{\cdot}10^{-2}$) (representative example in Figure 3A). One

of the other five patients (max fluorescence $4.57{\cdot}10^{-2}$) showed polypoid tissue on white light endoscopy, and at histology, residual tumor was confirmed in the submucosa (Figure 3B). In three of 22 (13%) fluorescence-positive cases, an ulcer was seen with white light endoscopy. In two of these ulcer cases, (max fluorescence at QFE: $2.32{\cdot}10^{-2}$ and $2.57{\cdot}10^{-2}$, respectively) histology showed mucosal tumor in one case and submucosal tumor in the other. The third patient (max fluorescence $2.02{\cdot}10^{-2}$) chose watchful waiting instead of surgery, so correlation with pathological staging was impossible at the time of QFE. However, residual tumor was likely in this case since tumor regrowth was detected at follow up white-light endoscopy 2 months later. Finally, one of the 22 (5%) fluorescence-positive patients (max fluorescence $3.09{\cdot}10^{-2}$) showed polypoid tissue with white light endoscopy containing high grade dysplasia without invasive tumor at histology (ypT0N0) (Figure 3C).

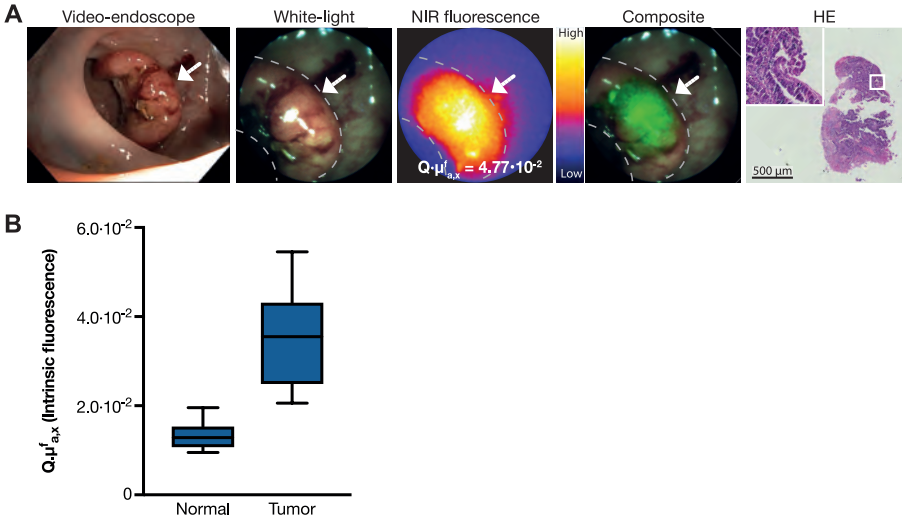

Figure 1. Baseline QFE prior to nCRT. (**A**) A representative example of baseline quantitative fluorescence endoscopy (QFE) prior to neoadjuvant chemoradiotherapy (nCRT). From left to right: a high-definition white-light video endoscope image of the rectal tumor before nCRT; a white-light image from the QFE fiberoptic, followed by the corresponding near infrared (NIR) fluorescence image captured with an exposure time of 100 ms and the composite image of both modalities. QFE clearly discriminates tumor from normal rectal tissue with wide-field fluorescence endoscopy. The maximum quantified fluorescence values, measured with multi diameter single fiber reflectance and single fiber fluorescence (MDSFR/SFF) spectroscopy is written on the NIR fluorescence image. The rightmost image shows the hematoxylin and eosin (HE) staining of a forceps biopsy of the fluorescent area, confirming adenocarcinoma. (**B**) Fluorescence quantification of tumor tissue and normal rectal tissue shows higher fluorescence in tumor compared to normal rectal tissue. Boxplot centerline is at median, the bounds of the box at 25th to 75th percentiles, the whiskers depict the min-max.

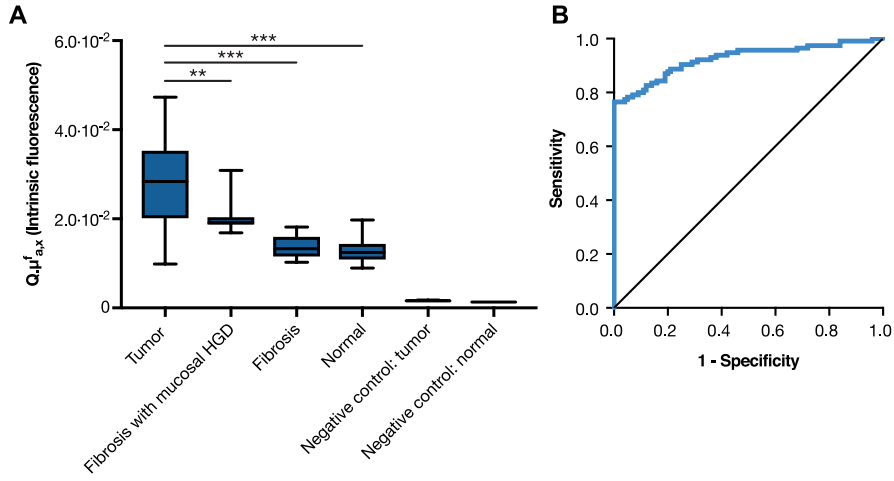

Figure 2. Bevacizumab-800CW distribution after nCRT. (**A**) Quantitative fluorescence endoscopy (QFE) measurements per tissue type demonstrates that tumor tissue shows significantly higher fluorescence compared to fibrosis and normal tissue. Negative control tissue of measurements of tumor tissue and normal rectal tissue from a patient without the tracer showed no detectable fluorescence, signifying the measured fluorescence originated from the tracer. All in vivo and ex vivo spectroscopy measurements were grouped. Boxplot centerline is at median, the bounds of the box at 25th to 75th percentiles, the whiskers depict the min-max. **, $P \leq 0.01$; ***, $P \leq 0.001$, One-way ANOVA test with Tukey post-hoc analysis. (**B**) A receiver operating characteristic (ROC) curve of quantified fluorescence of normal rectal tissue (n = 100) versus tumor tissue (n = 115) shows an area under the curve of 0.925. Normal rectal tissue included normal rectal tissue measurements of all patients and fibrosis measurements of pathological complete responders. Tumor tissue included all lesion measurements of all patients with residual tumor at pathological examination.

In three of 25 patients (12%) low fluorescence was observed compared to normal surrounding rectal tissue (i.e. fluorescence-negative, fluorescence < $2.00{\cdot}10^{2}$). One of these patients (max fluorescence $1.82{\cdot}10^{-2}$) showed white scar tissue at white light endoscopy. Histology showed a complete response (ypT0N0). The other two showed an ulcer at white light endoscopy. In one patient (max fluorescence $1.43{\cdot}10^{-2}$) the ulcer was large (> 3 cm); histology revealed a pCR (ypT0N0) (Figure 3D). In the other patient (max fluorescence $1.61{\cdot}10^{-2}$) a small ulcer (< 3 cm) was seen at white light endoscopy; histology showed a microscopic residual locus situated only in the submucosa.

Overall, QFE correctly identified 21 of the 22 patients with residual disease and two of the three patients with a pCR (Table 2).

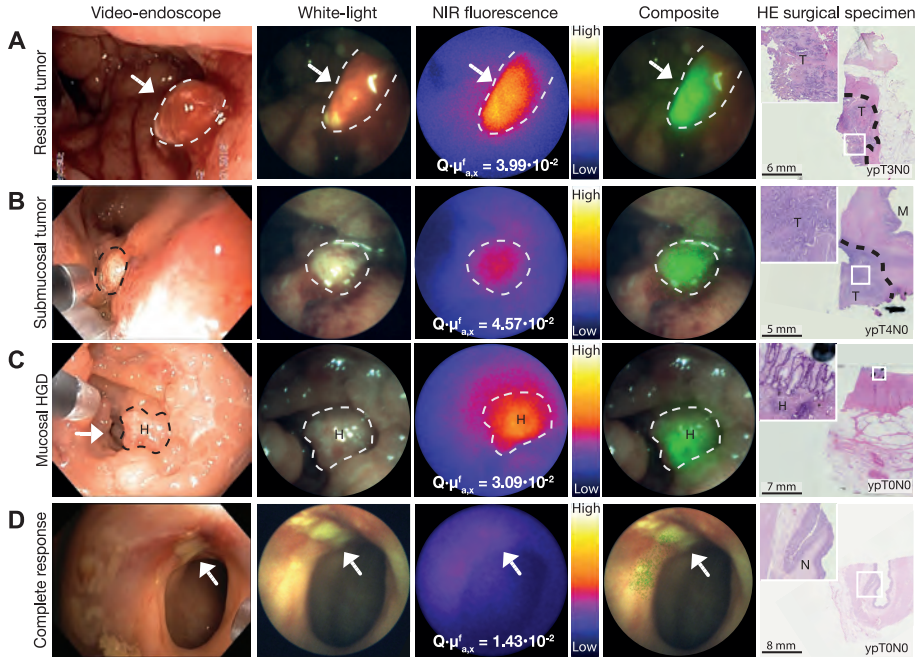

Figure 3. QFE after nCRT. One representative example per procedure. From left to right: a high-definition white-light video endoscope image of the rectal lumen after neoadjuvant chemoradiotherapy (nCRT); a white-light image; the corresponding near infrared (NIR) fluorescence image; the composite of both modalities. The maximum quantified fluorescence values, measured with multi diameter single fiber reflectance and single fiber fluorescence (MDSFR/SFF) spectroscopy, are depicted in the NIR fluorescence images. The NIR fluorescence images were acquired at 100ms exposure time. The rightest column depicts an hematoxylin and eosin (HE) staining of the surgical specimen, in which the pathological TNM stage is indicated. (**A**) Representative images of a patient with residual tumor. (**B**) Representative images of a patient with submucosal tumor. (**C**) Representative images of a patient with mucosal high-grade dysplasia. (**D**) Representative images of a patient with a pathological complete response (pCR).

QFE compared to conventional staging methods and pathological staging

Compared to the current clinical restaging methods, MRI and white-light endoscopy, QFE would have changed the diagnosis in four of 25 patients (16%) (Figure 4). QFE detected a clear fluorescence signal, indicating residual tumor, in three patients clinically categorized as potential complete responders. One of these patients chose watchful waiting, but tumor regrowth was detected at follow-up white-light endoscopy 2 months later (Figure 4A-C). In one patient, QFE showed low fluorescence, thus identifying a pCR in a patient categorized by conventional staging methods as having residual tumor (Figure 4D). In contrast, QFE yielded only one false positive, but the same patient was also shown as false positive on conventional imaging. All modalities indicated residual tumor in this case, but histological examination showed only high-grade dysplasia (Figure 4E). Although this case was classified

as false positive, surgery was required for the treatment of HGD since endoscopic resection was not feasible. One falsely negative patient (i.e. ulcer < 3 cm) was found to have only small microscopic submucosal tumor foci (Figure 4F).

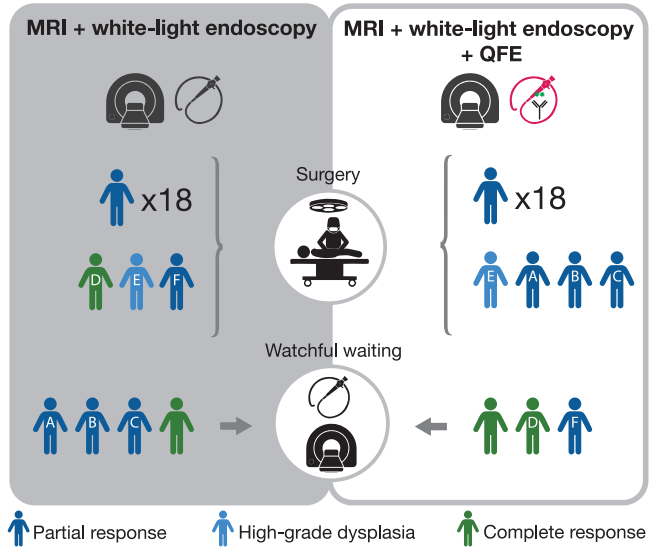

Figure 4. Schematic visualization of the potential added value of QFE to MRI and white-light endoscopy as restaging modality after nCRT. Clinical restaging with white-light endoscopy and magnetic resonance imaging (MRI) diagnosed 4 patients as having a clinical complete response, of which only 1 patient had a pathological complete response. Twenty-one patients were suspected of having residual tumor, of which 2 patients had a pathological complete response. However, by combining quantitative fluorescence endoscopy (QFE) findings with these clinical results, restaging would diagnose 3 patients with complete response, 22 patients suspected of having residual tumors. By adding QFE results, restaging diagnosis might be corrected in 4 of 25 patients (16%). In patients A-C, QFE detected clear fluorescence, indicating residual tumor in three patients clinically categorized as potential complete responders. In patient D, QFE showed low fluorescence, thus recognizing a complete response in a patient categorized by conventional staging methods as having residual tumor. In patient E, QFE showed the only false-positive result, which was also false positive on conventional imaging with suspected residual tumor, but high-grade dysplasia was shown at histological examination. In patient F, QFE was false-negative (i.e. ulcer < 3 cm) but the surgical specimen contained only small microscopic submucosal tumor foci.

Table 2. Contingency table

	Pathological residual tumor	Pathological complete response	Total
QFE positive $Q \cdot \mu^{f}_{a,x} \geq 2.00 \cdot 10^{-2}$	21	1*	22
QFE negative $Q \cdot \mu^{f}_{a,x} < 2.00 \cdot 10^{-2}$	1	2	3
Total	22	3	25

* High-grade dysplasia in surgical specimen

In our sample of 25 patients, the initial positive predictive value was 95% for QFE compared to 87.5% for MRI and 90% for white-light endoscopy. The accuracy of QFE was 92% compared to 84% for MRI and 80% for white-light endoscopy.

DISCUSSION

This is the first study demonstrating that VEGFA-targeted QFE using bevacizumab-800CW in patients with LARC is of additional value, adding functional imaging data, to MRI and white-light endoscopy in the selection of patients suitable for non-surgical management. QFE could improve the identification of patients with residual disease and complete response, leading to more accurate clinical restaging in a significant proportion of patients as compared with MRI and white-light endoscopy alone. These promising results warrant larger prospective studies with QFE aiming to improve personalized treatment decisions in LARC patients.

Clinical assessment of a pCR remains the biggest challenge in LARC patients treated with neoadjuvant chemoradiotherapy. FDG-PET has been extensively investigated to assess pCR, although lack of accuracy (ranging from 0.57-0.73) has hampered its use in clinical practice.[102] Currently, white light endoscopy and MRI is used most often to assess pCR. By using quantitative molecular fluorescence endoscopy, we observed an improved sensitivity and accuracy of respectively 95% and 92% for QFE compared to the reported 71% and 89% of MRI combined with white light endoscopy, but a lower specificity of 67%.[16] The latter can probably be explained by the relatively small number of patients with a pCR in our study. QFE is easy to perform, the QFE measurements are operator independent and together with the standard white light endoscopy procedure it takes only slightly more time (5-10 min extra). Importantly, no tracer or procedure related adverse events were observed in this study.

To enable quantification of the fluorescence signals, we used Multi Diameter Single Fiber Reflectance and Single Fiber Fluorescence (MDSFR/SFF) spectroscopy, a technique that corrects the measured fluorescence signals for tissue optical properties like scattering and absorption.[13,14] If fluorescence signals are not corrected for tissue optical properties, large differences in fluorescence result that do not reflect the true accumulation of the tracer and thus the actual biology. This can potentially lead to incorrect recommendations in clinical practice and thus to inferior outcomes for the patients.

In three of the 25 patients, examination of the surgical specimen revealed tumor situated only in the submucosa, not reaching the mucosa of the rectum lumen; QFE measured increased fluorescence of bevacizumab-800CW in two of these cases. Especially in patients without endoluminal tumor, but with tumor nests in deeper layers, we hypothesize that the microenvironment has not yet been normalized due to increased levels of VEGFA produced by the tumor cells. Therefore, a tracer that accumulates in the microenvironment of a tumor, like bevacizumab-800CW, and not only targets proteins on the tumor cell membranes, could offer an important advantage for restaging. Recent follow-up data has shown that 19% of watchful waiting patients experience early tumor regrowth within 12 months.[94] The majority

of these patients had ypT3 or ypT4 disease at salvage, indeed suggesting the presence of residual disease, not only intraluminal, but also in deeper layers of the rectum. QFE might help to identify these patients with submucosal disease and correctly stratify them to the optimal regimen, i.e., watchful waiting or surgical treatment.

Despite the promising results reported here, the detection of submucosal disease remains very challenging, though deeper bite-on-bite biopsies might improve sensitivity.[94,103] Although NIR wavelengths have a deeper penetration depth compared to light in the visible spectrum, optical imaging will always suffer from limited imaging penetration depth due to the intrinsic limitations of light propagation in tissue. Therefore, future complementary detection systems such as optoacoustic imaging, which combines the rich contrast of optical imaging with the higher penetration of radiofrequency waves, may further improve submucosal evaluation. Potentially, this approach could even visualize tumor-positive lymph nodes in the rectal fat, as most metastatic lymph nodes are located at the level of the initial tumor bed or just proximal to it.[104,105] Additionally, a higher tracer dose than the 4.5 mg bevacizumab used in the present study could provide stronger fluorescence signals. A clinical dose-finding study using bevacizumab-800CW for detection of adenomatous polyps in the colon reported that a higher tracer dose of 25 mg increases the target-to-background ratio almost twofold, thus improving the contrast between adenomatous and normal tissue.[14]

A limitation of our feasibility study is the relatively small sample size and the fact that only 12% of patients that received QFE after nCRT showed a pCR, which is lower than the 15-27% pCR after nCRT described in literature.[89,90] This is probably due to the fact that this study was carried out in a tertiary center with complex LARC patients (T4 in 40% and N2 in 64% of subjects).

In conclusion, these results, even in this small group of patients, are encouraging and are potentially a first step towards quantitative optical molecular imaging for tumor response evaluation following neoadjuvant treatment. Ultimately, the combination of MRI, white-light endoscopy and QFE may be a promising strategy for evaluating individual patient response and guiding clinical decision-making. To realize this strategy, the capability of clinical response evaluation in LARC patients with QFE, including determination of a definitive cut-off value that discriminates tumor from normal tissue, needs further evaluation in a larger prospective cohort.

Acknowledgments: We acknowledge and thank the LARC patients that participated in this study and the contribution of the personnel working at the endoscopy suite, the surgical theatre and the pathology department for their assistance at all study procedures. Special thanks to W. Boersma-van Ek for her technical assistance in the laboratory.

Funding: The research leading to these results was supported by a personal grant from the Dutch Cancer Society (WBN, RUG 2012-5416), a grant from the European Community's Seventh Framework Program (FP7/2007-2013 BetaCure project; MK, GMvD n° 602812), a grant from the Center for Translational Molecular Medicine (project MAMMOTH 03O-201), an Academy Professor Prize to EGEdV by the Royal Netherlands Academy of Arts and Sciences (KNAW), ERC advanced grant OnQview and by unrestricted research grants from SurgVision B.V. and Boston Scientific.

Competing Interests: GMvD and WBN received an unrestricted research grant made available to the institution for the development of optical molecular imaging from SurgVision BV ('t Harde, The Netherlands). GMvD and VN are members of the scientific advisory board of SurgVision BV.

SUPPLEMENTAL FIGURES

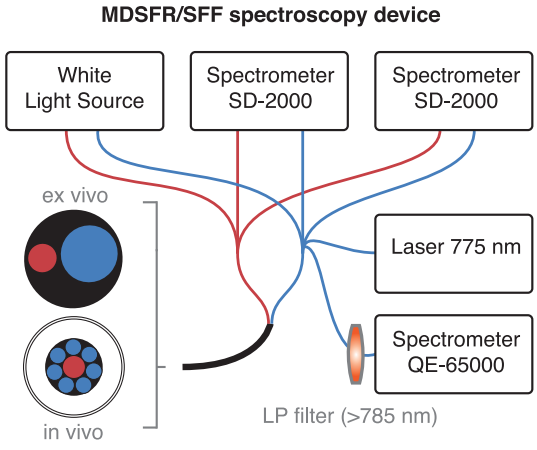

Supplemental Figure 1. Schematic representation of the MDSFR/SFF spectroscopy device. Two different reflection spectra are measured by using different diameters of an optical fiber-bundle. In vivo a concentric fiber-bundle was used. Ex vivo a fiber-bundle containing two fibers with different diameters (Ø 0.4 and 0.8 mm) was used. The reflection spectra are immediately followed by one fluorescence spectrum measurement via the largest fiber (775 nm fluorescence excitation light). *LP* long pass.

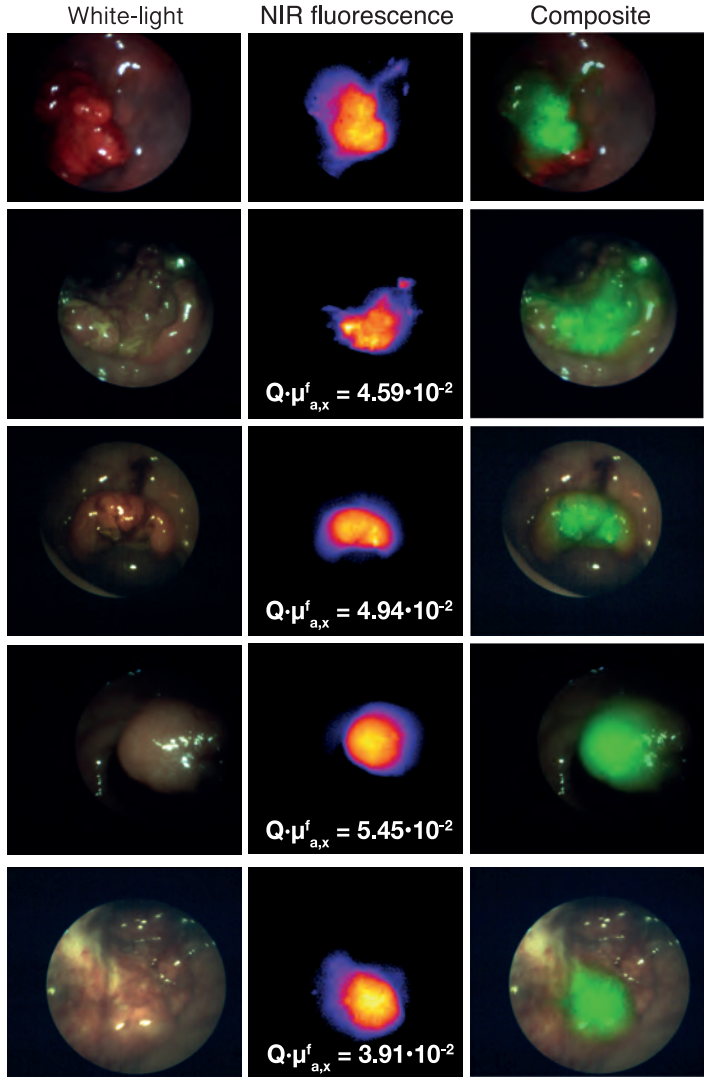

Supplemental Figure 2. Representative fiberoptic images of all 15 QFE procedures performed at baseline. In the left column, the QFE white-light images are shown. In the middle column, the QFE NIR fluorescence images are shown. The maximum quantified fluorescence of the depicted lesion is shown in all cases that were quantified. In right column, the QFE composite images of the former two are shown. All three images were also visible in real-time at video rate for the gastroenterologist during the endoscopy procedure. The fluorescence images in this figure were acquired with different exposure times and are not scaled to one another. Therefore, visual comparison of fluorescence intensities between different procedures is not possible. Many factors influence the wide-field fluorescence visualization, i.e. fiber age, varying distance between lesion and fiber tip and different tissue optical properties of the lesions.

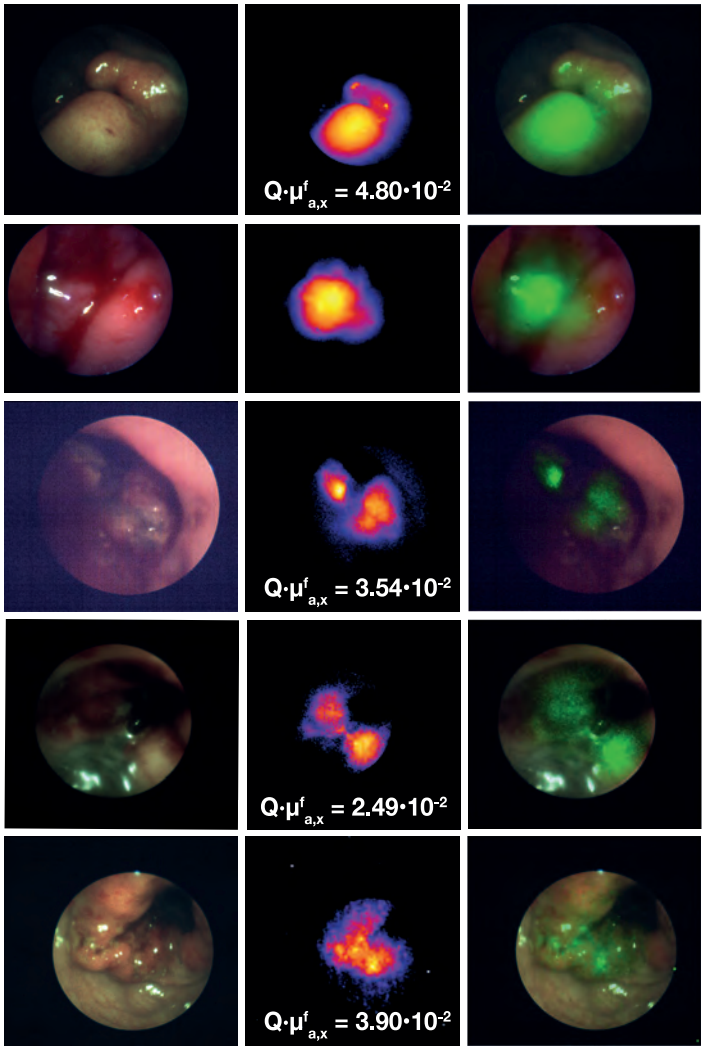

Supplemental Figure 2. Continued

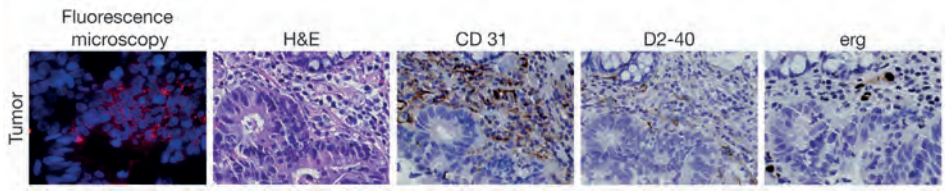

Supplemental Figure 3. Microscopy. The first image shows a fluorescence microscopy image of tumor tissue with bevacizumab-800CW depicted in red and the cell nuclei depicted in blue (after a Hoechst staining). The second image, a HE staining, shows that bevacizumab-800CW is localized in the stroma, not at the mucosal side of the rectum villi. The third image is a CD31 staining, demonstrating the presence of endothelial cells, a measure for the degree of tumor angiogenesis. The fourth image is a D2-40 staining, staining the endothelium of lymphatic channels. The fifth image shows an erg staining, a highly specific endothelial marker, used to assess lymphovascular invasion.

Supplemental Figure 4. Representative fiberoptic images of all 25 QFE procedures performed after nCRT. In the left column, the QFE white-light images are presented together with some additional observational notes. In the middle column, the QFE NIR fluorescence images are presented, the maximum quantified fluorescence of the lesion is depicted in all cases that were quantified. In right column, the QFE composite images of the former two columns are depicted. All three images were also visible in real-time at video rate for the gastroenterologist during the endoscopy procedure. The fluorescence images in this figure were acquired with different exposure times and are not scaled to one another. Therefore, visual comparison of fluorescence intensities between different procedures is not possible. Many factors influence the wide-field fluorescence visualization, i.e. fiber age, varying distance between lesion and fiber tip and different tissue optical properties of the lesions. ►

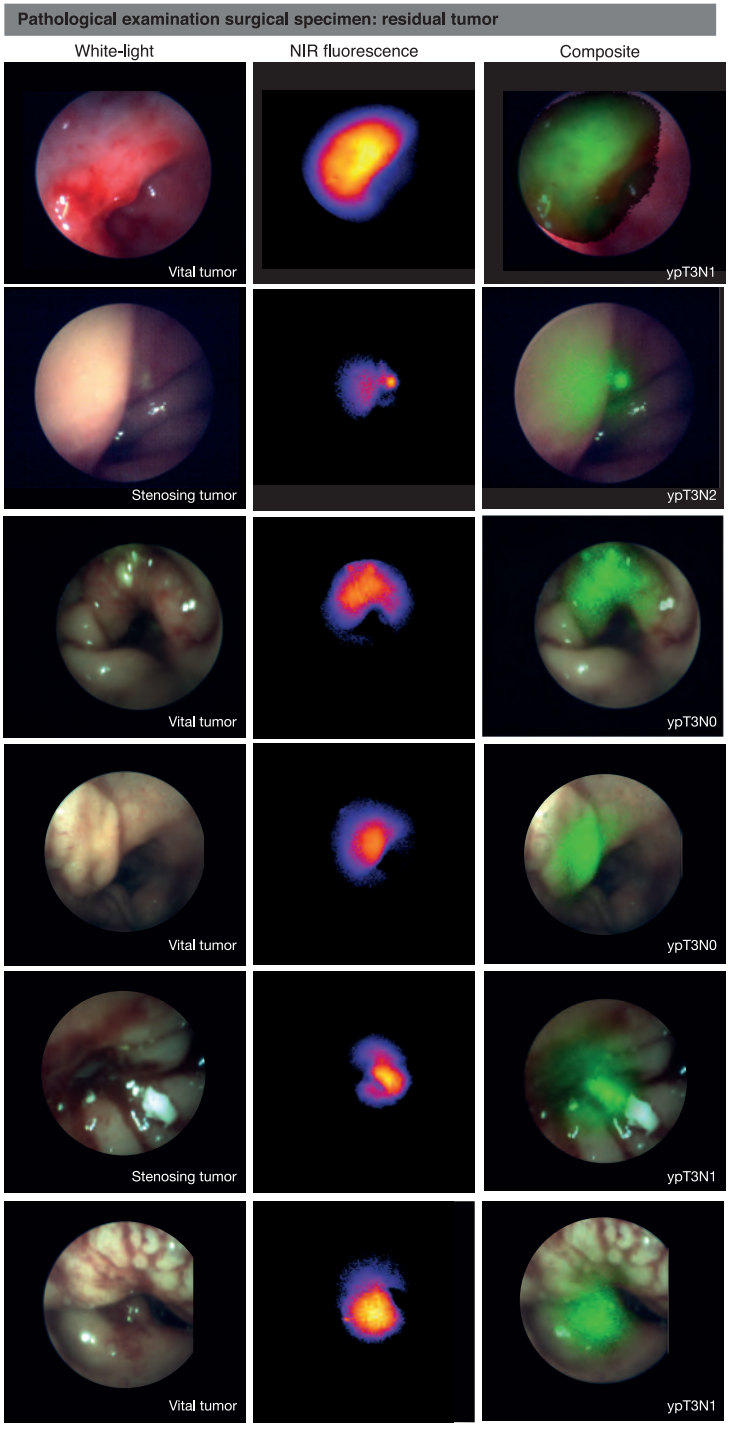
Pathological examination surgical specimen: residual tumor
White-light
NIR fluorescence
Composite
Vital tumor
ypT3N1
Stenosing tumor
ypT3N2
Vital tumor
ypT3N0
Vital tumor
ypT3N0
Stenosing tumor
ypT3N1
Vital tumor
ypT3N1

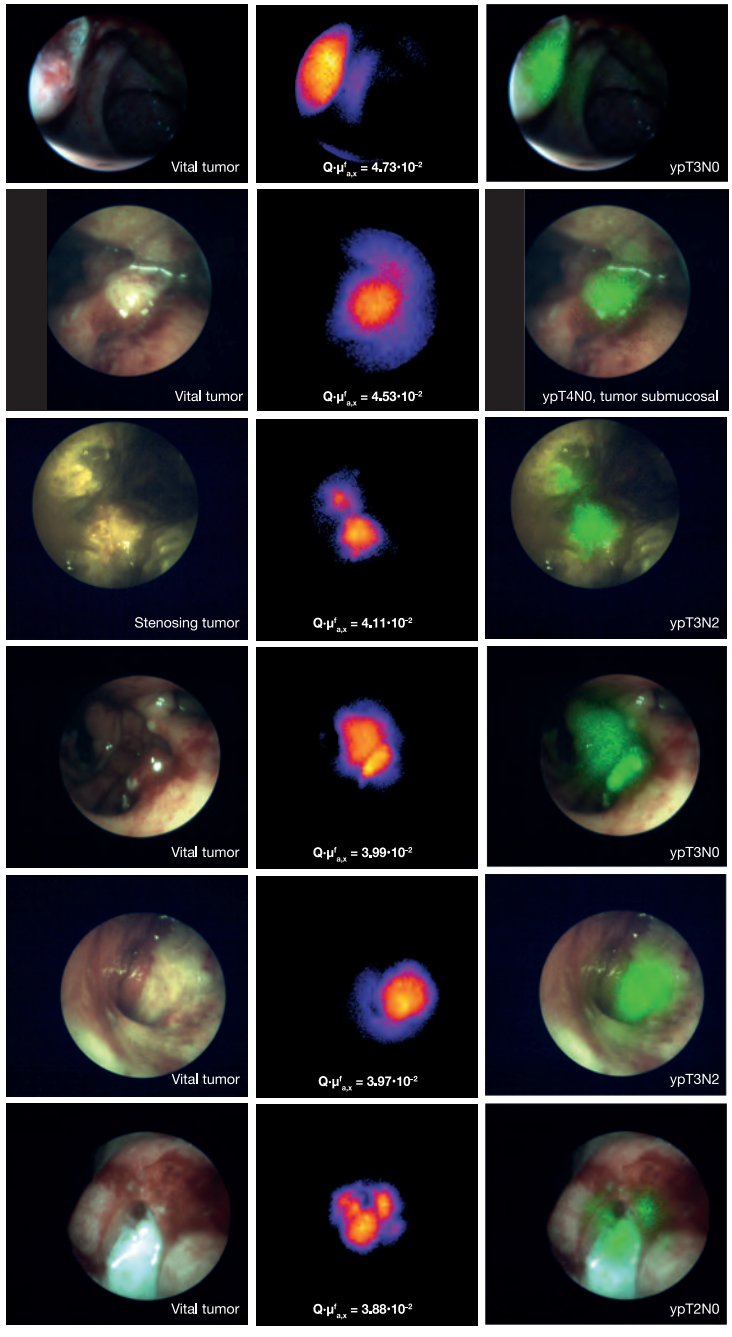

Supplemental Figure 4. Continued

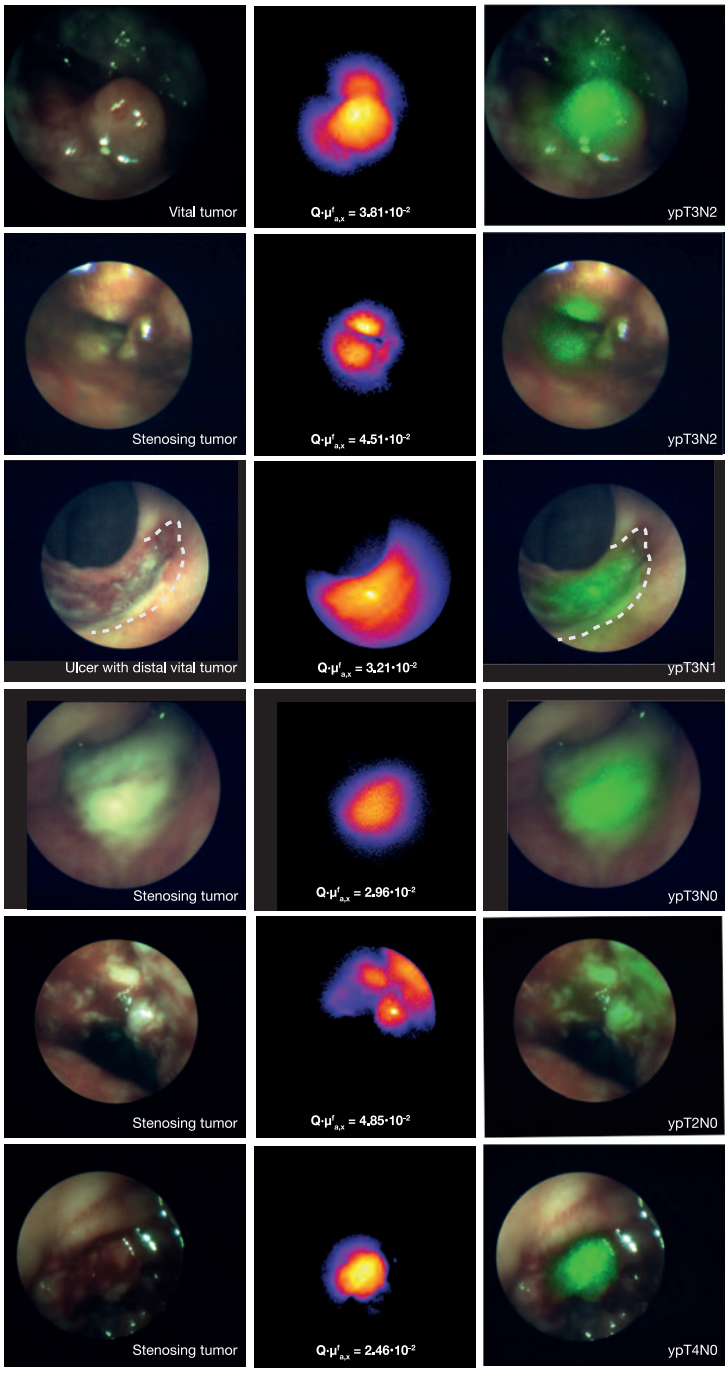

Supplemental Figure 4. Continued

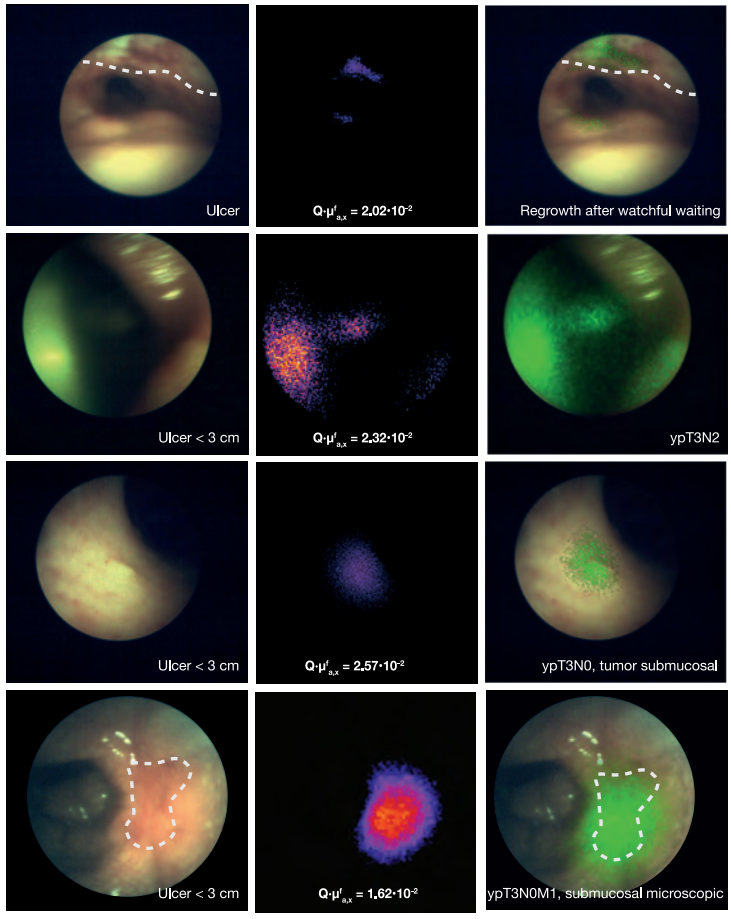

Supplemental Figure 4. Continued

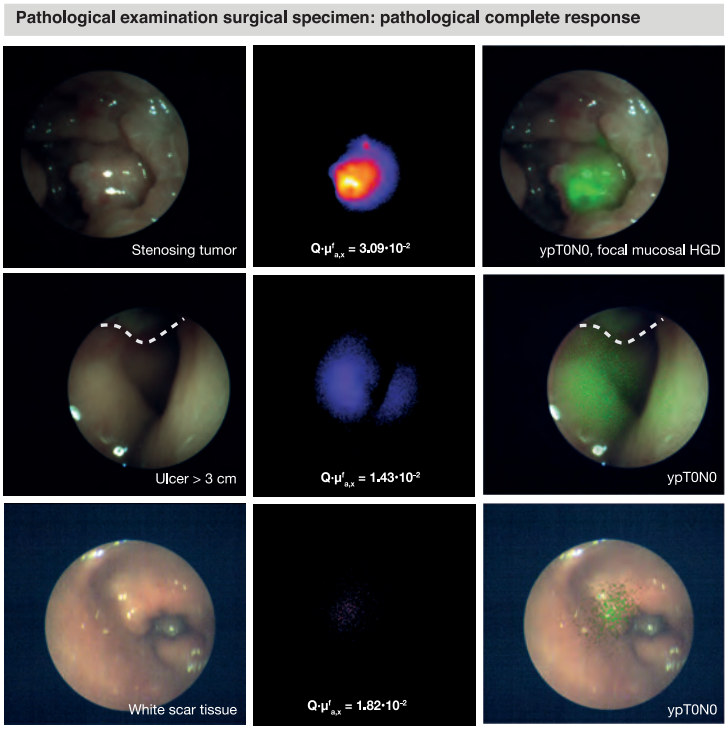

Supplemental Figure 4. Continued

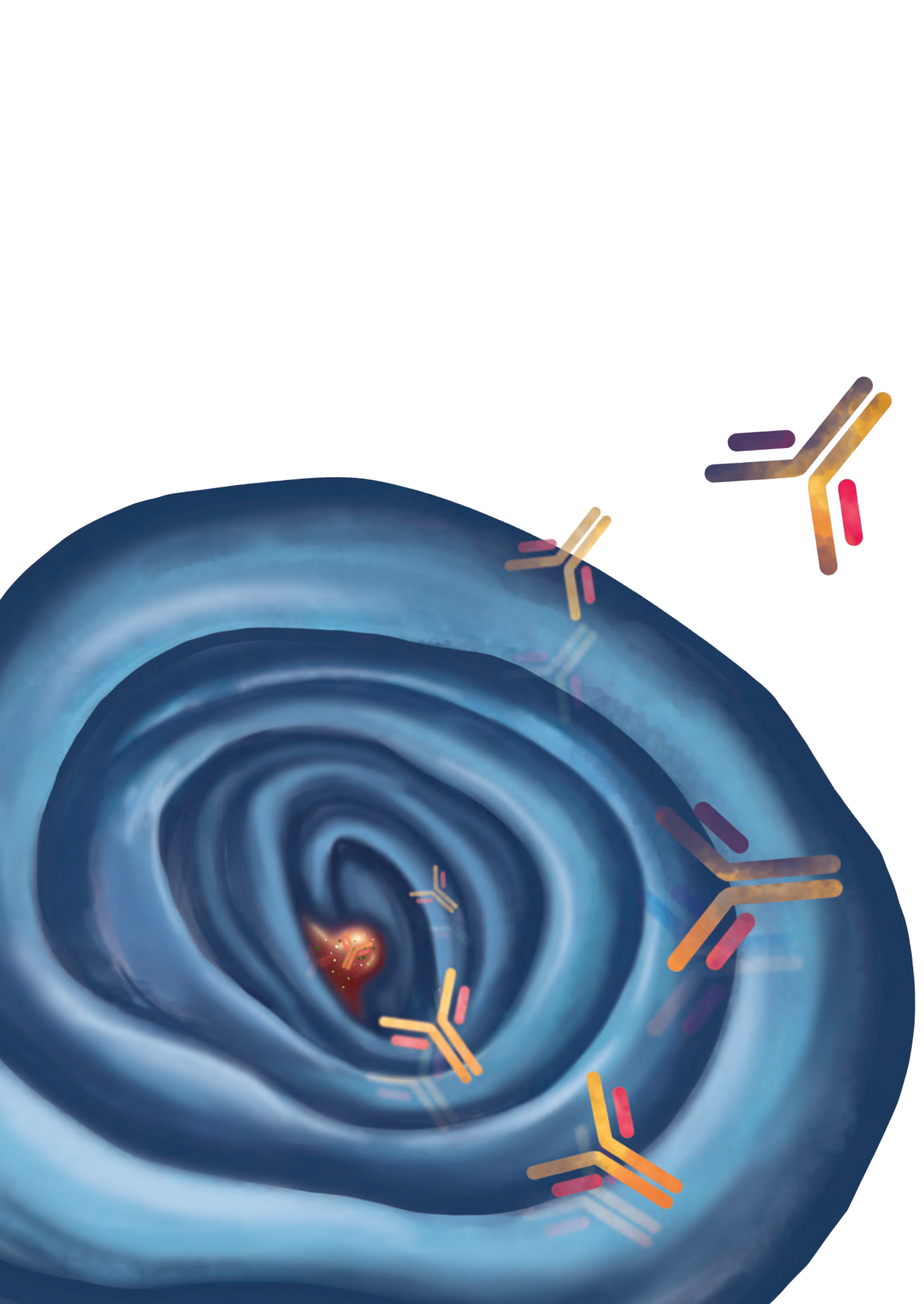

Chapter 6

Back-table fluorescence-guided imaging for circumferential resection margin evaluation in locally advanced rectal cancer patients using bevacizumab-800CW

Journal of Nuclear Medicine, 2020; 61: 655-661

Jolien J.J. Tjalma[1*], Steven J. de Jongh[1*], Marjory Koller[2], Matthijs D. Linssen[1,3], Jasper Vonk[1], Michael Dobosz[4], Annelies Jorritsma-Smit[3], Jan H. Kleibeuker[1], Geke A.P. Hospers[5], Klaas Havenga[2], Patrick H.J. Hemmer[2], Arend Karrenbeld[6], Gooitzen M. van Dam[2,7], Boudewijn van Etten[2], Wouter B. Nagengast[1]

**Contributed equally to this work*

[1]Department of Gastroenterology and Hepatology, [2]Department of Surgery, [3]Department of Clinical Pharmacy and Pharmacology, [5]Department of Medical Oncology, [6]Department of Pathology, [7]Department of Nuclear Medicine and Molecular Imaging - University of Groningen, University Medical Center Groningen, Groningen, The Netherlands; [4]Discovery Oncology, Pharmaceutical Research and Early Development, Roche Innovation Center Munich, Penzberg, Germany.

ABSTRACT

Introduction: Negative circumferential resection margins (CRM) are the cornerstone for curative treatment of patients with locally advanced rectal cancer (LARC). However, in up to 18% of patients tumor-positive resection margins are detected by final histopathology. In this proof-of-concept study, we investigated the feasibility of optical molecular imaging as a tool to evaluate the CRM directly after surgical resection in order to improve tumor-negative CRM rates.

Methods: LARC patients that were treated with neoadjuvant chemoradiotherapy received an intravenous bolus injection of 4.5 mg bevacizumab-800CW, a fluorescent tracer targeting vascular endothelial growth factor A (VEGFA), 2-3 days before surgery (NCT01972373). To evaluate the CRM status, back-table fluorescence-guided imaging (FGI) was performed of the fresh surgical specimens (n = 8). These results were correlated histopathology. Second, to determine the sensitivity and specificity of bevacizumab-800CW for tumor detection, a mean fluorescence intensity (MFI) cut-off value was determined on the formalin-fixed tissue slices (n = 42; 17 patients). Local bevacizumab-800CW accumulation was evaluated by fluorescence microscopy.

Results: Back-table FGI correctly identified a tumor-positive CRM by high fluorescence intensities in 1 of 2 patients (50%) with a tumor-positive CRM. The other patient showed low fluorescence intensities, although (sub-)millimeter tumor deposits were present <1 mm of the CRM. FGI correctly identified 5/6 tumor-negative CRMs (83). The one patient with false-positive findings had a marginal negative CRM of only 1.4 mm. ROC analysis of fluorescence intensities of formalin-fixed tissue slices gave an optimal MFI cut-off value for tumor detection of 5,775 (sensitivity and specificity of 96.2% and 80.4% respectively). Bevacizumab-800CW enabled a clear differentiation between tumor and normal tissue up to a microscopic level, with a tumor-to-background ratio of 4.7 ± 2.5 (mean ± SD).

Conclusion: In this proof-of-concept study, we showed the potential of back-table FGI to evaluate the CRM status in LARC patients. Optimization of this technique with adaptation of standard operating procedures could change perioperative decision-making with regard to extending resections or applying intraoperative radiation therapy in case of positive CRMs.

INTRODUCTION

In today's clinical practice, patients with locally advanced rectal cancer (LARC) receive long-course neoadjuvant chemoradiotherapy (nCRT) followed by surgical resection using the total mesorectal excision (TME) principles. nCRT induces tumor downsizing and downstaging, which facilitates complete resection by TME, resulting in significantly reduced local recurrence rates and increased opportunity for sphincter-sparing resections.[69,83-86]

Obtaining negative circumferential resection margins (CRM) is key in rectal cancer therapy. The CRM has proven to be one of the most important predictors for local recurrence and to a lesser extent the development of distant metastases and survival.[87] Restaging after nCRT occurs through a high-resolution MRI-scan for tumor staging and a CT-scan of thorax and abdomen for distant metastases and lymph node staging.[88-90] Accurate restaging can be highly challenging as differentiating between desmoplastic reaction and viable tumor tissue on preoperative imaging modalities is often difficult after nCRT.

Intraoperatively, surgeons mainly rely on visual and tactile inspection for margin assessment and differentiation between tumor and healthy tissue. This is often inaccurate, especially after nCRT, as small tumor deposits are frequently present within fibrotic parts.[91] When in doubt, resection margins can be evaluated intraoperatively by frozen section pathologic evaluation, but this is time-consuming, costly and poses a high risk of sampling error.[92]

Despite nCRT, TME-surgery and frozen section analysis, a tumor-positive CRM, defined as tumor presence ≤1 mm from the CRM, is detected in up to 18.6% of primary LARC surgeries upon final histopathology.[88-90] Peri-operative resection margin evaluation using optical molecular imaging could improve negative CRM rates by extending resections, applying intraoperative radiation therapy (IORT), or more innovative treatment modalities like photo-immunotherapy of the wound bed.[93] In contract, when a margin is evaluated to be tumor-negative, extended resections could be avoided.

The aim of this proof-of-concept study was to evaluate if back-table fluorescence-guided imaging (FGI) using the near-infrared fluorescent tracer bevacizumab-800CW, could aid in evaluating the CRM status at the surgical theater. Bevacizumab-800CW targets vascular endothelial growth factor A (VEGFA), which is overexpressed in LARC as well as many other solid tumors.[71,94,95] We retrospectively analyzed back-table FGI data of fresh surgical specimens of LARC patients that were treated with nCRT. This technique may eventually allow real-time determination of CRM during surgery, which could aid intraoperative clinical decision-making with regard to extending resections or applying IORT in case of a positive CRM, to improve the outcome of LARC patients.

MATERIALS AND METHODS

Study design and study population

Postoperative fluorescence imaging data were collected from 25 LARC patients enrolled in a clinical trial evaluating VEGFA-targeted molecular fluorescence endoscopy (Clinicaltrials.gov: NCT01972373). Eligibility criteria included histologically proven LARC, with the inferior margin within 16 cm from the anal verge and treatment with long-course nCRT. To determine if back-table FGI could aid in evaluating the CRM status, patients were included if fluorescence imaging data were available from at least the anterior and posterior sides of the fresh surgical specimen. Furthermore, to evaluate local bevacizumab-800CW accumulation and determine the sensitivity and specificity of bevacizumab-800CW for tumor detection using a fluorescence cut-off value, patients with high-resolution fluorescence images available of formalin-fixed tissue slices were included. The study was performed in the University Medical Center Groningen (UMCG), approved by the Institutional Review Board (METc 2013/067) an all subjects signed a written informed consent.

Surgery

After nCRT, all patients received an intended curative resection by either low anterior resection (LAR) for proximal rectum tumors or abdominal perineal resection (APR) for distal rectum tumors. Resections were performed outside the TME planes in case of tumor growth into adjacent organs. Patients only received IORT if judged necessary based on preoperative suspicion of mesorectal fascia involvement or intraoperative evaluation by the surgeons.

Histopathological processing

Histopathological processing of surgical specimens was performed by a board-certified gastrointestinal pathologist. After gross pathology, CRMs were inked black and staple lines were removed. Specimens were anteriorly opened from proximal to distal, except for specimens with an anterior lesion, which were opened until the rectal fold. All specimens were formalin-fixated for at least 48 hours and serially sliced perpendicular to the rectum, from distal to proximal into ±0.5 cm thick tissue slices. Distal and proximal resection surfaces plus additional areas of interest (i.e. regions with CRM involvement, perineural growth, vascular invasion, lymph nodes, etc.) were included for paraffin embedding. Formalin-fixed paraffin embedded (FFPE) tissue blocks were cut in 4 µm tissue sections and hematoxylin and eosin (HE) stained for routine histopathological examination. Immunohistochemistry was performed if required. A tumor-positive CRM was defined as tumor presence ≤1 mm from the inked CRM, in accordance with the Dutch national guidelines.

Bevacizumab-800CW

All patients received a 4.5mg IV bolus injection of bevacizumab-800CW (1 mg/ml) two-to-three days before surgery based on microdosing regulations (Figure 1). Bevacizumab-800CW was produced under cGMP conditions at the University Medical Center Groningen, as described previously.[48]

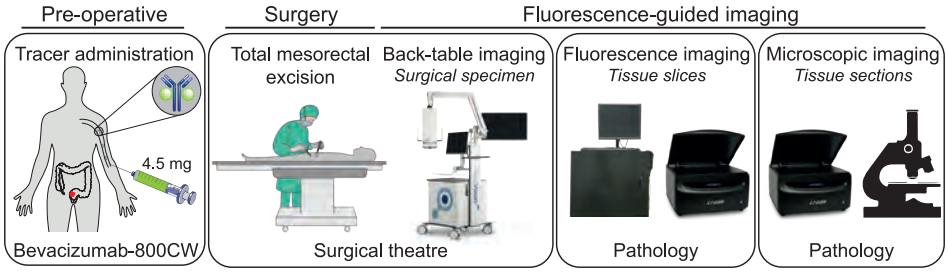

Figure 1. Schematic overview of study design. Bevacizumab-800CW (4.5 mg) was administered intravenously 2-3 days prior to surgery. Fluorescence-guided imaging was performed at every step during pathological processing: back-table of the fresh surgical specimen, of the tissue slices and tissue sections. Results were correlated to histopathology.

Back-table FGI

To evaluate the CRM status, back-table FGI of the fresh surgical specimens was performed in a light-tight room directly after surgery using the Explorer Air fluorescence camera (SurgVision BV, Groningen, The Netherlands, Figure 1). Areas with high fluorescence signals were marked with a pin and subsequently inked with a different color from the CRM during pathological processing, to ensure an accurate correlation of fluorescence with histopathology.

Fluorescence imaging of tissue slices and sections

To evaluate the local tracer accumulation, fluorescence imaging of both sides of all formalin-fixed tissue slices was performed using the Explorer Vault, a standardized and light-tight fluorescence imaging system (SurgVision BV). Thereafter, two-to-three tissue slices containing tumor and/or normal rectal tissue were imaged per patient using the high-resolution Odyssey CLx fluorescence imaging system (LI-COR Biosciences Inc., Lincoln, NE, USA). Additional areas of interest based on fluorescence imaging were also paraffin embedded, sliced in 4 µm tissue sections and HE stained. All FFPE tissue blocks were fluorescently scanned using the Odyssey CLx (Figure 1). For comparison purposes, all fluorescence images were thresholded to minimum-maximum values per imaging modality for each individual patient.

To broaden our understanding of the overall penetration, distribution, and accumulation of bevacizumab-800W in rectal cancer tissue, a combination of optical tissue clearing and light-sheet fluorescence microscopy was performed on selected tissue slices, as previously described for preclinical tissue samples (Supplemental Materials and Methods).[97]

Fluorescence grid analysis

Finally, to evaluate the sensitivity and specificity of bevacizumab-800CW for tumor detection, a fluorescence grid analysis was used based on histopathology as a gold standard to determine a fluorescence cut-off value (Supplemental Materials and Methods).

Statistical analysis

Normally distributed data is presented as mean values with standard deviation (SD) and skewed data as median values with interquartile range (IQR). A receiver operating characteristics (ROC) curve was plotted to determine the MFI cut-off value for tumor detection. *P*-values <0.05 were considered statistically significant. Statistical analyses were performed using Prism (version 7.0, GraphPad Software).

RESULTS

Patient characteristics

In this retrospective proof-of-concept study, eight of 25 patients met the criteria to determine the feasibility of back-table FGI for the evaluation of the CRM status (Supplemental Figure 1). For the second aim of this study, to evaluate local bevacizumab-800CW distribution and determine the sensitivity and specificity of bevacizumab-800CW for tumor detection on high-resolution tissue slices, 17 of 25 patients met the inclusion criteria. Patient characteristics are depicted in Table 1. All patients received 4.5 mg bevacizumab-800CW IV, 2-3 days prior to surgery. Ten patients underwent a LAR and 7 patients underwent an APR. There were no tracer-related (serious) adverse events in any of the patients.

Evaluation of the CRM status

Of eight evaluated cases, two patients (25%) presented with a tumor-positive CRM on final histopathology. Back-table FGI correctly predicted the tumor-positive CRM in one of these patients due to increased fluorescence signals in the CRM (50%, Figure 2). This patient was treated with an APR with en-bloc resection of the sacrum and a wide perineal excision because of a fistula. Intraoperatively, two frozen section analyses were performed of the lateral resection surface, both of which were benign. Interestingly, during back-table FGI of the fresh surgical specimen, high fluorescence signals were observed at the lateral resection margin (Figure 2A). Fluorescence imaging of the corresponding tissue slice also showed high fluorescence that seemed to reach into the CRM, while the surrounding non-tumor tissue showed low fluorescence (Figure 2B). Final histopathology proved that this exact location was a tumor-positive CRM (Figure 2C, orange arrows).

The second patient with a tumor-positive CRM received a LAR. Back-table FGI of the fresh surgical specimen and subsequent fluorescence imaging of the tissue slices showed low fluorescence intensities in the CRM, apart from fluorescence in two enlarged suspicious mesorectal lymph nodes that proved to be tumor-positive (Supplemental Figure 2A). However, the pathologist reported a tumor-positive CRM that was solely based on the presence of isolated microscopic vital-looking tumor deposits of (sub-)millimeter size within a distance of 0.2-1 mm of the CRM (Supplemental Figure 2B; orange arrow). The tumor volume was limited due to the (sub-)millimeter size of the tumor deposits, which explains the negative imaging results.

Six out of 8 patients (75%) had a tumor-negative CRM, of which 5 were correctly predicted by low fluorescence intensities during back-table FGI (representative example in Supplemental Figure 3). Subsequent fluorescence imaging of tissue slices also showed low fluorescence in

relation to the CRM, although fluorescence was observed in the (intra)luminal tumor, except for the patient with a pathologic complete response. IORT was applied to 1 of these patients due to a macroscopic suspicion of a tumor-positive CRM, while histopathology showed a tumor-negative CRM (>1 cm).

Table 1. Patient and tumor characteristics.

Characteristics	CRM evaluation (*n* = 8) No. %		Fluorescence cut-off value (*n* = 17) No. %	
Sex				
Male	5	62.5%	12	70.6%
Female	3	37.5%	5	29.4%
Age (years)				
Median (range)	56 (54 - 61)		56 (31 - 76)	
Duration between nCRT - Surgery (days)				
Median (interquartile range)	87 (76-111)		87 (77-117)	
Surgery				
Low-anterior resection	5	62.5%	10	58.8%
- Including adjacent organs	1	-	2	-
Abdominoperineal resection	3	37.5%	7	41.2%
- Including adjacent organs	3	-	5	-
Intraoperative radiation therapy				
Not standby	3	37.5%	-	-
Standby	4	50%		
Applied	1	12.5%		
Histopathological staging (pTNM)				
pT0 N0 M0 (pCR)	1	12.5%	1	5.9%
pT2 N0 M0	2	25.0%	2	11.8%
pT3 N0 M0	1	12.5%	4	23.5%
pT3 N1 M0	0	-	3	17.6%
pT3 N2 M0	2	25.0%	5	29.4%
pT4 N0 M0	2	25.0%	2	11.8%
Circumferential resection margin (CRM)				
≤ 1 mm (tumor-positive)	2	25.0%	3	17.6%
1-2 mm	1	12.5%	2	11.8%
> 2 mm	4	50.0%	11	64.7%
pCR	1	12.5%	1	5.9%
Distal resection margin				
≤ 1 mm (tumor-positive)	0	-	0	-
1-2 mm	0	-	1	5.9%
> 2 mm	7	87.5%	15	88.2%
pCR	1	12.5%	1	5.9%

CRM circumferential resection margin, *nCRT* neoadjuvant chemoradiotherapy, *pCR* pathological complete response, *TNM* tumor, node, metastasis.

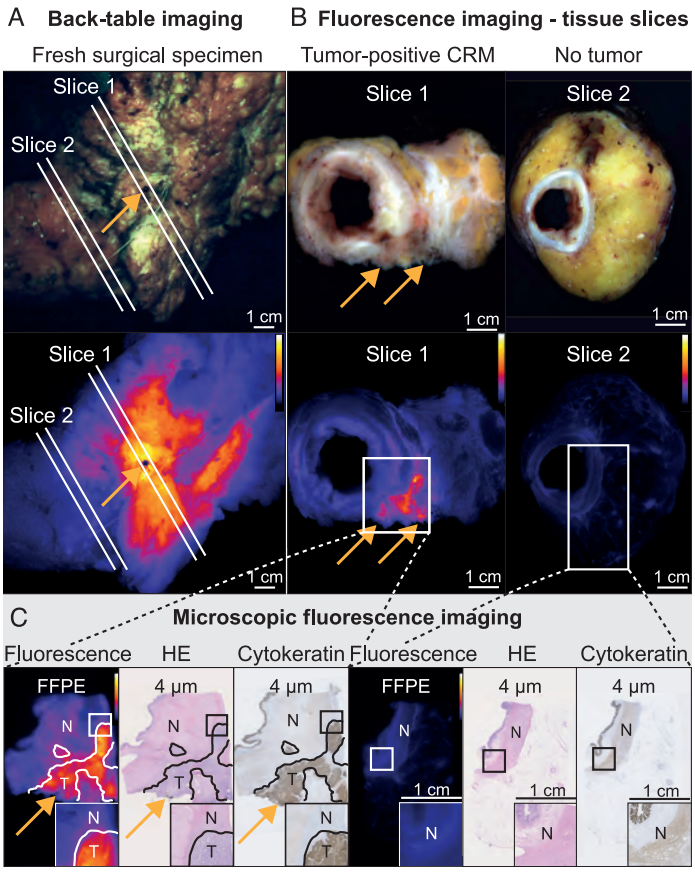

Figure 2. Back-table fluorescence-guided imaging of a patient with a tumor-positive CRM. At back-table imaging, a black pin was placed at the location showing increased fluorescence, to enable accurate correlation with histology (**A**, orange arrow). Fluorescence imaging of two corresponding tissue slices (**B**) and further microscopic fluorescence imaging and histological correlation (**C**), with orange arrows indicating the location of the tumor-positive CRM. High fluorescence is observed at the CRM of tissue slice 1 containing the tumor-positive CRM, whereas low fluorescence was observed in the non-tumor tissue slice 2, corresponding to the microscopy results. *FFPE* formalin-fixed paraffine-embedded, *HE* hematoxylin and eosin; *N* non-tumor; *T* tumor.

Six out of 8 patients (75%) had a tumor-negative CRM, of which 5 were correctly predicted by low fluorescence intensities during back-table FGI (representative example in Supplemental Figure 3). Subsequent fluorescence imaging of tissue slices also showed low fluorescence in relation to the CRM, although fluorescence was observed in the (intra)luminal tumor, except for the patient with a pathologic complete response. IORT was applied to 1 of these patients due to a macroscopic suspicion of a tumor-positive CRM, while histopathology showed a tumor-negative CRM (>1 cm).

The remaining patient with a tumor-negative CRM received a low-anterior resection with en-bloc resection of the uterus, cervix, adnexa and the distal right ureter due to tumor ingrowth. Increased fluorescence was observed at the cervix during back-table FGI and subsequent fluorescence imaging of the tissue slices, potentially indicating a tumor-positive CRM. Although the fluorescence colocalized with a tumor deposit upon histopathology, the CRM was defined as tumor-negative as the distance to the CRM was 1.4 mm.

Fluorescence cut-off value and local bevacizumab-800CW accumulation

High-resolution fluorescence Odyssey scans of formalin-fixed tissue slices (n = 42) available from 17 patients were used to determine a semi-quantitative fluorescence cut-off value for tumor detection. A total of 5,101 grid-squares were analyzed, of which 446 were classified as tumor-positive and 4,655 as tumor-negative (Figure 3A, C). Significantly higher fluorescence intensities were observed in tumor areas (median MFI: 12,000) compared to surrounding non-tumor tissue (median MFI: 2,140; $P < 0.0001$, Figure 3D). This resulted in a ratio between tumor-to-surrounding tissue of 4.7 ± 2.5 (mean ± SD). Receiver operating characteristics (ROC) curves were plotted per patient (Figure 3E) and for all patients combined, with an area under the curve of 0.94 (std. error 0.0039, Figure 3F). In our limited sample size, an optimal MFI cut-off value of 5,775 was calculated using Youden's J statistics (J = 0.77), with a sensitivity and specificity of 96.2% and 80.4% respectively.

Finally, we evaluated the distribution and accumulation of bevacizumab-800CW on a microscopic level. Bevacizumab-800CW was mainly localized in the micro-environment of the tumor cells (Figure 4), which was in line with the expected location of VEGFA (Supplemental Video 1).

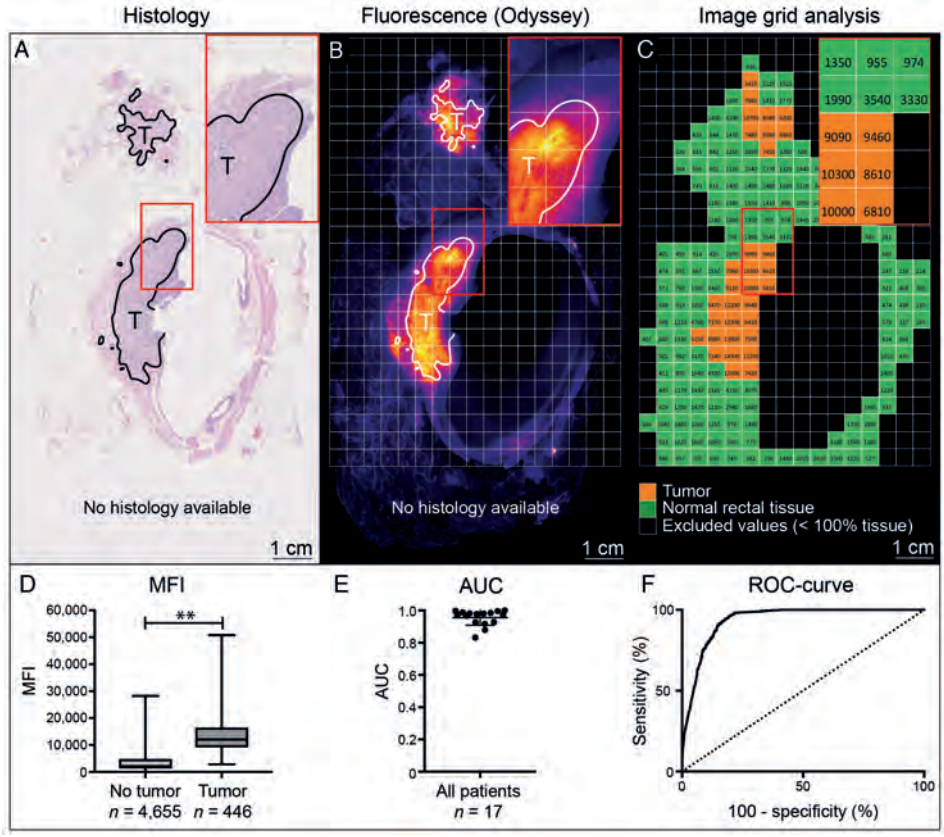

Figure 3. Fluorescence grid analysis. All tumor tissue was delineated on a hematoxylin eosin (HE)-staining (**A**) and subsequently overlaid on the high-resolution fluorescence images of tissue slices (**B**). Each 3-by-3 mm square was selected as tumor-positive (**C**, orange) or tumor-negative (**C**, green). Median fluorescence intensities (MFI) were calculated per square, with significantly higher fluorescence in tumor tissue compared to surrounding non-tumor tissue (12,000 versus 2,140; $P < 0.001$; **D**). Individual areas under the curve were determined per patient (**E**) and a receiver operating characteristic (ROC)-curve was plotted, showing an area under the curve (AUC) of 0.94 (**F**).

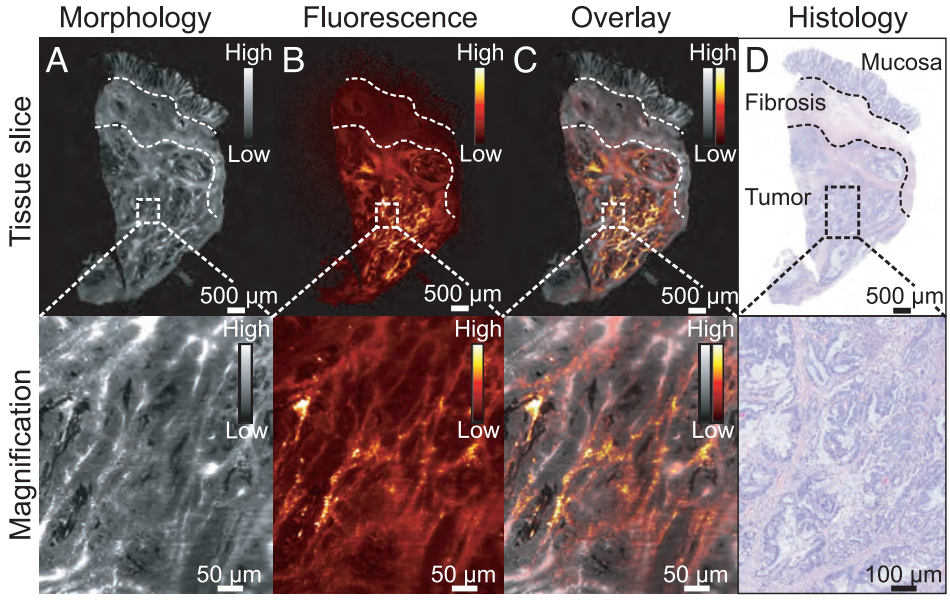

Figure 4. Light-sheet fluorescence microscopy. Representative example of light-sheet fluorescence microscopy to evaluate the local tracer accumulation in a rectal cancer tissue slice, showing the tissue morphology based on autofluorescence (**A**), the fluorescence (**B**), a morphology and fluorescence overlay (**C**) and the corresponding histology (**D**). A magnification is depicted in the bottom row. Increased bevacizumab-800CW binding can be seen in the micro-environment of the tumor cells compared to surrounding normal mucosa and fibrosis.

DISCUSSION

Accurate perioperative evaluation of resection margins is highly important for the prognosis of LARC patients. In this explorative study, we demonstrate for the first time the feasibility of back-table FGI for identification of tumor-positive resection margins in LARC patients. Our data suggest that FGI may have the potential to guide current clinical decision-making with regard to additional targeted resections or application of IORT. Future studies using a standardized imaging protocol with larger patient samples should confirm these results.

Over the past decade, optical molecular imaging has predominantly been applied for intraoperative guidance and surgical navigation. Two clinical studies have demonstrated the feasibility and potential benefit of fluorescence-guided surgery in colorectal cancer.[50,103] However, fluorescence-guided surgery is subject to several limitation related to the currently available hardware, such as variation in image-acquisition parameters and interference of ambient light. Moreover, homogenous tracer excitation is difficult especially in rectal cancer surgery, as the pelvic region is a confined surgical field often situated deep in the patient. Possibly, the development of fluorescence laparoscopes and robotic systems sensitive enough to detect micro-dosed fluorescent tracers may enable more reliable intraoperative evaluation of rectal cancer resection margins in the future.

Back-table FGI circumvents these limitations, as it makes use of a controlled, standardized, and closed-field imaging environment that results in a consistent field-of-view, imaging distance and image-acquisition parameters.[98] This enables a highly sensitive and semi-quantitative evaluation of resection margins, within a maximum of one hour after specimen excision at the OR.

The potential added value of back-table FGI was clearly demonstrated by the patient in which a tumor-positive CRM was detected at the OR, while surgical assessment and frozen section analysis false-negative. Although intraoperative frozen section analysis is recommended for low and mid rectal tumors, it is prone to sampling error, labor-intensive and significantly prolongs anesthesia.[99,100] By ‘bringing pathology to the operating theatre’ using back-table FGI, both surgeons and pathologist may be guided in correctly assessing the CRM status and evaluating the need for extended surgery or application of IORT, thereby improving personalized treatment.

In rectal cancer surgery, caution is to be taken with unnecessarily extending TME surgery to a partial or total resection of adjacent pelvic organs or applying IORT, as this can result in substantial postoperative complications and is associated with the need for reinterventions.[101] Back-table FGI correctly predicted five out of six tumor-negative CRMs, which might have

prevented unnecessary IORT application in one patient. In contrast, one close margin of 1.4 mm of was identified as tumor-positive based on fluorescence. Although currently a tumor-positive margin is defined as tumor cells ≤1 mm of the CRM, this definition is under debate, as both patients with a CRM of 0.0 – 1.0 mm and 1.1 – 2.0 mm are shown to have an equally increased 2-year risk of local recurrence and distant metastases.[89,102]

Application of fluorescence may highlight the location of a (potentially) tumor-positive CRM, which allows the surgeon to perform more 'targeted' intraoperative frozen section analysis.

FGI may also support the pathologist by differentiating tumor from healthy tissue, i.e. fluorescence-guided pathology. Currently, tissue sampling is performed by gross examination of the surgical specimen and tissue slices, which can be challenging as the tissue architecture is changed by nCRT. Using the fluorescence-grid analysis, we showed a tumor-to-background ratio of 4.7 ± 2.5 on tissue slices, with a high sensitivity (96.2%) and specificity (80.4%) for tumor detection. A fluorescence cut-off value provides more objective information and may enable targeted tissue sampling, potentially saving labor, time and money. In addition, the fluorescence-grid analysis can be used to evaluate tracer biodistribution and can easily be implemented on other closed-field imaging devices.

This study has several limitations. First of all, the number of patients included for CRM evaluation was relatively low, as this was a retrospective proof-of-concept analysis of a clinical trial evaluating molecular fluorescence endoscopy (NCT01972373), and imaging techniques as well as ex vivo imaging procedures have developed throughout the study. Second, a dose-escalation was not incorporated in this study design. Currently available evidence from two bevacizumab-800CW dose-escalation studies suggests that increasing the dose above microdosing levels may result in higher tracer accumulation without significantly increasing background fluorescence.[13,104] This may further improve the detection of tumor-positive CRMs that are based on small tumor deposits, which proved to be challenging in one of our patients.

We propose a standardized imaging protocol that can be used in future research and for the development of FGI, based on our findings in the current study and our recently reported analytical workflow (Figure 5).[104] Fluorescence imaging is performed at fixed time-points. First, when feasible, intraoperative fluorescence-guided surgery is performed. After resection, back-table FGI of the fresh surgical specimen is performed to evaluate the resection margin status, preferably using a closed-field imaging. In case high fluorescence is observed during intraoperative or back-table FGI, several treatment options can be considered, such as frozen section analysis, an additional or extended resection, IORT or potentially more innovative treatment modalities like photo immunotherapy.[93] Subsequently, to correlate fluorescence

with histology, fluorescence imaging is performed during histopathological processing: of the fresh surgical specimen formalin-fixed tissue slices and paraffin-embedded tissue sections. Additionally, fluorescence microscopy can evaluate local tracer accumulation. Altogether, this can give more insight in tissue biodistribution, important for tracer or drug development, or to evaluate potential off- and on-target effects of fluorescent tracers. We believe such a standardized imaging protocol is widely applicable for the validation of FGI in different tumor types and with different fluorescent tracers.

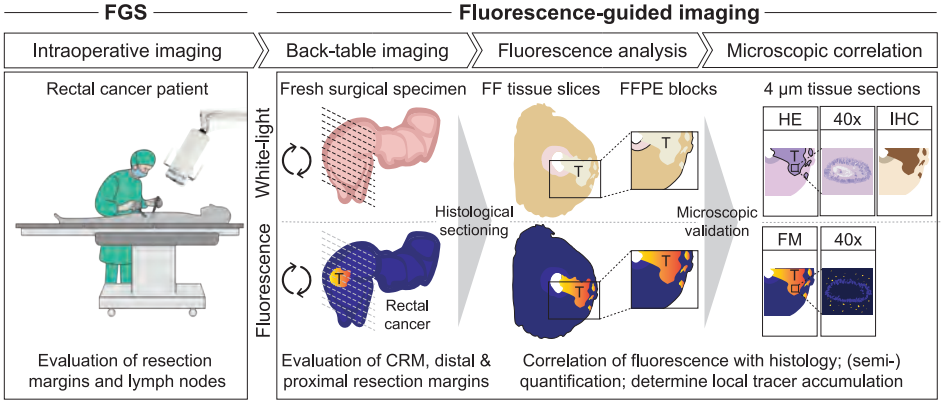

Figure 5. Proposed data collection and data analysis design for resection margin evaluation. Fluorescence-guided surgery is performed to evaluate resection margins and identify potential lymph nodes and/or peritoneal metastasis. Subsequently back-table fluorescence-guided imaging of the fresh surgical specimen is performed to evaluate resection margins, and further fluorescence analysis of tissue slices, formalin-fixed paraffin-embedded (FFPE) tissue blocks and tissue sections for cross-reference and correlation of fluorescence with histology. *T* tumor, *HE* hematoxylin and eosin, *IHC* immunohistochemistry, *FM* fluorescence microscopy.

In conclusion, our study shows the high potential of back-table FGI using the near-infrared fluorescent tracer bevacizumab-800CW targeting VEGFA for margin evaluation at the surgical theatre in patients with LARC. The technique itself proved to be safe, feasible, and shows potential to guide intraoperative clinical decision-making with a high sensitivity in patients with a threatened tumor-positive resection margin. A phase II study using a standardized imaging protocol is in development to confirm these results. Future studies will provide evidence if FGI will be beneficial for all patients, or will only be applied in selected cases to guide clinical decision-making.

Disclosures: The research leading to these results was supported by a personal grant from the Dutch Cancer Society (WBN; RUG2012-5416), a grant from the European Community's Seventh Framework Program (MK, GMvD; FP7/2007-2013 BetaCure project; n°602812), and by unrestricted research grants from SurgVision BV (GMvD, WBN) and Boston Scientific (WBN). GMvD is member of the scientific advisory board of SurgVision BV, founder, shareholder and CEO of TRACER Europe BV (Groningen, The Netherlands). No other potential conflicts of interest relevant to this article exists.

Acknowledgements: We would like to thank the contribution of the personnel working at the endoscopy suite, the surgical theatre and the pathology department for their assistance at all study procedures. Special thanks to W. Boersma-van Ek for her technical assistance in the laboratory.

SUPPLEMENTAL MATERIALS AND METHODS

Fluorescence grid analysis

Tumor locations were delineated on 4 µm HE stained tissue sections by a board-certified gastrointestinal pathologist, who was blinded for fluorescence imaging results. The histological delineation was merged with the high-resolution fluorescence images of the formalin-fixed tissue slices (Odyssey CLx), to enable a direct correlation of fluorescence with histology. Subsequently, a fluorescence grid analysis was performed, which was adapted from Gao et al.[106] A 3 x 3 mm grid was drawn on the merged image using ImageStudio software (version 5.0, LI-COR Biosciences Inc., Lincoln, NE, USA), dividing it into identical 9 mm^2 squares. Each square was classified as tumor-negative or tumor-positive if more than 20% of the square consisted of tumor-tissue, based on the histological delineation. ImageStudio software automatically calculated mean fluorescence intensities (MFI) for each square. A receiver operating characteristics (ROC) curve was determined per patient and for all patients combined, to determine an optimal cut-off value for tumor detection based on optimal sensitivity and specificity as determined by Youden's J statistics.

Three-dimensional tissue analysis by light-sheet fluorescence microscopy.

Light-sheet fluorescence microscopy enables a multicolor 3D analysis of optical transparent whole-mount tissue specimen at cellular resolution. Tissue slices were formalin fixated, dehydrated, and incubated in an organic clearing solution (one-part benzylalcohol & two-parts benzylbenzoate, incubation condition: 24-48 hours, 4°C, dark) to obtain high optical tissue transparency. Subsequently, the fluorescence signal intensity of bevacizumab-800CW as well as the tissue autofluorescence (providing detailed morphological tissue information) were measured within the cleared rectal cancer tissue using a commercially available light-sheet microscope (UltraMicroscope II, LaVision Biotec GmbH, Bielefeld, Germany). The obtained fluorescence imaging results were visualized as single and co-registered data sets, combining information of drug penetration/accumulation with morphological tissue context. In addition, the performed virtual 3D tissue analysis was also correlated to conventional histology.

Fluorescence imaging parameters

Throughout the study, the same imaging parameters were used for data acquisition per imaging device. In case of saturation of fluorescence images, the fluorescence exposure time or gain was decreased to ensure adequate data collection.

SUPPLEMENTAL TABLES AND FIGURES

Supplemental Table 1. Contingency table.

	Tumor-positive CRM	Tumor-negative CRM	Total
High fluorescence	1	1*	**2**
Low fluorescence	1**	5	**6**
Total	**2**	**6**	**8**

A qualitative evaluation of fluorescence intensities was performed on the fresh surgical specimens. Low fluorescence was assessed as a homogenous background fluorescence; localized increased fluorescence was assessed as high fluorescence. *Distance to the circumferential resection margin (CRM) of 1.4 mm. **Tumor-positive CRM based on isolated microscopic tumor deposits £ 1 mm of the CRM.

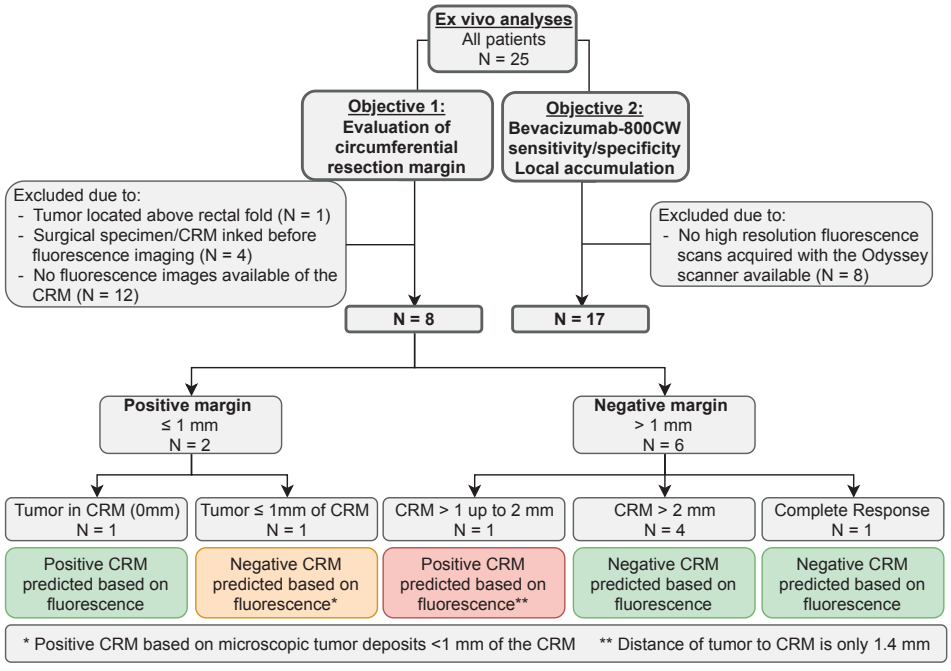

Supplemental Figure 1. Flow diagram of the study. Flow diagram of the study. From 25 patients, eight patients were included in this explorative analysis for the use of back-table fluorescence-guided imaging to evaluate the circumferential resection margins (CRM) status on the fresh surgical specimens. Out of two tumor-positive margins, one was identified correctly using back-table, whereas the other was considered tumor-negative, despite the presence of (sub)millimeter tumor deposits <1 mm of the CRM. Five out of six tumor-negative CRMs were identified correctly. The remaining CRM was identified to be tumor-positive based, although the CRM was marginally negative CRM with 1.4 mm. Seventeen patients were included to determine the sensitivity and specificity of bevacizumab-800CW and evaluate local tracer accumulation, including the eight patients included for CRM evaluation.

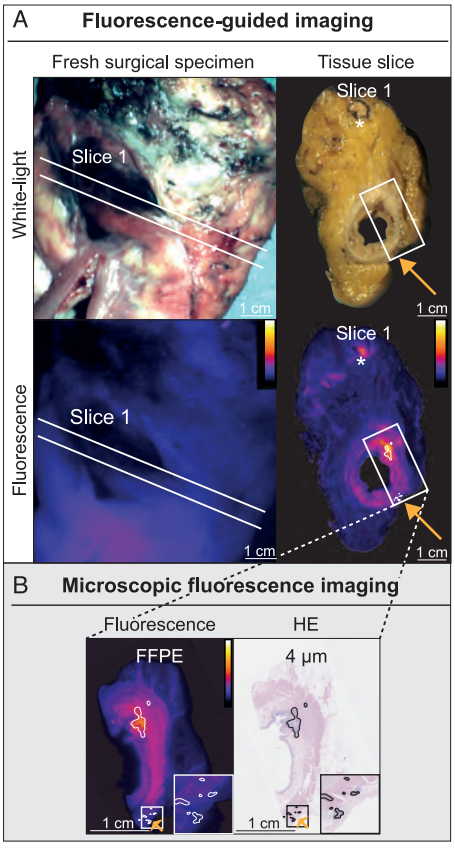

Supplemental Figure 2. Tumor-positive CRM with low fluorescence intensities during back-table FGI. Low fluorescence intensities during back-table FGI of the fresh surgical specimen and fluorescence imaging of a subsequent tissue slice (**A**). The orange arrows indicate the location of the tumor-positive CRM that was based on isolated microscopic tumor deposits as determined on final histopathology (**B**). The asterix (*) indicates a tumor-positive lymph node. *FFPE* formalin-fixed paraffin-embedded, *HE* hematoxylin and eosin.

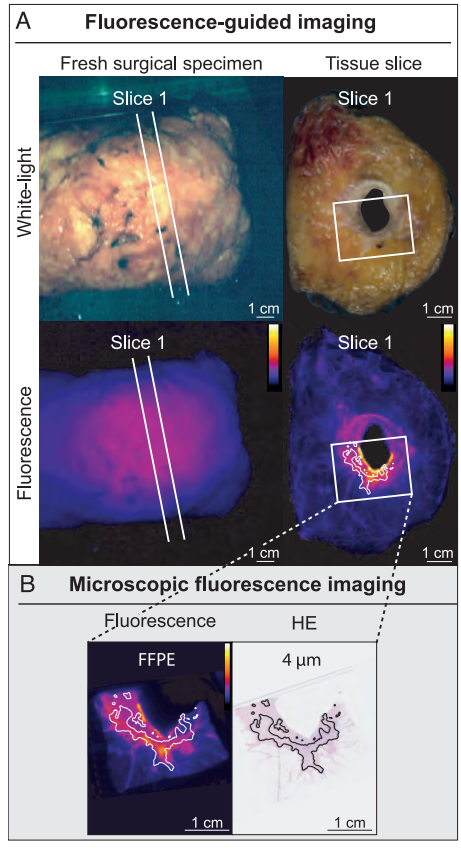

Supplemental Figure 3. Tumor-negative CRM with low fluorescence during back-table FGI. Low fluorescence intensities during back-table FGI of the fresh surgical specimen. A corresponding tissue slice shows high fluorescence at the location of the luminal tumor, though low fluorescence near the CRM (**A**), which was confirmed during microscopic fluorescence imaging and correlated to histology (**B**). *FFPE* formalin-fixed paraffin-embedded, *HE* hematoxylin and eosin.

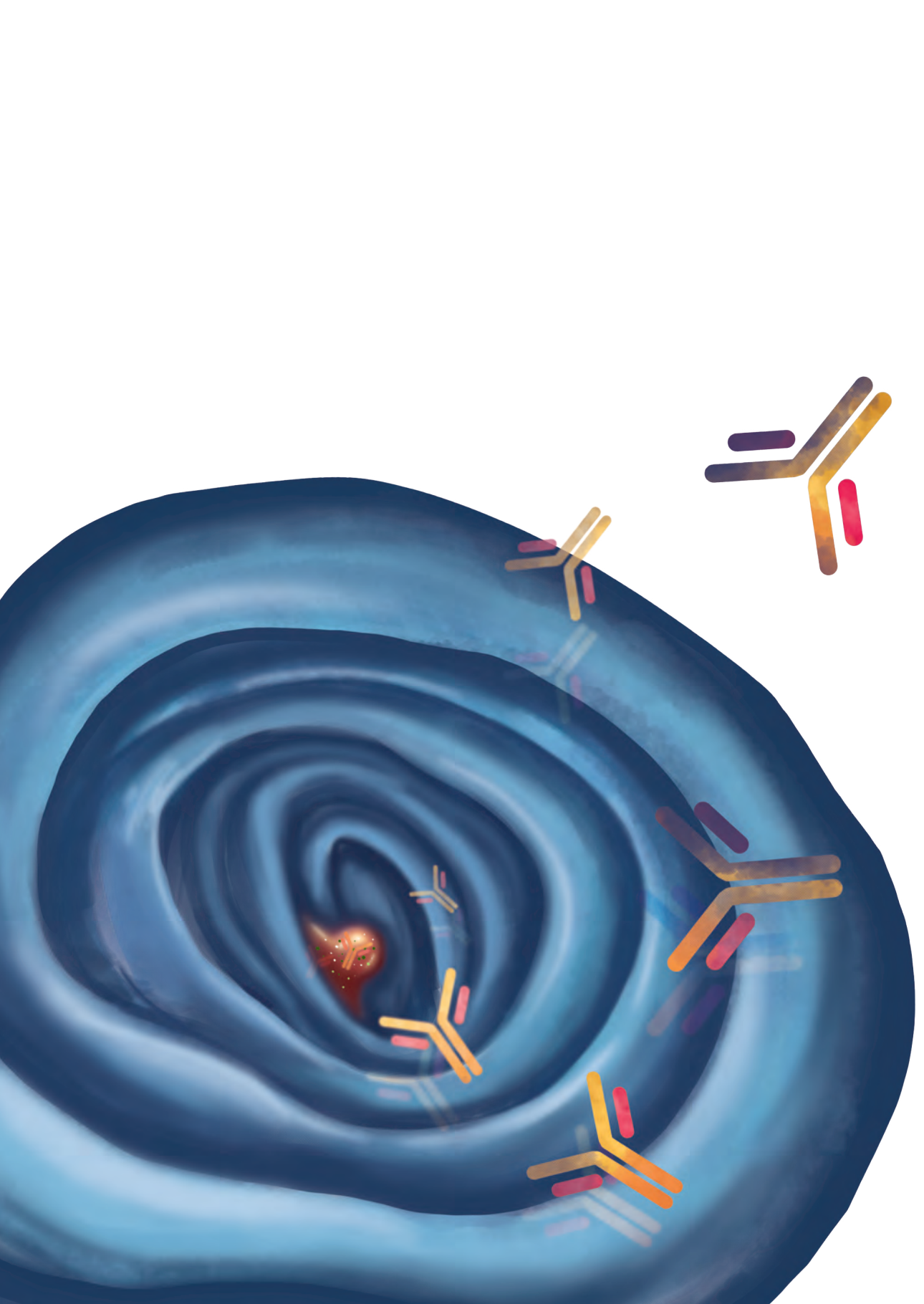

Chapter 7

Summary, general discussion and future perspectives

SUMMARY

In **chapter 1** we provide a short introduction and outline of this thesis. **Part I** describes the validation of molecular fluorescence endoscopy (MFE) for screening purposes. In **chapter 2** we describe the search for targets suitable for MFE and the preclinical validation of MFE. The protein expression of VEGFA and EGFR was determined by immunohistochemistry in a large subset of archival human colorectal samples (hyperplastic polyps, sporadic adenomas, sessile serrated adenomas/polyps, and adenomatous and carcinomatous tissue of patients with Lynch syndrome). VEGFA showed a high protein expression (79-96%), especially in sessile serrated adenomas/polyps and Lynch adenomas, and is therefore an interesting target for endoscopic screening purposes in high-risk patients, while EGFR was overexpressed in only approximately 50% of all adenoma lesions. A MFE procedure was simulated with VEGFA- and EGFR-targeted intraperitoneal xenograft tumors stitched in a human colon specimen. This showed the feasibility to visualize colorectal lesion in real-time, using our in house developed fluorescence endoscopy platform combined with VEGFA- and EGFR-targeting NIR fluorescent tracers.

In **chapter 3** a dose-escalation study is described in seventeen patients with familial adenomatous polyposis (FAP), who have a high probability of occurrence of colorectal adenomas. Eight patients received 4.5 mg, three patients 10 mg and another six patients 25 mg bevacizumab-800CW intravenously, three days later followed by MFE. For all three tracer-dose cohorts, VEGFA-targeted MFE visualized all adenomas concurrently identified with white-light HD inspection (sensitivity 100%). However, fluorescence visualization improved in the 25 mg dose cohort, as very small dysplastic adenomas showed high in vivo fluorescent contrast even at video rate. These finding were confirmed by fluorescence quantification by multi-diameter single fiber reflectance and single fiber fluorescence (MDSFR/SFF) spectroscopy, with the highest adenoma-to-normal ratio of 1.84 for the 25 mg cohort. Ex vivo fluorescence analyses demonstrated NIR fluorescence within the dysplastic areas of the adenomas. This study suggests that VEGFA-targeted MFE is clinically feasible as a real-time, red-flag technique for colorectal adenoma detection. Therefore, this first feasibility and dose-finding study, paves the way to start a study in high-risk patients like those with Lynch syndrome, to objectify its ‘red-flag’ ability in identifying and improving detection rate of flat and depressed adenomas.

Part II of this thesis describes imaging in patients with locally advanced rectal cancer (LARC). In the clinic, LARC patients undergo a pelvic magnetic resonance imaging (MRI) scan for locoregional staging and a computed tomography (CT) scan of chest and abdomen for detection of distant metastases. This is followed by neoadjuvant chemoradiotherapy. The international guidelines recommend re-assessment of the primary tumor and circumferential resection margin (CRM) prior to surgery with digital rectal examination, MRI scan and

proctoscopy. At the time the study in **chapter 4** was published, a preoperative restaging CT scan of chest and abdomen to rule out distant metastases was not recommended in the international guidelines.[107] Since formerly non-detectable distant metastases may appear in the time interval between diagnosis and surgery (at least eleven weeks), we performed a retrospective study in a homogenous cohort of LARC patients (*n* = 153) determining the value of restaging CT scan after neoadjuvant chemoradiotherapy. In 11% of patients a change in treatment strategy was made due to the detection of new metastases on the restaging CT scan. On average, 10 restaging CT scans could spare 1 patient from rectal surgery. This is relevant, as total mesorectal excision (TME) of rectal cancer has a high morbidity (up to 31%) and mortality rate (up to 1.6%).[22] These results underscore the relevance of the CT scan after neoadjuvant chemoradiotherapy in patients with LARC. Two years after this publication, the guidelines were updated and restaging CT scan is now recommended in patients with more advanced cT4 cancers, threatened CRM and the presence of extramural venous invasion (EMVI), within 3 months of original staging to exclude metastatic disease prior to surgery.[108]

In total, 15-27% of LARC patients respond so well to neoadjuvant chemoradiotherapy that pathological examination of the surgical specimen shows no residual tumor, *i.e.* a pathological complete response (pCR; ypT0N0). A series of studies have suggested that these patients could benefit from watchful waiting instead of the standard TME.[17] It seems to result in good local disease control and may lead to organ preservation in nearly 80% of watchful waiting patients.[109] This watchful waiting strategy is carried out by experienced centers, but is not yet standard clinical care. Unfortunately, it is difficult to select patients who might benefit from watchful waiting. On one hand, tumor response can be overestimated by for example tumor fragmentation, reflected in the 16-28% of watchful waiting patients that showed tumor regrowth.[108-110] On the other hand, tumor response can be underestimated due to poor discrimination between residual tumor and radiation-induced fibrosis. Namely, in 9-16% of patients with suspected residual tumor by MRI and white-light endoscopy no tumor is detected in the surgical resection specimen.[15-17] In **chapter 5** we evaluate whether VEGFA-targeted quantitative fluorescence endoscopy (QFE) (i.e. MFE together with MDSFR/SFF spectroscopy in vivo) could aid in clinical response assessment by identifying residual tumor in 25 patients with LARC after neoadjuvant chemoradiotherapy. The QFE measurements were compared to the findings of clinical restaging (MRI scan and white-light endoscopy) and correlated to gold standard: pathological staging of the surgical specimen. We observed an initial positive predictive value of 95% for QFE, 87.5% for MRI, and 90% for white-light endoscopy; and accuracy of 92% for QFE, 84% for MRI, and 80% for white-light endoscopy. This shows that QFE can assess residual tumor in patients otherwise considered as having a potential complete response. QFE would have changed the restaging diagnosis correctly in 4 of 25 patients (16%). This study shows that VEGFA-targeted QFE has the potential to improve the identification of patients with residual disease and complete response.

As the VEGFA-targeted QFE took place at day of surgery to enable direct correlation to histopathology, we decided to image the NIR fluorescence of the surgical specimen immediately after surgery: back-table fluorescence-guided imaging (FGI). A tumor-negative circumferential resection margin (CRM) is the cornerstone for curative treatment, but tumor-positive margins are detected in up to 18% of LARC patients. Therefore, we wanted to evaluate the feasibility of optical molecular imaging as a tool for the surgeon and pathologist to evaluate the CRM peri-operatively. This proof-of-concept side study is described in **chapter 6**. First, fluorescence intensities of fresh surgical specimens (n = 8) were retrospectively correlated to standard histopathology. Of the 2 patients with a tumor-positive CRM (tumor ≤1 mm of the CRM), 1 was correctly identified with FGI. The other did not show increased fluorescence, possibly because there were only (sub-)millimeter tumor deposits within 1 mm of the CRM. FGI correctly identified negative CRMs in 5 out of 6 patients with a tumor-negative CRM. The one patient with negative CRM that showed a fluorescent spot at back-table imaging underscored the sensitivity of the technique, as tumor was present at 1.4 mm distance of the CRM. Second, to determine the sensitivity and specificity of bevacizumab-800CW for tumor detection, a mean fluorescence intensity (MFI) cut-off value was determined on the formalin-fixed tissue slices (n = 42, 17 patients). Local tracer accumulation was evaluated by fluorescence microscopy. ROC analysis of fluorescence intensities of formalin-fixed tissue slices gave an optimal MFI cut-off value for tumor detection of 5085 (sensitivity and specificity of 98.2% and 76.8% respectively). Bevacizumab-800CW enabled a clear differentiation between tumor and normal tissue up to a microscopic level, with a tumor-to-background ratio of 4.7 ± 2.5 (mean ± SD). These results show the potential of back-table FGI to evaluate the CRM status in LARC patients. Optimization of this technique with adaptation of standard operating procedures could change perioperative decision-making with regard to extending resections or applying intraoperative radiation therapy in case of positive CRMs.

GENERAL DISCUSSION AND FUTURE PERSPECTIVES

Clinical translation beyond proof-of-concept

The two clinical studies described in this thesis are early-phase trials addressing safety, feasibility and dose finding for optimal fluorescence imaging. As we were one of the first conducting clinical studies toward optical molecular imaging, no framework let-alone guideline was available. In the following years, we and others obtained experience with working with fluorescence imaging devices (e.g. calibration and threshold-adjusting), fluorescence image analyses, and comparison with histopathological examination. Recently, discussion sessions and expert meetings were held within the field, resulting in the development of research guidelines and standards.[111-113] This will take research in the field of optical molecular imaging to a higher plan. Now the time has come to confirm the use of optical molecular imaging in larger patient populations, ideally as part of randomized controlled trials.

Molecular fluorescence endoscopy (MFE) is capable of visualizing targeted fluorescent lesions in a wide field-of-view. It is therefore particularly of interest to use in screening programs, in a selected category of patients at high-risk of developing dysplasia and/or malignancies. For example, a multicenter randomized controlled trial with cross-over design could address the effect of MFE on the adenoma detection rate and the clinical benefit in patients with Lynch syndrome.

Quantitative fluorescence endoscopy (QFE) does not only visualize fluorescence qualitatively, but can also quantify the intensity of the fluorescence signal using multidiameter single fiber reflection and single fiber fluorescence (MDSFR/SFF) spectroscopy. As sometimes the fluorescence signal is hard to judge because of tissue optical properties, QFE can still measure its presence and is therefore imperative in for example restaging setting. In **chapter 6** we showed that QFE could aid in clinical response assessment in patients with locally advanced rectal cancer (LARC). It can assess residual tumor in patients otherwise considered as having a potential complete response, or can give extra arguments in selecting patients suitable for non-operative management. These promising results make QFE of interest for larger prospective studies towards response evaluation.

However, non-operative management of patients with LARC that showed a good response to neoadjuvant chemoradiotherapy (nCRT), i.e. watchful waiting, is currently not part of standard clinical care. Evidence in favor for watchful waiting is based on small-to-moderate sized patient series from specialized centers. It seems to result in good local disease control and may lead to organ preservation in nearly 80% of patients, it is associated with good survival rates and a reduction of long-term morbidity by avoiding surgery.[93,109] Nevertheless, concerns are raised for watchful waiting patients who develop local tumor regrowth, as they show a

higher incidence of distant progression compared with the patients that did not show local regrowth; and they have a worse survival compared with pCR patients.[112] Recently, a large-scale registry of pooled individual patient data has started, the International Watch & Wait Database (IWWD), to provide the necessary data in the future.[93] It would be worthwhile to incorporate QFE in a study setting in patients opting for a watchful waiting strategy to further assess the positive and negative predictive value of QFE.

Future perspective on back-table FGI

As for back-table fluorescence guided imaging (FGI), we proposed an imaging study protocol in **chapter 6** which can be used for the development of fluorescence-guided imaging in different tumor types and with different imaging probes. This set-up enables correlation of observed fluorescence to histology from a macroscopic to a microscopic level. It gives insight in tracer distribution in the tissue of interest and can evaluate potential off- and on-target effects of fluorescence tracers. We do not specifically recommend the use of specific imaging devices or acquisition parameters, but we emphasize the need for standardization in fluorescence imaging, i.e. similar imaging parameters and procedures.

Currently, when surgeons are in doubt if the CRM is free of tumor, biopsies are taken and send to the pathology department for frozen section analysis. This is time-consuming and labor-intensive as the surgeons and anesthesiologist should wait and pathologists should always be on-call. Back-table FGI is way faster as it is performed at the operating theater, requires several minutes for image acquisition, followed by evaluation of the fluorescence images to judge the CRM status by the surgeon. Ultimately however, this technique may even improve the surgical workflow in terms of time and quality as it can potentially prevent second surgery and improve tumor-negative resection margin rates.

A subsequent study would need to determine which cases benefit the most. We can only hypothesize that the main added value of back-table FGI may lie in the cases with for example a close margin on preoperative imaging modalities, when the surgeon has doubts on the CRM status intraoperatively, or for very distal LARCs.

MDFSFR/SFF spectroscopy in drug- and tracer development

We envision a crucial role for MDSFR/SFF spectroscopy, embedded in QFE or as stand-alone device, in future drug- and tracer development. When new drugs are developed, blood samples are taken to give insight in the pharmacokinetics and pharmacodynamics of the drug. Sometimes whole-body information on drug distribution is available by positron emission tomography (PET) imaging, which can be related to target expression when biopsies are also taken. However, MDSFR/SFF spectroscopy measures drug's concentrations at selected target sites in vivo. By measuring the in vivo local drug accumulation, it can support the

identification of the optimal dose in a dose-escalation study design. For example, in chapter 3 it showed us that raising the bevacizumab-800CW dose from 10 to 25 mg, raised the tracer availability at the target site with 40% (from 0.48 mmol/mL to 0.69 mmol/mL). Meanwhile, the intrinsic fluorescence intensities of normal tissue remained constant. This was helpful in determining the optimal bevacizumab-800CW tracer dose.

MDSFR/SFF spectroscopy could also play a role in personalized medicine. Many targeted drug therapies are developed, but only a limited number of patients benefit from these therapies. The percentage of non-responders is often high. When MDSFR/SFF spectroscopy could measure if the targeted drug reaches its target site in a patient, it might help selecting the patients that benefit from the particular drug, guiding individualized patient care. Also, it can give insight in heterogeneous expression of a drug target within a tumor, which has shown to predict therapy failure in some tumor types.[113] Thus, it provides tailored treatment based on individual tumor target expression, target engagement, and response for each patient.

MDSFR/SFF spectroscopy can also be valuable in the development and characterization of optical imaging devices. For example, in chapter 3, our MFE device was sensitive enough to visualize fluorescent adenomas in real-time at a bevacizumab-800CW dose of 25 mg. MDSFR/SFF spectroscopy measured the corresponding amount of intrinsic fluorescence and calculated the adenoma-to-normal ratio, and in this way provided us more objective information on the performance of our MFE device. The ratios usually given in fluorescence studies provide information on the contrast that can be gained in the images of the imaging device, rather than the in vivo available contrast, as they are obtained from reflectance images. MDSFR/SFF spectroscopy provides an objective way to value the performance of a fluorescence imaging device.

Future fluorescent tracer development

The ideal optical imaging probe has a high affinity toward the molecular target, a rapid clearance from non-target tissue, a favorable pharmacokinetic profile and a safe toxicity profile. IgG monoclonal antibodies like bevacizumab have a high functional affinity for their target antigen, and are therefore of interest for tracer development. Antibody fragments, proteins, peptides, aptamers, small molecules and nanoparticle conjugates are also under investigation in different optical imaging studies. With different size range comes different binding and pharmacokinetic properties.

The only FDA-approved fluorophore so far is fluorescein, which emits fluorescence in the visible light spectrum (515 nm). There is however great interest in fluorophores that emit fluorescence in the near-infrared (NIR) light spectrum, like IRDye800CW. One advantage

is the relatively low tissue autofluorescence in the NIR light spectrum, improving in vivo contrast. Also, photon absorption characteristics of especially hemoglobin are minimal in the NIR light spectrum, which is beneficial for penetration depth. The ideal fluorophore has a high quantum yield, is chemical and photostable and has a narrow excitation and narrow emission spectrum that are spectrally separated.

Next level optical imaging probes that are in development are smart activatable probes (who are fluorescent only after for example enzymatic cleavage or cellular internalization) and theranostic probes (simultaneous diagnosis and treatment) such as used in photoimmunotherapy. Also, multimodal tracers are in development, tracers that can be visualized by different techniques, for example a fluorophore probe combined with a PET probe.

Route of administration

The route of administration of the tracer depends on pharmacokinetic profile as well as the imaging purpose. Intravenous injection is required when the imaging surface is rather large, for example in diagnostic endoscopic screening of the colon and rectum. This is also the case when deep tissue penetration is needed, to for example endoscopically determine presence of tumor remnant in deeper layers of the intestinal wall. Topical spraying is well possible on smaller surfaces such as diagnostic or therapeutic fluorescence endoscopy of the esophagus.[99] Evaluation of the circumferential resection margin (CRM) after oncological surgery using fluorescence guided imaging (FGI) is in this thesis performed after intravenous administration of the optical tracer. It is op interest if topical spraying the tracer reaches sufficient penetration depth (at least 1 mm) to reliable evaluate the CRM. This would enable the use of FGI also in patients where doubt has arisen on the CRM status during surgery, additional to patients that are selected already with (re)staging modalities.[114]

Tracer dose

Most likely the optimal tracer dose will have to be determined per tracer, organ of interest and indication. A dose must be low enough to minimize potential; adverse events, and high enough to gain sufficient contrast in vivo.

Bevacizumab-800CW

As for the tracer bevacizumab-800CW itself, the results presented in this thesis show it is a suitable optical imaging tracer for many diagnostic purposes. It can play an important role in gastrointestinal endoscopic screening, whereas its target vascular endothelial growth factor A (VEGFA) is known to be upregulated already early in the colorectal adenoma-carcinoma sequence and our immunohistochemistry results demonstrated high VEGFA expression in high-risk adenomas such as sessile serrated adenomas/polyps (SSA/P) and low- and high-

grade dysplastic adenomas of patients with Lynch syndrome.[14] Moreover, bevacizumab-800CW can be used outside the gastrointestinal tract, as VEGFA is highly upregulated in the microenvironment of many solid tumors.[95] The imaging probe has already successfully been used in breast cancer and Barret esophagus, and it is currently evaluated in esophageal cancer (NCT03558724), pancreatic cancer (NCT02743975), cholangiocarcinoma (NCT03620292), sarcomas (NCT03913806), head and neck squamous cell carcinoma (NCT03134846) and sinosal inverted papilloma (NCT03925285).[14,50,98,99,115]

Future technical developments

Refining of wide-field endoscopic fluorescence visualization

The MFE approach used in this thesis is probe-based: it consists of a small fiber bundle that can be inserted in the working channel of a clinical video endoscope. The advantage of this approach is that it meets the current clinical standards for endoscopic surveillance; it adds sensitive molecular fluorescence to the clinical standard of high-definition white-light images in real time. Moreover it is safe, fast and relatively inexpensive.[27] The choice for an approach that uses a tracer that emits fluorescence in the near-infrared (NIR) light spectrum makes it technically feasible to concurrently capture full visible light as well as NIR fluorescence, allowing us to superimpose fluorescent signals on the morphologic images without sacrificing visible light image quality.

However, the existing technical set-up can still be optimized. First, the fiber bundle has a field of view of 85°, versus 140° of general clinical video endoscopes, so there is space for technical improvement. Second, the image quality of the optical fiber bundle declines by regular use, as single-fibers can break. We are developing a standardization method to test the quality of optical imaging fibers, to guarantee quality control. Third, the current fiber bundle contains 30,000 single fibers, thus providing a wide-field fluorescence image of 30,000 pixels, versus the high-definition images of the video endoscope. Ideally, at this moment in time when highly sensitive NIR-CCDs are developed that fit in the tip of a video endoscope, our probe-based approach can be changed into an endoscope-based approach. Furthermore, software can be developed that scan for NIR fluorescence and warn the endoscopist or surgeon when fluorescence is detected above a certain threshold. In this way the human factor is reduced, there is less dependency on operator expertise.

Standardization of fluorescence imaging devices

Optical molecular imaging is a rather new and fast-evolving research field where many early phase trials have been established, predominantly for intraoperative guidance in oncological surgery. All these trials use different fluorescence imaging devices. One can easily compare the technical parameters of imaging devices such as field-of-view, camera and spatial resolution, wave-lengths and sensitivity, but their overall performance, for example their

performance in relation to factors such as tissue optical properties and light illumination homogeneity, is difficult to test or to compare.[116] Several standardized assessments, varying from simple to composite fluorescent phantoms, are under development to correct and benchmark fluorescence imaging devices.[117-119] To date, no widely accepted standard phantom for optical imaging or minimum requirements for device performance exist. One broadly accepted standardization would be an important step forward in clinical translation of fluorescence imaging devices, as it enables a better comparison, offers quality control and in the future even data referencing.

Fluorescence interpretation and quantification

As propagation of light through tissue is influenced by tissue optical properties such as photon scattering and photon absorption (mainly by hemoglobin), reliable fluorescence interpretation, let alone quantification, cannot be performed on the images gained with wide-field fluorescence visualization.[120] There are methods in development to concurrently capture and revert the effect of optical properties on the fluorescence images, to make fluorescence interpretation more reliable.[121] However, this is still in an early stage and improvements need to be made for more accurate acquisition and better fitting, and it needs to be greatly accelerated before it can be applied during real-time fluorescence visualization in clinical setting.

A different and far more reliable fluorescence quantification approach is spectroscopy. In this thesis multidiameter single fiber reflection, single fiber fluorescence (MDSFR/SFF) spectroscopy is used. This technique point-measures the fluorescence and corrects it for scattering and absorption.[13,14] The imaging probe is held directly onto the tissue of interest and measures two different reflection spectra via concentric rings (using a small and a large diameter), see Figure 1. This is immediately followed by one fluorescence spectrum measurement. From the reflectance spectra, the scattering and absorption coefficients are determined, which are used to correct the raw fluorescence signal, resulting in the intrinsic fluorescence.[13,57-59] The intrinsic fluorescence can afterwards be used to approximate the actual tracer concentration present in the tissue, with the assumption that the in silico measured fluorescence quantum yield and extinction coefficient of the fluorescent tracer are representative for the in vivo conditions. Therefore, it is an ideal technique to be used in tracer- and drug development.

At the moment, we are testing if it is possible to endoscopically perform deep tissue MDSFR/SFF spectroscopy measurements. The spectroscopy probe is led into the tissue of interest via a needle, comparable to endoscopic ultrasound guided via fine needle aspiration (FNA). In this way fluorescence measurements could be performed on cancer tissue located in for example the submucosa of the rectum wall.

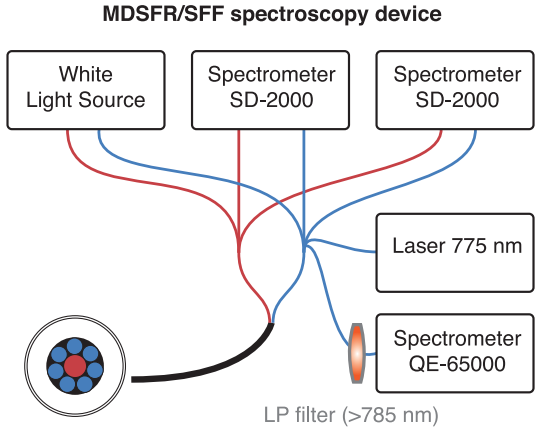

Figure 1. Schematic representation of the MDSFR/SFF spectroscopy device.

Clinical implementation of optical molecular imaging

Moving the research field forward toward clinical implementation is a big challenge, since it encounters many hurdles like choosing the device, the tracer, arranging funding and obtain FDA approval. Consultation of the FDA taught us that optical molecular imaging is considered as a significant risk, as it takes place in real-time. Therefore, patient benefit needs to be established before an application for FDA approval can be filed. So far, there is only one study showing beneficial outcome.[122] As clear clinical endpoints like survival are difficult to establish, detection rate of positive margins after oncological resection can be taken, since the correlation between positive margins, local recurrence and survival is already well established for many types of cancer.[123] Clinical benefit can also be shown if optical molecular imaging confirms tissue sparing, improves intraoperative tumor assessment, and improved pathological assessment. When this is available, FDA approval for clinical use becomes possible.[123, 124]

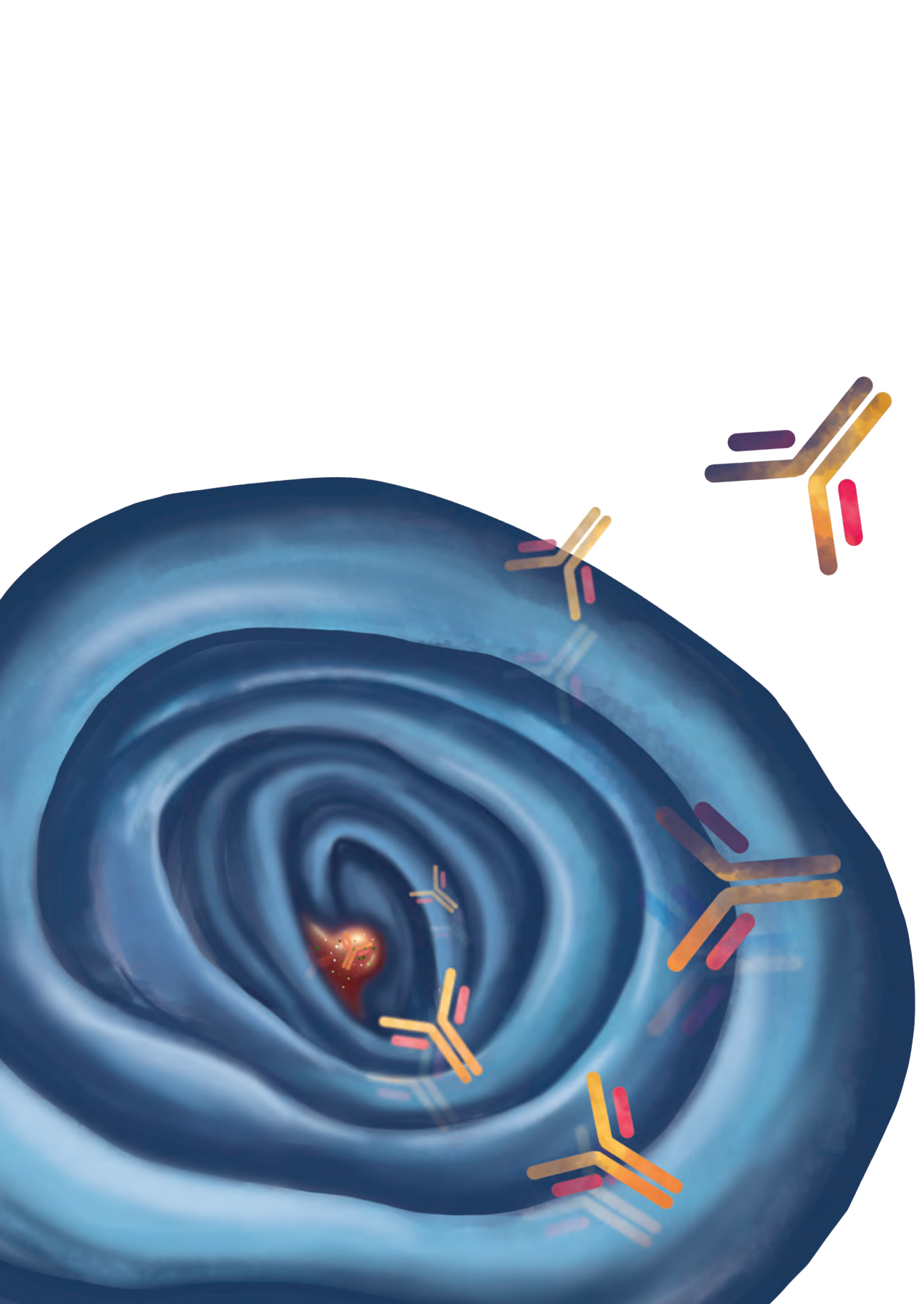

Chapter 8

Nederlandse samenvatting (Dutch summary)

Introductie

Het colorectaal carcinoom is het op-één-na meest voorkomende tumortype wereldwijd. Bij het verbeteren van de uitkomst van patiënten met een colorectaal carcinoom spelen verschillende facetten een rol, waaronder o.a. preventie van ontstaan van kanker door detectie van adenomen, vroegdetectie van laag-stadium colorectale tumoren, optimaliseren van stagering om zodoende de best aansluitende behandeling te kiezen, het bepalen van de respons op behandeling met betrekking tot chirurgische strategie, en het verbeteren van de follow-up.

Ten aanzien van adenomen en vroegdetectie van laag-stadium tumoren is het van belang om een techniek te gebruiken met een optimale sensitiviteit. De huidige gouden standaard is wit-licht endoscopie, waarbij op basis van morfologie en verstoring van de normale architectuur afwijkingen opgespoord worden. Deze techniek is echter suboptimaal, aangezien ongeveer 20-25% van de adenomen gemist worden gedurende endoscopie, hetgeen een bewezen risicofactor is voor het ontstaan van zogenaamde 'intervalcarcinomen', met name in hoog-risico patiënten zoals die met Lynch syndroom.

Voor wat betreft stagering wordt gebruik gemaakt van MRI en CT. Op basis van stagering worden patiënten geselecteerd voor direct chirurgie, vooraf kort neoadjuvant radiotherapie, of een intensiever traject met chemoradiotherapie. Met name in die laatste groep zitten verscheidene uitdagingen die de toekomstige behandeling van het gevorderd rectumcarcinoom zouden kunnen verbeteren. In de eerste plaats was het onduidelijk of restadiering met een CT scan vlak voor de geplande operatie, na afronden van neoadjuvante chemoradiotherapie, zinvol was. Mogelijk zouden hiermee afstandsmetastasen gedetecteerd kunnen worden die tijdens neoadjuvante therapie zijn ontstaan, waardoor een grote chirurgische ingreep mogelijk herzien moet worden. Daarnaast is het moeilijk om de lokale respons op neoadjuvante therapie goed te beoordelen. Het inschatten van de respons op neoadjuvante therapie is van belang voor het bepalen van de uitgebreidheid van chirurgie. Ook zijn er de laatste jaren meer data die suggereren dat ‘watchful waiting’ een veilig alternatief zou kunnen zijn in patiënten die een complete respons hebben op neoadjuvante therapie. Volgens de huidige standaard wordt een MRI-scan gemaakt om de respons op neoadjuvante therapie te evalueren. In studieverband is ook de conventionele wit-licht endoscopie onderzocht. Beide methoden zijn echter suboptimaal, omdat responsevaluatie bemoeilijkt wordt door fibrose, oedeem, en ulcera die ontstaan onder invloed van de neoadjuvante chemoradiotherapie en moeilijk te onderscheiden zijn van tumorresidu.

In dit proefschrift onderzochten we een nieuwe techniek die mogelijk aan zowel het verbeteren van de detectie van premaligne adenomen kan bijdragen, als ook bij het evalueren van de respons op neoadjuvante chemoradiotherapie: optische moleculaire beeldvorming met fluorescente probes, geschikt voor endoscopische detectie. Hierbij wordt gebruikt gemaakt van fluorescent-gelabelde antilichamen die kunnen binden aan een specifiek target. Op die manier kunnen moleculaire eigenschappen met behulp van een fluorescent signaal zichtbaar worden gemaakt. In combinatie met een endoscoop, die geschikt is gemaakt voor zowel fluorescente beeldvorming alsmede verkrijgen van conventionele wit-licht beelden, kan zodoende zowel anatomische als moleculaire informatie in *real-time* in de patiënt worden gevisualiseerd.

We beschrijven in dit proefschrift de ontwikkeling en klinische validatie van deze nieuwe moleculaire fluorescentie endoscopie techniek.

Samenvatting van dit proefschrift

In **hoofdstuk 1** wordt een korte introductie en overzicht van de studies in dit proefschrift gegeven. **Deel I**, bestaande uit hoofdstuk 2 en 3, beschrijft de validatie van moleculaire fluorescentie endoscopie als screenings techniek. In **hoofdstuk 2** is eiwitexpressie van VEGFA en EGFR bepaald met behulp van immuunhistochemie op archiefweefsel van patiënten met hyperplastische poliepen, sporadische adenomen, sessiele adenomen, en adenomen en carcinomen van patiënten met Lynch syndroom. Er bleek verhoogde VEGFA-expressie te zijn in 79-96% van de laesies, afhankelijk van het subtype, met de hoogste expressie in sessiele poliepen en adenomen van Lynch patiënten. Gezien de hoge expressie en de aanwezigheid hiervan in een zeer groot percentage van premaligne laesies, lijkt VEGFA een goed target om de sensitiviteit van endoscopie middels fluorescente imaging te verbeteren. Dit gold in veel mindere mate voor EGFR, hetgeen in slechts 50% van de adenomen tot overexpressie kwam. Ter validatie werd moleculaire fluorescentie endoscopie nagebootst met behulp van intraperitoneale xenograft tumoren die werden vastgehecht in menselijke restweefsel na darmchirurgie. Hierbij werd aangetoond dat het mogelijk is om laesies in het colon of rectum, *real-time* te visualiseren met behulp van het door onszelf ontwikkelde moleculaire fluorescentie endoscopie platform en fluorescente tracers gericht tegen de eiwitten VEGFA en EGFR.

In **hoofdstuk 3** wordt onze moleculaire fluorescentie endoscopie techniek klinisch gevalideerd voor de detectie van colorectale adenomen. In een dosis escalatie studie in 17 patiënten met familiaire adenomateuze polyposis (FAP), die een verhoogd risico hebben op ontstaan van colorectale adenomen, werd de optimale dosis voor fluorescent-gelabeld bevacizumab onderzocht. Patiënten werden geïnjecteerd met 4,5 mg, 10 mg, of 25 mg bevacizumab-800CW, gevolgd door moleculaire fluorescentie endoscopie. Met alle drie onderzochte doseringen was het mogelijk om adenomen te visualiseren, maar de beste resultaten werden bereikt met de dosering van 25 mg, waarbij ook zeer kleine dysplastische adenomen werden gezien. Deze bevindingen werden bevestigd door kwantificatie van het fluorescente signaal *in vivo* met behulp van spectroscopie, hetgeen de hoogste adenoom:normaal ratio opleverde van 1.84 voor het 25 mg cohort. *Ex vivo* analyse toonde fluorescent signaal aan in de dysplastische gedeelten van adenomen. Deze studie toont aan dat moleculaire fluorescentie endoscopie met een tracer gericht tegen VEGFA mogelijk is in een klinische setting, *real-time* informatie kan geven, en kan helpen met detectie van dysplastische poliepen.

Deel II van dit proefschrift, bestaande uit hoofdstuk 4, 5 en 6, betreft studies in patiënten met een lokaal gevorderd rectumcarcinoom. In **hoofdstuk 4** onderzochten we de waarde van een CT-scan voor het restageren van patiënten na afronden van neoadjuvante

chemoradiotherapie. Internationale richtlijnen bevelen aan om na neoadjuvante chemoradiotherapie de primaire tumor en de circumferentiële resectiemarge (CRM) opnieuw in kaart te brengen met een MRI-scan van het bekken, rectaal toucher en proctoscopie. Op moment van publicatie van dit hoofdstuk werd het niet aanbevolen de CT-thorax/abdomen opnieuw te verrichten om eventueel nieuw ontstane afstandsmetastasen in kaart te brengen. Wij onderzochten in een retrospectieve studie in een homogene populatie van patiënten met lokaal gevorderd rectumcarcinoom (n = 153) de waarde van restagering middels CT. In 11% van de patiënten bleek op basis van CT-scan een andere behandelstrategie te zijn gekozen door de detectie van afstandsmetastasen. Het aantal scans om 1 patiënt te sparen van onnodige rectumchirurgie was 10. Gegeven de hoge morbiditeit (tot 31%) en mortaliteit (tot 1.6%) van totale mesorectale excisie een relevante uitkomst, en inmiddels zijn internationale richtlijnen ook aangepast en is restagering standaard geworden voor cT4 tumoren, bedreiging van de circumferentiële resectiemarge, en aanwezigheid van extramurale veneuze invasie.

Daar waar in een deel van de patiënten chirurgie niet zinvol is door het ontstaan van afstandsmetastasen, is er aan de andere kant van het spectrum ook een groep patiënten die een complete respons op neoadjuvante chemoradiotherapie hebben: geen aanwijsbare ziekte meer. Ongeveer 15-27% van de patiënten met gevorderd rectumcarcinoom heeft een complete pathologisch respons (pCR, ypT0N0) bij histopathologisch onderzoek van het resectiepreparaat. In deze patiënten zou mogelijk chirurgie ook achterwege gelaten kunnen worden. Hoewel dit momenteel nog geen standaardbeleid is, laten studies tot op heden goede lokale controle en behoud van orgaanfunctie zien in bijna 80% van de patiënten met een watchful-waiting strategie. Om de kans op lokale terug-groei zo klein mogelijk te maken, is het belangrijk patiënten die in aanmerking kunnen komen voor watchful-waiting heel nauwkeurig te selecteren. Dit is echter lastig, doordat enerzijds de respons soms wordt overschat op beeldvorming door tumor fragmentatie, wat terug te zien is in de 16-28% van de patiënten die terug-groei heeft vanuit tumorresidu. Anderzijds wordt er bij 9-16% van de patiënten waarin op beeldvorming geen volledige respons wordt gezien bij histopathologisch onderzoek alsnog een pCR gezien. Dit laatste kan worden verklaard door fibrose, oedeem, en ulcera die kunnen ontstaan onder invloed van neoadjuvante chemoradiotherapie.

In **hoofdstuk 5** evalueerden we of moleculaire fluorescentie endoscopie met een tracer gericht tegen VEGFA kan helpen bij het vaststellen van respons na neoadjuvante chemoradiatie bij 25 patiënten met een lokaal gevorderd rectumcarcinoom. De fluorescentie werd gekwantificeerd en vergeleken met pathologie als gouden standaard. Er werd een positief voorspellende waarde gevonden voor kwantitatieve fluorescente endoscopie van 95% vergeleken met 87,5% voor MRI en 90% voor wit-licht endoscopie. De accuratesse was 92% voor kwantitatieve fluorescente endoscopie vergeleken met 84% voor MRI en 80% voor wit-licht endoscopie. Kwantitatieve fluorescente endoscopie kon tumorresidu

beter vaststellen dan conventionele technieken, waarbij minder patiënten ten onrechte als complete responder werden geclassificeerd, en toevoegen van deze techniek zou de restageringsdiagnose correct hebben gewijzigd in 4 van de 25 patiënten.

In dezelfde patiënten werd de opname van de fluorescente tracer niet alleen endoscopisch beoordeeld op de dag van chirurgie, maar werd zo mogelijk ook perioperatief fluorescente beeldvorming verricht van het chirurgisch preparaat. Het doel hiervan was om te kijken of de circumferentiële resectiemarge vrij was van fluorescentie, als maat voor vrije snijvlakken. Het is van groot belang een negatieve circumferentiële resectiemarge te hebben bij rectumchirurgie, aangezien een positief snijvlak een sterke voorspeller is voor lokaal tumorrecidief/residu (waarbij een marge van 1 mm of minder als positief wordt beschouwd). Helaas wordt een positieve circumferentiële resectiemarge gezien in tot 18% van de patiënten met een lokaal gevorderd rectumcarcinoom. In **hoofdstuk 6** beschrijven we 8 patiënten waarbij fluorescente beeldvorming van het chirurgisch preparaat werd gecorreleerd aan de standaard histopathologische uitkomsten. Van de 2 patiënten met een positieve circumferentiële resectiemarge werd dit in 1 patiënt correct geïdentificeerd met behulp van perioperatieve fluorescente analyse van het resectiepreparaat. De patiënt zonder positief fluorescent signaal had slechts enkele microscopische tumorveldjes binnen 1mm van de circumferentiële resectiemarge. Dit laat mogelijk de beperkte resolutie van deze techniek bij zeer kleine (<1mm) laesies zien. Van 6 patiënten met een negatieve circumferentiële resectiemarge hadden 5 patiënten ook geen fluorescentiesignaal. De patiënt waarin wel een fluorescent signaal werd gezien had op 1,4 mm van de circumferentiële resectiemarge een tumor, hetgeen de fluorescentie goed kon verklaren. In deze studie werd als validatie nu gekozen voor het meten van fluorescentie in het resectiepreparaat, maar idealiter zou uiteindelijk intra-operatief het inwendige snijvlak in de patiënt gemeten kunnen worden. De uitkomsten van deze studie tonen aan dat er bij aanwezigheid van fluorescentie sterk rekening gehouden moet worden met aanwezigheid van tumor, het is dan immers niet relevant of de dracht van het fluorescente signaal afkomstig is van meer of minder dan 1mm van het resectievlak omdat in de patiënt gekeken wordt. Anderzijds lijkt negatieve fluorescentie aanwezigheid van tumorresidu nagenoeg uit te sluiten, waarbij de techniek echter waarschijnlijk niet sensitief genoeg is voor submillimetrische afwijkingen.

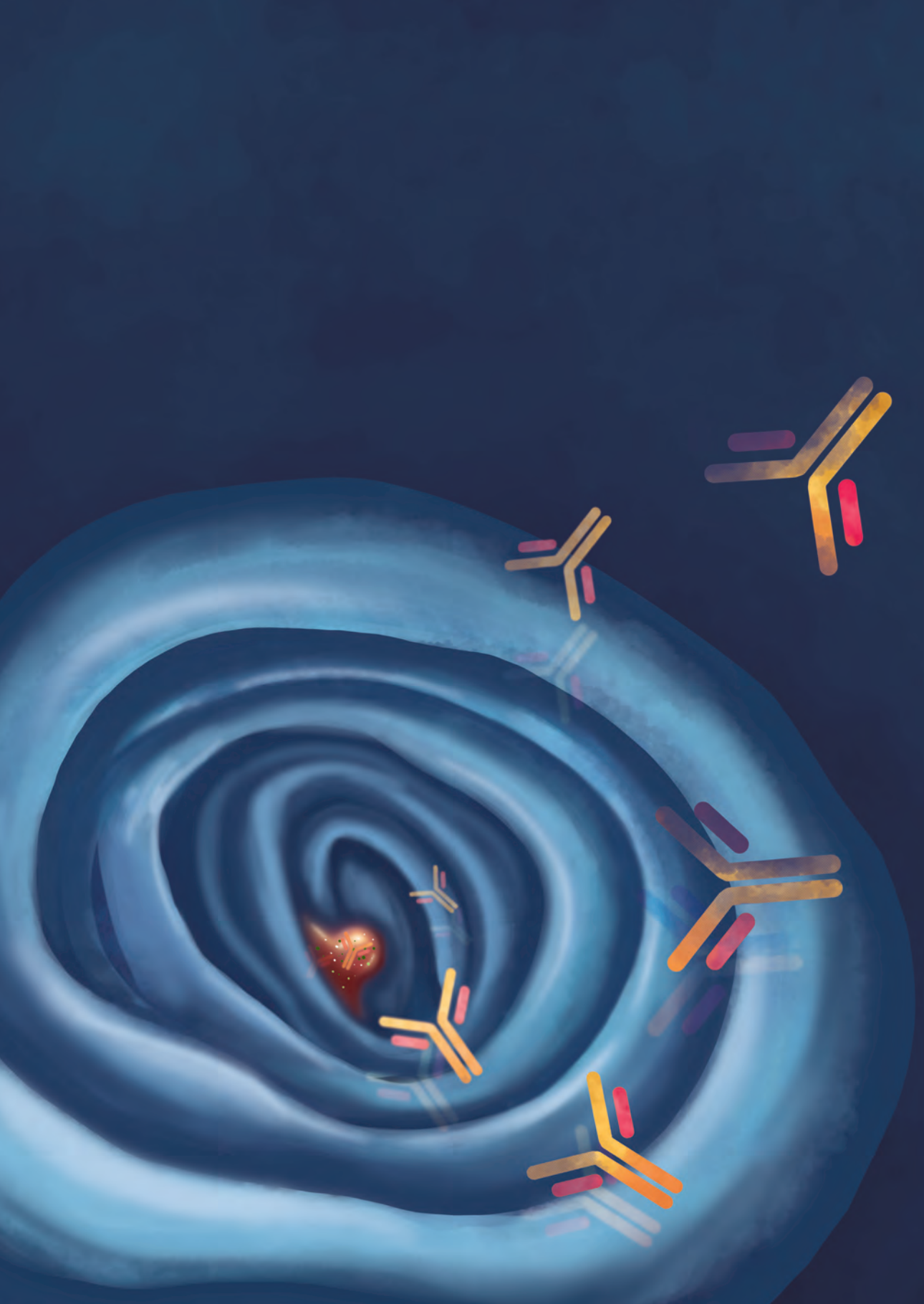

Appendices

References & Dankwoord

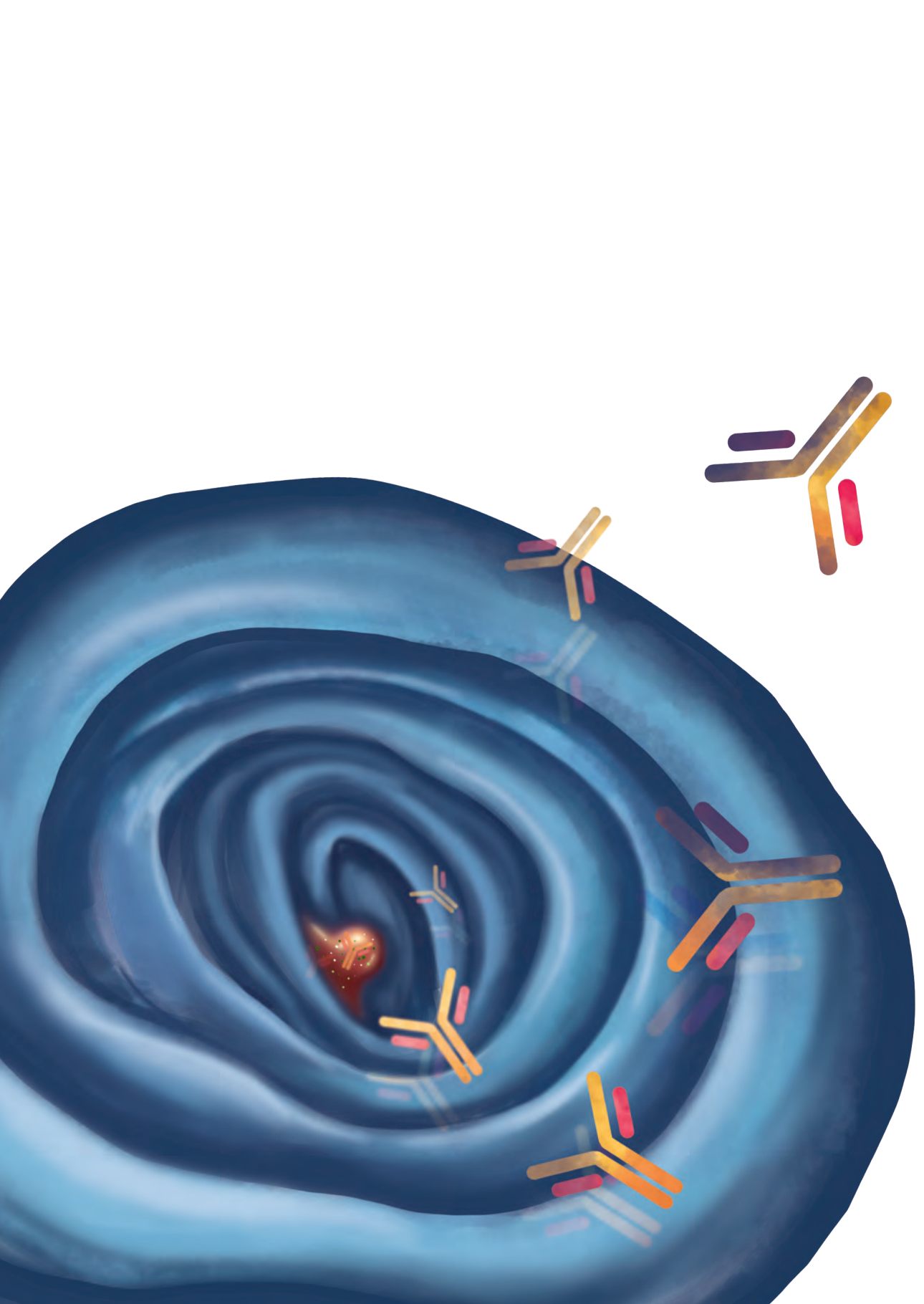

Appendix

References

REFERENCES

1. Rockey DC, Paulson E, Niedzwiecki D, et al. Analysis of air contrast barium enema, computed tomographic colonography, and colonoscopy: prospective comparison. *The Lancet*. 2005;365(9456):305-311.
2. Heresbach D, Barrioz T, Lapalus M, et al. Miss rate for colorectal neoplastic polyps: a prospective multicenter study of back-to-back video colonoscopies. *Endoscopy*. 2008;40(4):284-290.
3. Stoffel EM, Turgeon DK, Stockwell DH, et al. Missed adenomas during colonoscopic surveillance in individuals with Lynch syndrome (Hereditary Nonpolyposis Colorectal Cancer). *Cancer Prev Res*. 2008;1(6):470-475.
4. Mecklin JP, Aarnio M, Läärä E, et al. Development of colorectal tumors in colonoscopic surveillance in Lynch syndrome. *Gastroenterology*. 2007;133(4):1093-1098.
5. Rijcken FEM, Hollema H, Kleibeuker JH. Proximal adenomas in hereditary non-polyposis colorectal cancer are prone to rapid malignant transformation. *Gut*. 2002;50(3):382-386.
6. Corley DA, Jensen CD, Marks AR, et al. Adenoma detection rate and risk of colorectal cancer and death. *N Engl J Med*. 2014;370(14):1298-1306.
7. Staton CA, Chetwood ASA, Cameron IC, Cross SS, Brown NJ, Reed MWR. The angiogenic switch occurs at the adenoma stage of the adenoma carcinoma sequence in colorectal cancer. *Gut*. 2007;56(10):1426-1432.
8. van Dam GM, Themelis G, Crane LMA, et al. Intraoperative tumor-specific fluorescence imaging in ovarian cancer by folate receptor-[alpha] targeting: first in-human results. *Nat Med*. 2011;17(10):1315-1319.
9. Hanrahan V, Currie MJ, Gunningham SP, et al. The angiogenic switch for vascular endothelial growth factor (VEGF)-A, VEGF-B, VEGF-C, and VEGF-D in the adenoma-carcinoma sequence during colorectal cancer progression. *J Pathol*. 2003;200(2):183-194.
10. Siegel RL, Miller KD, Jemal A. Cancer statistics, 2018. *CA Cancer J Clin*. 2018;68(1):7-30.
11. Rex DK, Ahnen DJ, Baron JA, et al. Serrated Lesions of the Colorectum: Review and Recommendations From an Expert Panel. *Am J Gastroenterol*. 2012;107(9):1315-1329.
12. van Rijn JC, Reitsma JB, Stoker J, Bossuyt PM, van Deventer SJ, Dekker E. Polyp miss rate determined by tandem colonoscopy: a systematic review. *Am J Gastroenterol*. 2006;101(2):343-350.
13. Middelburg TA, Hoy CL, Neumann HAM, Amelink A, Robinson DJ. Correction for tissue optical properties enables quantitative skin fluorescence measurements using multi-diameter single fiber reflectance spectroscopy. *J Dermatol Sci*. 2015;79(1):64-73.
14. Hartmans E, Tjalma JJJ, Linssen MD, et al. Potential red-flag identification of colorectal adenomas with wide-field molecular fluorescence endoscopy. *Theranostics*. 2018;8(6):1458-1467.
15. Creavin B, Ryan E, Martin ST, et al. Organ preservation with local excision or active surveillance following chemoradiotherapy for rectal cancer. *Br J Cancer*. 2017;116(2):169-174.
16. Maas M, Lambregts DMJ, Nelemans PJ, et al. Assessment of clinical complete response after chemoradiation for rectal cancer with digital rectal examination, endoscopy, and MRI: selection for organ-saving treatment. *Ann Surg Oncol*. 2015;22(12):3873-3880.
17. Habr-Gama A, Perez R, Nadalin W, et al. Long-term results of preoperative chemoradiation for distal rectal cancer correlation between final stage and survival. *J Gastrointest Surg*. 2005;9(1):90-101.

18. Ryan JE, Warrier SK, Lynch AC, Ramsay RG, Phillips WA, Heriot AG. Predicting pathological complete response to neoadjuvant chemoradiotherapy in locally advanced rectal cancer: a systematic review. *Colorectal Dis*. 2016;18(3):234-246.
19. Habr-Gama A, Perez RO, Proscurshim I, et al. Patterns of failure and survival for nonoperative treatment of stage c0 distal rectal cancer following neoadjuvant chemoradiation therapy. *J Gastrointest Surg*. 2006;10(10):1319-1329.
20. Smith JD, Ruby JA, Goodman KA, et al. Nonoperative management of rectal cancer with complete clinical response after neoadjuvant therapy. *Ann Surg*. 2012;256(6):965-972.
21. Appelt AL, Ploen J, Harling H, et al. High-dose chemoradiotherapy and watchful waiting for distal rectal cancer: a prospective observational study. *Lancet Oncol*. 2015;16(8):919-927.
22. Maas M, Beets-Tan RGH, Lambregts DMJ, et al. Wait-and-see policy for clinical complete responders after chemoradiation for rectal cancer. *J Clin Oncol*. 2011;29(35):4633-4640.
23. Renehan AG, Malcomson L, Emsley R, et al. Watch-and-wait approach versus surgical resection after chemoradiotherapy for patients with rectal cancer (the OnCoRe project): a propensity-score matched cohort analysis. *Lancet Oncol*. 2016;17(2):174-183.
24. East JE, Suzuki N, Stavrinidis M, Guenther T, Thomas HJW, Saunders BP. Narrow band imaging for colonoscopic surveillance in hereditary non-polyposis colorectal cancer. *Gut*. 2008;57(1):65-70.
25. Ramsoekh D, Haringsma J, Poley JW, et al. A back-to-back comparison of white light video endoscopy with autofluorescence endoscopy for adenoma detection in high-risk subjects. *Gut*. 2010;59(6):785-793.
26. Chung SJ, Kim D, Song JH, et al. Comparison of detection and miss rates of narrow band imaging, flexible spectral imaging chromoendoscopy and white light at screening colonoscopy: a randomised controlled back-to-back study. *Gut*. 2014;63(5):785-791.
27. de Vries EGE, Oude Munnink TH, van Vugt MATM, Nagengast WB. Toward molecular imaging–driven drug development in oncology. *Cancer Discov*. 2011;1(1):25-28.
28. Hoetker MS, Goetz M. Molecular imaging in endoscopy. *United European Gastroenterol J*. 2013;1(2):84-92.
29. Terwisscha van Scheltinga AG, van Dam GM, Nagengast WB, et al. Intraoperative near-infrared fluorescence tumor imaging with vascular endothelial growth factor and human epidermal growth factor receptor 2 targeting antibodies. *J Nucl Med*. 2011;52(11):1778-1785.
30. Cohen R, Stammes MA, de Roos IH, Stigter-van Walsum M, Visser GW, van Dongen GA. Inert coupling of IRDye800CW to monoclonal antibodies for clinical optical imaging of tumor targets. *EJNMMI Res*. 2011;1(1):31.
31. Marshall MV, Draney D, Sevick-Muraca EM, Olive DM. Single-dose intravenous toxicity study of IRDye 800CW in Sprague-Dawley rats. *Mol Imaging Biol*. 2010;12(6):583-594.
32. Zinn KR, Korb M, Samuel S, et al. IND-directed safety and biodistribution study of intravenously injected cetuximab-IRDye800 in cynomolgus macaques. *Mol Imaging Biol*. 2015;17(1):49-57.
33. Themelis G, Yoo JS, Soh K-S, Schulz R, Ntziachristos V. Real-time intraoperative fluorescence imaging system using light-absorption correction. *J Biomed Opt*. 2009;14(6):064012.
34. Garcia-Allende PB, Glatz J, Koch M, et al. Towards clinically translatable NIR fluorescence molecular guidance for colonoscopy. J *Biomed Opt*. 2013;5(1):78-92.
35. Nagengast WB, de Vries EG, Hospers GA, et al. In vivo VEGF imaging with radiolabeled bevacizumab in a human ovarian tumor xenograft. *J Nucl Med*. 2007;48(8):1313-1319.
36. Eiblmaier M, Meyer LA, Watson MA, Fracasso PM, Pike LJ, Anderson CJ. Correlating EGFR expression with receptor-binding properties and internalization of 64Cu-DOTA-cetuximab in 5 cervical cancer cell lines. *J Nucl Med*. 2008;49(9):1472-1479.

37. Ferrara N. Vascular endothelial growth factor: basic science and clinical progress. *Endocr Rev*. 2004;25(4):581-611.
38. Bansal A, Liu X, McGregor DH, Singh V, Hall S. Correlation of epidermal growth factor receptor with morphological features of colorectal advanced adenomas: a pilot correlative case series. *Am J Med Sci*. 2010;340(4):296-300.
39. Neumann H, Kiesslich R, Wallace MB, Neurath MF. Confocal laser endomicroscopy: technical advances and clinical applications. *Gastroenterology*. 2010;139(2):388–392
40. Goetz M, Ziebart A, Foersch S, et al. In vivo molecular imaging of colorectal cancer with confocal endomicroscopy by targeting epidermal growth factor receptor. *Gastroenterology*. 2010;138(2):435-446.
41. Sturm MB, Joshi BP, Lu S, et al. Targeted imaging of esophageal neoplasia with a fluorescently labeled peptide: first-in-human results. *Sci Transl Med*. 2013;5(184):184ra61-184ra61.
42. Joshi BP, Miller SJ, Lee CM, Seibel EJ, Wang TD. Multispectral endoscopic imaging of colorectal dysplasia in vivo. *Gastroenterology*. 2012;143(6):1435-1437.
43. Miller SJ, Joshi BP, Feng Y, Gaustad A, Fearon ER, Wang TD. In vivo fluorescence-based endoscopic detection of colon dysplasia in the mouse using a novel peptide probe. Minna J, ed. *PLoS ONE*. 2011;6(3):e17384.
44. Bird-Lieberman EL, Neves AA, Lao-Sirieix P, et al. Molecular imaging using fluorescent lectins permits rapid endoscopic identification of dysplasia in Barrett's esophagus. *Nat Med*. 2012;18(2):315-321.
45. Burggraaf J, Kamerling IMC, Gordon PB, et al. Detection of colorectal polyps in humans using an intravenously administered fluorescent peptide targeted against c-Met. *Nat Med*. 2015;21(8):955-961.
46. Oosting SF, Brouwers AH, van Es SC, et al. ^{89}Zr-bevacizumab PET visualizes heterogeneous tracer accumulation in tumor lesions of renal cell carcinoma patients and differential effects of antiangiogenic treatment. *J Nucl Med*. 2015;56(1):63-69.
47. Tjalma JJ, Garcia-Allende PB, Hartmans E, et al. Molecular fluorescence endoscopy targeting vascular endothelial growth factor A for improved colorectal polyp detection. *J Nucl Med*. 2016;57(3):480-485.
48. ter Weele EJ, Terwisscha van Scheltinga AGT, Linssen MD, et al. Development, preclinical safety, formulation, and stability of clinical grade bevacizumab-800CW, a new near infrared fluorescent imaging agent for first in human use. *Eur J Pharm Biopharm*. 2016;104:226-234.
49. van Cutsem E, Cervantes A, Nordlinger B, Arnold D, ESMO Guidelines Working Group. Metastatic colorectal cancer: ESMO clinical practice guidelines for diagnosis, treatment and follow-up. *Ann Oncol*. 2014;25 Suppl 3:iii1-9.
50. Harlaar NJ, Koller M, de Jongh SJ, et al. Molecular fluorescence-guided surgery of peritoneal carcinomatosis of colorectal origin: a single-center feasibility study. *Lancet Gastroenterol Hepatol*. 2016;1(4):283-290.
51. Hirsch FR, Varella-Garcia M, Bunn PA, et al. Epidermal growth factor receptor in non-small-cell lung carcinomas: correlation between gene copy number and protein expression and impact on prognosis. *J Clin Oncol*. 2003;21(20):3798-3807.
52. Inoue Y, Izawa K, Kiryu S, Tojo A, Ohtomo K. Diet and abdominal autofluorescence detected by in vivo fluorescence imaging of living mice. *Mol Imaging*. 2008;7(1):7290.2008.0003.
53. Rabinsky EF, Joshi BP, Pant A, et al. Overexpressed Claudin-1 can be visualized endoscopically in colonic adenomas in vivo. *Cell Mol Gastroenterol Hepatol*. 2016;2(2):222-237.

54. Mayinger B, Neumann F, Kastner C, Haider T, Schwab D. Hexaminolevulinate-induced fluorescence colonoscopy versus white light endoscopy for diagnosis of neoplastic lesions in the colon. *Endoscopy*. 2010;42(01):28-33.
55. Joshi BP, Dai Z, Gao Z, et al. Detection of Sessile Serrated Adenomas in the Proximal Colon Using Wide-Field Fluorescence Endoscopy. *Gastroenterology*. 2017;152(5):1002-1013.e9.
56. Fang J, Nakamura H, Maeda H. The EPR effect: Unique features of tumor blood vessels for drug delivery, factors involved, and limitations and augmentation of the effect. *Adv Drug Deliv Rev*. 2011;63(3):136-151.
57. Kanick SC, Robinson DJ, Sterenborg HJCM, Amelink A. Extraction of intrinsic fluorescence from single fiber fluorescence measurements on a turbid medium. *Opt Lett*. 2012;37(5):948-950.
58. Hoy CL, Gamm UA, Sterenborg HJCM, Robinson DJ, Amelink A. Method for rapid multidiameter single-fiber reflectance and fluorescence spectroscopy through a fiber bundle. *J Biomed Opt*. 2013;18(10):1560-2281.
59. van Leeuwen-van Zaane F, Gamm UA, van Driel PBAA, et al. In vivo quantification of the scattering properties of tissue using multi-diameter single fiber reflectance spectroscopy. *Biomed Opt Express*. 2013;4(5):696-708.
60. Cohen R, Vugts DJ, Walsum MS-V, Visser GWM, van Dongen GAMS. Inert coupling of IRDye800CW and zirconium-89 to monoclonal antibodies for single- or dual-mode fluorescence and PET imaging. *Nat Protoc*. 2013;8(5):1010-1018.
61. Rosenthal EL, Warram JM, de Boer E, et al. Safety and tumor specificity of cetuximab-IRDye800 for surgical navigation in head and neck cancer. *Clin Cancer Res*. 2015;21(16):3658-3666.
62. van Leeuwen-van Zaane F, Gamm UA, van Driel PBAA, et al. Intrinsic photosensitizer fluorescence measured using multi-diameter single-fiber spectroscopy in vivo. *J Biomed Opt*. 2014;19(1):1560-2281.
63. Hoy CL, Gamm UA, Sterenborg HJCM, Robinson DJ, Amelink A. Use of a coherent fiber bundle for multi-diameter single fiber reflectance spectroscopy. *Biomed Opt Express*. 2012;3(10):2452-2464.
64. Leung K. IRDye 800CW-Human serum albumin. *MICAD*. 2012;102:107-112.
65. ferlay J, Soerjomataram I, Ervik M. GLOBOCAN 2012 v1.0, cancer incidence and mortality worldwide: IARC CancerBase no. 11. Lyon, France: international agency for research on cancer. globocan.iarc.fr.
66. McCarthy K, Pearson K, Fulton R, Hewitt J. Pre-operative chemoradiation for non-metastatic locally advanced rectal cancer. Cochrane Colorectal Cancer Group, ed. *Cochrane Database Syst Rev*. 2012;12(3):CD008368.
67. Leporrier J, Maurel J, Chiche L, Bara S, Segol P, Launoy G. A population-based study of the incidence, management and prognosis of hepatic metastases from colorectal cancer. *Br J Surg*. 2006;93(4):465-474.
68. Nordholm-Carstensen A, Krarup P-M, Jorgensen LN, Wille-Jørgensen PA, Harling H, Danish Colorectal Cancer Group. Occurrence and survival of synchronous pulmonary metastases in colorectal cancer: a nationwide cohort study. *Eur J Cancer*. 2014;50(2):447-456.
69. Evans J, Patel U, Brown G. Rectal cancer: primary staging and assessment after chemoradiotherapy. *Semin Radiat Oncol*. 2011;21(3):169-177.
70. Samee A, Selvasekar CR. Current trends in staging rectal cancer. *World J Gastroenterol*. 2011;17(7):828-834.
71. Bipat S, Niekel MC, Comans EFI, et al. Imaging modalities for the staging of patients with colorectal cancer. *Neth J Med*. 2012;70(1):26-34.

72. Chua TC, Chong CH, Liauw W, Morris DL. Approach to rectal cancer surgery. *Int J Surg Oncol*. 2012;2012(1):247107-247109.
73. Gérard A, Buyse M, Nordlinger B, et al. Preoperative radiotherapy as adjuvant treatment in rectal cancer. Final results of a randomized study of the European Organization for Research and Treatment of Cancer (EORTC). *Ann Surg*. 1988;208(5):606-614.
74. Sauer R, Becker H, Hohenberger W, et al. Preoperative versus postoperative chemoradiotherapy for rectal cancer. *N Engl J Med*. 2004;351(17):1731-1740.
75. Bosset J-F, Collette L, Calais G, et al. Chemotherapy with preoperative radiotherapy in rectal cancer. *N Engl J Med*. 2006;355(11):1114-1123.
76. Gérard J-P, Conroy T, Bonnetain F, et al. Preoperative radiotherapy with or without concurrent fluorouracil and leucovorin in T3-4 rectal cancers: results of FFCD 9203. *J Clin Oncol*. 2006;24(28):4620-4625.
77. Garajová I, Di Girolamo S, de Rosa F, et al. Neoadjuvant treatment in rectal cancer: actual status. *Chemother Res Pract*. 2011;2011(8):839742–12.
78. Integraal kankercentrum Nederland (IKNL). Richtlijn colorectaal carcinoom en colorectale levermetastasen. https://richtlijnendatabase.nl.
79. National Institute for Health and Clinical Excellence. Colorectal cancer. https://guidance.nice.org.uk/CG131.
80. Schmoll HJ, Van Cutsem E, Stein A, et al. ESMO Consensus Guidelines for management of patients with colon and rectal cancer. a personalized approach to clinical decision making. *Ann Oncol*. 2012;23(10):2479-2516.
81. Tjandra JJ, Kilkenny JW, Buie WD, et al. Practice parameters for the management of rectal cancer (revised). *Diseases of the Colon & Rectum*. 2005;48(3):411-423.
82. Benson AB, Bekaii-Saab T, Chan E, et al. Rectal cancer. *J Natl Compr Canc Netw*. 2012;10(12):1528-1564.
83. Ayez N, Alberda WJ, Burger JWA, et al. Is restaging with chest and abdominal CT scan after neoadjuvant chemoradiotherapy for locally advanced rectal cancer necessary? *Ann Surg Oncol*. 2013;20(1):155-160.
84. Hanly AM, Ryan EM, Rogers AC, et al. Multicenter evaluation of rectal cancer reimaging post neoadjuvant (MERRION) therapy. *Ann Surg*. 2014;259(4):723-727.
85. Law WL, Chu KW. Abdominoperineal resection is associated with poor oncological outcome. *Br J Surg*. 2004;91(11):1493-1499.
86. Parnaby CN, Bailey W, Balasingam A, et al. Pulmonary staging in colorectal cancer: a review. *Colorectal Dis*. 2012;14(6):660-670.
87. Chung C-C, Hsieh C-C, Lee H-C, et al. Accuracy of helical computed tomography in the detection of pulmonary colorectal metastases. *J Thorac Cardiovasc Surg*. 2011;141(5):1207-1212.
88. Parsons AM, Detterbeck FC, Parker LA. Accuracy of helical CT in the detection of pulmonary metastases: is intraoperative palpation still necessary? *Ann Thorac Surg*. 2004;78(6):1910–6–discussion1916–8.
89. Ferrari L, Fichera A. Neoadjuvant chemoradiation therapy and pathological complete response in rectal cancer. *Gastroenterol Rep (Oxf)*. 2015;3(4):277-288.
90. Maas M, Nelemans PJ, Valentini V, et al. Long-term outcome in patients with a pathological complete response after chemoradiation for rectal cancer: a pooled analysis of individual patient data. *Lancet Oncol*. 2010;11(9):835-844.
91. Park IJ, You YN, Agarwal A, et al. Neoadjuvant treatment response as an early response indicator for patients with rectal cancer. *J Clin Oncol*. 2012;30(15):1770-1776.

92. Nilsson PJ, van Etten B, Hospers GAP, et al. Short-course radiotherapy followed by neo-adjuvant chemotherapy in locally advanced rectal cancer-the RAPIDO trial. *BMC Cancer*. 2013;13(1):279.
93. van der Valk MJM, Hilling DE, Bastiaannet E, et al. Long-term outcomes of clinical complete responders after neoadjuvant treatment for rectal cancer in the International Watch & Wait Database (IWWD): an international multicentre registry study. *Lancet*. 2018;391(10139):2537-2545.
94. Habr-Gama A, Gama-Rodrigues J, São Julião GP, et al. Local recurrence after complete clinical response and watch and wait in rectal cancer after neoadjuvant chemoradiation: impact of salvage therapy on local disease control. *Int J Radiat Oncol Biol Phys*. 2014;88(4):822-828.
95. Ferrara N, Gerber H-P, LeCouter J. The biology of VEGF and its receptors. *Nat Med*. 2003;9(6):669-676.
96. Breugom AJ, Swets M, Bosset J-F, et al. Adjuvant chemotherapy after preoperative (chemo) radiotherapy and surgery for patients with rectal cancer: a systematic review and meta-analysis of individual patient data. *Lancet Oncol*. 2015;16(2):200-207.
97. Lappin G. The expanding utility of microdosing. *Clin Pharmacol Drug Dev*. 2015;4(6):401-406.
98. Lamberts LE, Koch M, de Jong JS, et al. Tumor-specific uptake of fluorescent bevacizumab-irdye800CW microdosing in patients with primary breast cancer: a phase I feasibility study. *Clin Cancer Res*. 2017;23(11):2730-2741.
99. Nagengast WB, Hartmans E, Garcia-Allende PB, et al. Near-infrared molecular fluorescence endoscopy detects dysplastic oesophageal lesions using topical and systemic tracer of vascular endothelial growth factor A. *Gut*. 2019;68(1):7-10.
100. Maas M, Lambregts DMJ, Nelemans PJ, Heijnen LA, Martens MH, Leijtens JWA, et al. Assessment of clinical complete response after chemoradiation for rectal cancer with digital rectal examination, endoscopy, and MRI: selection for organ-saving treatment. *Ann Surg Oncol*. 2015;22(12):3873-3880.
101. Gamm UA, Kanick SC, Robinson DJ, Sterenborg HJ, Amelink A. Measurements of tissue scattering properties using multi-diameter single fiber reflectance spectroscopy: experimental validation. *Biomed Opt*. April 2012.
102. Memon S, Lynch AC, Akhurst T, et al. Systematic review of FDG-PET prediction of complete pathological response and survival in rectal cancer. *Ann Surg Oncol*. 2014;21(11):3598-3607.
103. Noordman BJ, Spaander MCW, Valkema R, et al. Detection of residual disease after neoadjuvant chemoradiotherapy for oesophageal cancer (preSANO): a prospective multicentre, diagnostic cohort study. *Lancet Oncol*. 2018;19(7):965-974.
104. Heijnen LA, Lambregts DMJ, Lahaye MJ, et al. Good and complete responding locally advanced rectal tumors after chemoradiotherapy: where are the residual positive nodes located on restaging MRI? *Abdom Radiol (NY)*. 2016;41(7):1245-1252.
105. He H, Wissmeyer G, Ovsepian SV, Buehler A, Ntziachristos V. Hybrid optical and acoustic resolution optoacoustic endoscopy. *Opt Lett*. 2016;41(12):2708-2710.
106. Gao RW, Teraphongphom NT, van den Berg NS, et al. Determination of tumor margins with surgical specimen mapping using near-infrared fluorescence. *Cancer Research*. 2018;78(17):5144-5154.
107. Glimelius B, Tiret E, Cervantes A, Arnold D. Rectal cancer: ESMO clinical practice guidelines for diagnosis, treatment and follow-up. *Ann Oncol*. 2013;24 Suppl 6:vi81-88.
108. Glynne-Jones R, Wyrwicz L, Tiret E, et al. Rectal cancer: ESMO Clinical Practice Guidelines for diagnosis, treatment and follow-up. *Ann Oncol*. 2017;28(4):22-40.
109. Dattani M, Heald RJ, Goussous G, et al. Oncological and survival outcomes in watch and wait patients with a clinical complete response after neoadjuvant chemoradiotherapy for rectal cancer: a systematic review and pooled analysis. *Ann Surg*. 2018;268(6):955-967.

110. Rullier E, Perez RO. Surgery or a watch-and-wait approach for rectal cancer? *Lancet Oncol*. 2019;20(2):189-190.
111. de Jongh SJ, Voskuil FJ, Schmidt I, et al. C-Met targeted molecular fluorescence endoscopy in Barrett's esophagus patients and identification of outcome parameters for phase-I studies. *Theranostics*. 2020;10(12):5357-5367.
112. Smith JJ, Strombom P, Chow OS, et al. Assessment of a watch-and-wait strategy for rectal cancer in patients with a complete response after neoadjuvant therapy. *JAMA Oncol*. 2019;5(4):e185896.
113. Metzger-Filho O, Tutt A, de Azambuja E, Saini KS, Piccart-Gebhart M. Dissecting the heterogeneity of triple-negative breast cancer. *J Clin Oncol*. 2012;30(15):1879-1887.
114. de Jongh SJ, Tjalma JJJ, Koller M, et al. Back-table fluorescence-guided imaging for circumferential resection margin evaluation using bevacizumab-800CW in patients with locally advanced rectal cancer. *J Nucl Med*. 2020;61:655-661.
115. Koller M, Qiu S-Q, Linssen MD, et al. Implementation and benchmarking of a novel analytical framework to clinically evaluate tumor-specific fluorescent tracers. *Nat Commun*. 2018;9(1):3739.
116. Snoeks TJA, van Driel PBAA, Keereweer S, et al. Towards a successful clinical implementation of fluorescence-guided surgery. *Mol Imaging Biol*. 2014;16(2):147-151.
117. De Grand AM, Lomnes SJ, Lee DS, et al. Tissue-like phantoms for near-infrared fluorescence imaging system assessment and the training of surgeons. *J Biomed Opt*. 2006;11(1):014007.
118. Zhu B, Tan IC, Rasmussen JC, Sevick-Muraca EM. Validating the sensitivity and performance of near-infrared fluorescence imaging and tomography devices using a novel solid phantom and measurement approach. *Technol Cancer Res Treat*. 2012;11(1):95-104.
119. Gorpas D, Koch M, Anastasopoulou M, Klemm U, Ntziachristos V. Benchmarking of fluorescence cameras through the use of a composite phantom. *J Biomed Opt*. 2017;22(1):16009.
120. Kim A, Khurana M, Moriyama Y, Wilson BC. Quantification of in vivo fluorescence decoupled from the effects of tissue optical properties using fiber-optic spectroscopy measurements. *J Biomed Opt*. 2010;15(6):067006.
121. Anastasopoulou M, Gorpas D, Koch M, et al. Fluorescence imaging reversion using spatially variant deconvolution. *Sci Rep.* 2019;9(1):18123.
122. Stummer W, Pichlmeier U, Meinel T. Fluorescence-guided surgery with 5-aminolevulinic acid for resection of malignant glioma: a randomised controlled multicentre phase III trial. *Lancet Oncol*. 2006;7(5):392-401.
123. Tummers WS, Warram JM, Tipirneni KE, et al. Regulatory Aspects of Optical Methods and Exogenous Targets for Cancer Detection. *Cancer Research*. 2017;77(9):2197-2206.
124. Rosenthal EL, Warram JM, de Boer E, et al. Successful translation of fluorescence navigation during oncologic surgery: a consensus report. *J Nucl Med*. 2016;57(1):144-150.

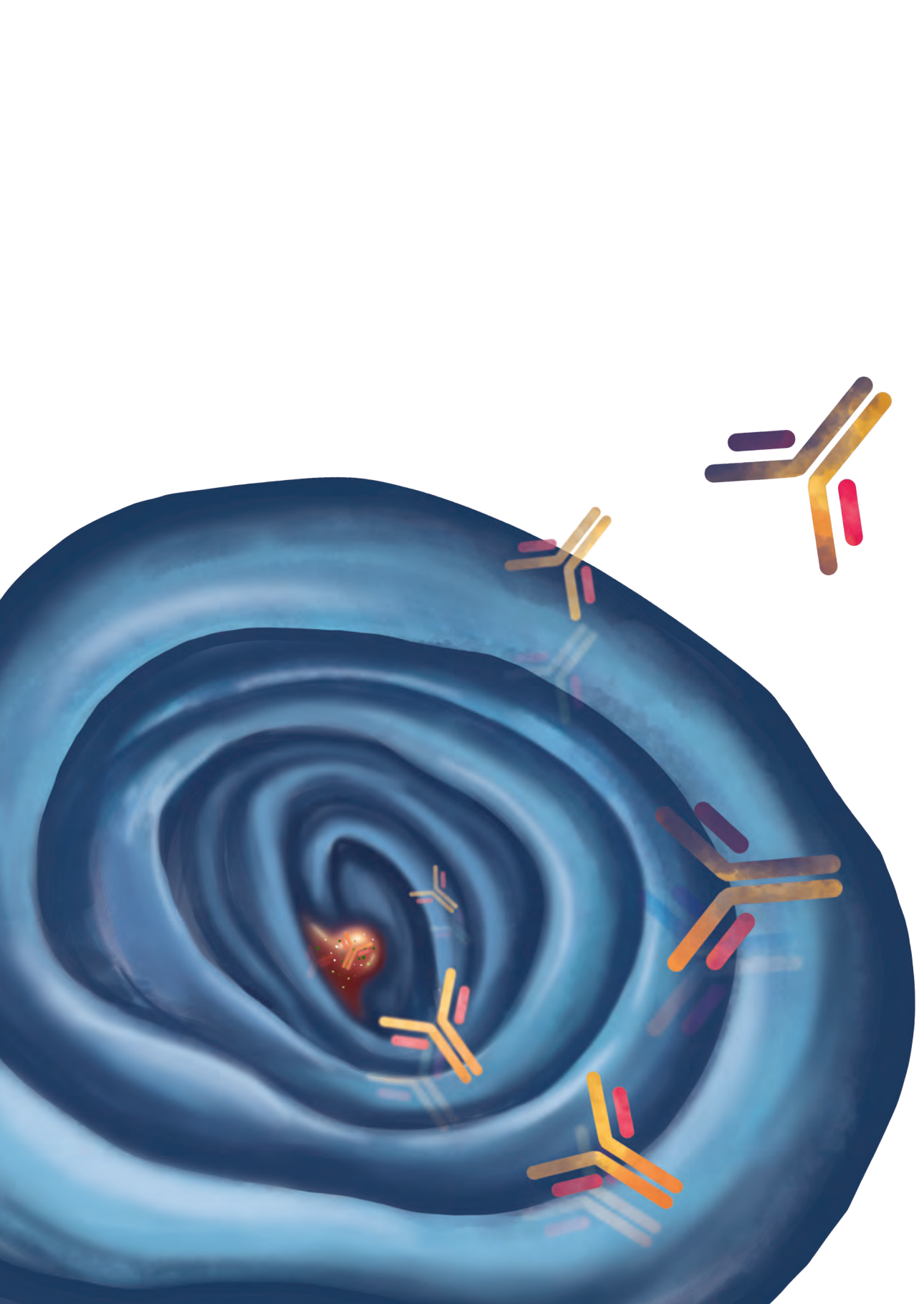

Appendix

Dankwoord
(Acknowledgements)

DANKWOORD

Een proefschrift is een team effort, en dat geldt zeker voor dit multidisciplinaire proefschrift. Ik heb geluk met de vele mensen om mij heen die allen op hun eigen wijze de afgelopen jaren hebben bijgedragen aan de totstandkoming van dit proefschrift.

Als eerste wil ik alle *patiënten* bedanken die hebben mee gewerkt aan de klinische studies beschreven in dit proefschrift, met in het bijzonder de deelnemers van de TRACT-studie (beschreven in hoofdstuk 5 en 6). Ik benaderde hen in een onzekere fase in hun leven, op het moment dat zij de diagnose endeldarmkanker kregen of wanneer zij pas chemoradiotherapie hadden ondergaan en voor een grote operatie stonden. Ik ben hen ontzettend dankbaar dat zij hun tijd en energie wilden steken in dit onderzoek naar de werking van moleculaire fluorescentie endoscopie.

Prof. dr. Wouter Nagengast, beste Wouter, ik reed op een dinsdagavond met je mee terug van Enschede naar Groningen voor een hospiteeravond. Tijdens deze autorit wist je zo bevlogen je onderzoeksplannen te delen dat ik besloot mijn wetenschappelijke stage bij je te doen, de dierstudie beschreven in hoofdstuk 2. Je enthousiasme werkte zo aanstekelijk dat ik besloot je eerste PhD-student te worden. In de jaren die volgden bouwde jij een heuse onderzoeksgroep op waardoor je nu niet meer mijn copromotor bent, maar eerste promotor. Veel dank voor je goede begeleiding, de gegeven vrijheden en het aanhoudende vertrouwen!

Prof. dr. Geke Hospers, beste Geke, jouw vrolijkheid, eerlijkheid en positiviteit werkten inspirerend. Bij overleg zat je altijd vol ideeën en je had vaak een andere kijk op zaken. Het was heel leerzaam om als beginnende arts onder jouw supervisie RAPIDO-patiënten te begeleiden bij hun neoadjuvante chemotherapie traject. Veel dank voor jouw warme rol als tweede promotor.

Prof. dr. Jan Kleibeuker, beste Jan, dank voor de kritische noot tijdens overleggen en je waardevolle feedback op de manuscripten. De ruimte die jij creëerde heeft de onderzoekslijn laten groeien tot wat het nu is.

Prof. dr. Go van Dam en *prof. dr. Liesbeth de Vries*, hartelijk dank voor jullie vakoverstijgende visie. Jullie enthousiasme en drive voor onderzoek is voor velen inspirerend!

De leden van de leescommissie, *prof. dr. Rinze Weersma*, *prof. dr. Esther Consten* en *prof. dr. Johannes de Boer* wil ik hartelijk bedanken voor de beoordeling, suggesties en goedkeuring van mijn proefschrift.

De twee klinische studies zijn een succes geworden dankzij de hulp en ondersteuning van vele medewerkers van verschillende afdelingen binnen het UMCG. Dankzij de flexibiliteit van de endoscopieplanning, endoscopieverpleegkundigen, operatieassistenten en pathologiemedewerkers, hebben we onderzoek kunnen doen tijdens klinische programma's. Afdeling Maag,- Darm-, en Leverziekten: alle MDL-artsen en AIOS bedankt die hebben bijgedragen aan moleculaire fluorescentie endoscopie, met name *drs. Rina Bijlsma*, *dr. Frans Peters* en *dr. Jan Jacob Koornstra*. Afdeling Chirurgie: ik wil de colorectaal chirurgen *dr. Boudewijn van Etten*, *dr. Klaas Havenga* en *drs. Patrick Hemmer* speciaal bedanken voor hun enthousiasme en bijdrage aan de TRACT-studie (H5 en 6). Hopelijk volgt er nog een intra-operatieve studie! Afdeling Pathologie: *drs. Arend Karrenbeld*, dankzij jouw rustige uitleg gedurende die vele uren samen achter de microscoop ben ik histologie gaan waarderen. Jouw hulp als patholoog bij het beoordelen van rectumpreparaten, HE-coupes en kleuringen was onmisbaar. *Jacko Duker*, dank voor de logistiek en scanner ruimte. Afdeling Klinische Farmacie en Farmacologie: *dr. Annelies Jorritsma,* dank je wel voor alle input tijdens de imaging meeting en je belangrijke rol bij de tracerontwikkeling. *Matthijs Linssen* zonder jouw inzet bij het opzetten, plannen en uitvoeren van de GMP-labelingen waren deze studies niet mogelijk geweest, petje af! Het Multidisciplinair Oncologisch Laboratorium (MOL): *dr. Hetty Timmer* en *dr. Coby Meijer*, jullie maken het mogelijk dat zoveel jonge mensen zich kunnen ontwikkelen tot goede onderzoekers. Jullie enthousiasme en betrokkenheid zorgt ervoor dat velen zich gauw thuis voelen. *Wytske Boersma-van Ek*, zoveel coupes gesneden, gekleurd en gescoord, zoveel gelletjes gerund, dank je wel voor je labtechnische ondersteuning. Dank *Anton*, *Arjan* en *Martin* voor het wegwijs maken in het proefdieronderzoek en in het laboratorium, niets zo mindfull als cellijnen kweken! Ook mijn *feestcommissiegenootjes*, dank! Ik wil ook alle ondersteuning bedanken die ik heb ontvangen van *Erna Lont, Jurya Glansbeek, Gretha Beuker, Hilda Tooi, Bianca Smit* en alle researchverpleegkundigen *Arja, Gerrie* en *Greetje*.

Naast het UMCG, zijn er veel samenwerkingsverbanden ontstaan met andere universiteiten en bedrijven. Technical University of Munich: dear *Beatrice*, *Jürgen* and *Max*, so many times you've traveled to Groningen to convert the first camera from wide-field to endoscopy set-up, in a small dark room that was never cleaned. Thank you for the technical support in the first clinical procedures and our fruitful discussions on quantification in optical imaging. SurgVision: *Ben* en *Adrian*, dank jullie wel voor het vele samen sleutelen aan de camera. Erasmus MC: dr. *Dominic Robinson*, ik heb ontzettend veel geleerd van onze gesprekken over het kwantificeren van fluorescentie. Bedankt voor je ondersteuning bij MDSFR/SFF spectroscopie, ik ben heel benieuwd naar de verdere ontwikkeling!

Graag wil ik ook alle coauteurs bedanken voor de samenwerking.

Y3.187 en *U4.313 guppen*, arts-onderzoekers van het eerste uur Rob, Hink, Titia, Martine, Sietske, Lars, Frederike, Niek, Sjoukje, Kees, Pieter, Hilde, Thijs, Harm, Grytsje, Clarieke, Kirsten, Suzanne, Lotte en Maaike. Met jullie als collega's voelden de eerste jaren een verlenging van mijn studententijd. Het is een feestje om naar je werk te gaan als er zo'n gezellige groep arts-onderzoekers aan soortgelijke projecten werkt. Ik bewaar mooie herinneringen aan onze vrijdagmiddagborrels, barbecues, sinterklaasvieringen en weekendjes weg. Brieven van de arbeid & gezondheid bekijk ik nog altijd met argusogen.

Elmire, *Marjory* en *Steven*, jullie zijn met stip mijn promotiemaatjes! Samen klinische studies opzetten, patiënten voorlichten, fluorescentie endoscopie en chirurgie in goede banen leiden, rectumpreparaten afbeelden, muizen behandelen (of reanimeren), congressen onveilig maken (San Diego, Utrecht, Honolulu, New York)... Jullie hebben zelfs het kolven achter mijn Macbook getolereerd en mijn eeuwige chaos het hoofd weten te bieden ☺. Zonder jullie geen promotie! *Niels* en *Michael*, ik zal onze cabriotour over Hawaï niet gauw vergeten. Alle overige *OMIG-onderzoekers*: Matthijs, Floris, Iris, Pascal, Wouter, Bobbie, Siqi, Pieter, dank jullie wel voor de gezellige en leerzame onderzoeksbijeenkomsten. O ja, mannen, er is slechts één klein voordeel aan het feit dat we niet mogen borrelen na de verdediging, nu zal de filmgrap die jullie uithaalden nooit het witte doek zien ☺.

Dan zijn er nog een aantal vrienden die ik graag wil noemen, jullie hebben mijn promotietijd verrijkt en nog steeds! *Sjaakies*, fijn om als zij-instroomvriendinnen het medische wereldje te delen maar ook zoveel daarbuiten. Succes met jouw bikkeltraject Yvet! *Lutske*, jouw poëtische kaartjes en bezoekjes verlichten. *Kitty* en *Merlijn*, onze biologie vriendschap is uitgegroeid tot iets bijzonders, ik geniet van onze jaarlijkse weekendjes. *Harm,* we delen gelukkig meer dan alleen dezelfde humor. *Henk* en *Machteld*, genieten is hoofdzaak, klaverjassen slechts bijzaak. *Chris* en *Renée*, wat heerlijk om altijd te kunnen komen aanwaaien en alleen bij jou was 'het boekje' geen verboden onderwerp, misschien omdat jij zelf altijd aan het schrijven bent? Ik bewonder je doorzettingsvermogen en veerkracht. *Floor*, er is geen beter basis dan samen onkruid wieden! *Aagje*, wat fijn om bij jou altijd thuis te komen. *Anaïs*, you are the most positive and inspiring person I know. *Carmen,* in coronatijd is Madrid plots ver weg, maar jij weet dat toch te overbruggen. *Wouter*, wat beter dan als goede buur uitgroeien tot goede vriend? *Rob* en *Gerrie*, dank voor alle gezellige avonden samen muren bouwen, gauw weer? *Mariëlle*, ik volg jouw voorbeeld westwaarts ☺. *Taco* en *Kirsten*, jullie zijn inspirerende vrienden, die mij blijven prikkelen om te geloven in, en te werken aan, een groenere toekomst. *Wies*, jij volgt je gevoel als geen ander, powervrouw! *Hugo* en *Isa*, ik kom altijd graag bij jullie over de vloer, zoveel levendigheid. *#momlife* wat is het lekker om onbeperkt te kunnen kletsen over kinderen en mannen; maar vooral om hen af en toe allemaal thuis te laten! *WoesteLanders, Boschlusters* en *Pancho'ers,* ik kijk met warme gevoelens terug naar mijn jaren met jullie!

AIOS Huisartsgeneeskunde, in het huisartsvak voel ik me helemaal op mijn plek. Ik wil jullie bedanken voor de getoonde belangstelling tijdens de laatste loodjes van dit proefschrift. Maar vooral voor de gezellige opleidingsjaren; wekelijks een dag onderwijs, intervisie en bijkletsen is een luxe! *Ton* en *Rik*, dank voor de extra tijd die ik kreeg voor de afronding, ik heb jullie beiden hoog zitten!

René & Laura, dank jullie wel voor jullie betrokkenheid en de vele oppasuren. *Mayke & Francesco,* een leukere schoonzus en cognato kan ik me niet wensen.

Margreet, na alle bijzondere momenten die wij hebben gedeeld, ben jij natuurlijk mijn paranimf! Jij weet als geen ander in het oog te houden wat belangrijk is in het leven. Je liet me relativeren als schaamte de kop opstak voor het feit dat ik mijn proefschrift zo lang op de plank had laten liggen. Onze vriendschap is mij heel dierbaar.

Hanna, jij kent mij als geen ander. Onze zussenband is tegen alles bestand. Nu onze tropenjaren gelijk opgaan geeft dat een extra dimensie. Dank voor je onvoorwaardelijke support! *Indra*, grote kleine broer, ik zie je zo graag.

Papa en *mama*, fijnere ouders kan ik me niet wensen. Jullie hebben me veel ruimte en vrijheid gegeven om mijn eigen weg te volgen en me te ontwikkelen tot de persoon die ik nu ben. Dank voor jullie aanmoediging om mijn promotietraject toch af te ronden, zonder jullie steun was dat zeker niet gelukt. Het blijft bijzonder om jullie als pake en make mee te mogen maken, genieten!

Michel, wat startte als een bezoekje aan de lab imaging meeting, resulteerde in kamergenootschap, stiekem koffiedrinken, samen een pubquiz organiseren en een nacht onder de sterrenhemel slapen. Nu vormen we een prachtig gezin met Milou, Mare en Jonas. Ik geniet van ons samenzijn, iedere dag opnieuw.

Jolien Tjalma